22

UTILIZATION OF *IN VITRO* CYTOCHROME P450 INHIBITION DATA FOR PROJECTING CLINICAL DRUG–DRUG INTERACTIONS

JANE R. KENNY, DERMOT F. MCGINNITY, KEN GRIME, AND ROBERT J. RILEY

AstraZeneca R&D Charnwood, Loughborough, United Kingdom

Contents

Preclinical Development Handbook: ADME and Biopharmaceutical Properties, edited by Shayne Cox Gad

22.1 INTRODUCTION

Adverse drug reactions (ADRs) are recognized as a significant cause of hospitalizations and up to 2.8% of hospital admissions may be a consequence of drug–drug interactions (DDIs) [1, 2]. The possibility of DDIs presents whenever two or more drugs are administered simultaneously; an ever more likely occurrence in an aging population often exposed to polypharmacy [3]. Moreover, it has been estimated that >90% of ADRs are also associated with dose-dependent pharmacokinetic/pharmacodynamic (PK/PD) events, which are one of the top five causes of death in the United States, resulting in over 100, 000 deaths each year [1, 2, 4]. While this is alarming, it is noteworthy that of the drugs associated with preventable drug-related hospital admissions, only four drug groups account for more than 50% of ADRs [5]. Indeed, drug concentration-dependent pharmacological reactions (classified as type A adverse reactions) account for approximately 75% of all ADRs and in principle should be preventable [6]. Such statistics highlight the need for improved mechanistic understanding and clear risk avoidance strategies, both during the drug discovery/development process and in the clinic.

DDIs may occur at the metabolic level with impact on drug clearance at the site of gastrointestinal absorption, on plasma or tissue binding, by inhibition or induction of hepatic drug metabolizing enzymes, and on carrier mediated transport (including renal and hepatic uptake and biliary efflux) [7]. All these interactions may induce changes in the PK profiles of the drugs involved, resulting in altered PD response or promotion of a toxicological effect not associated with the primary pharmacology [8, 9]. Several clinically relevant and severe DDI cases, such as those resulting in the withdrawal of terfenadine and cerivastatin [10], have increased the focus on metabolism-based interactions, particularly those involving cytochrome P450 (CYP) enzymes. Indeed, CYP inhibition is reported to account for as much as half of all reported DDIs [11]. These metabolic interactions can occur whenever the metabolism of one "victim" drug is inhibited by the presence of another "perpetrator" drug. The resultant decrease in clearance of the victim drug leads to increased systemic concentrations that are pronounced if the inhibited pathway is the major route of elimination. Several CYP mediated DDIs have resulted in severe clinical reactions and fatalities in extreme cases [10, 12], so real emphasis is placed on the prediction and hence avoidance of DDIs in drug discovery [7, 13–15]. Indeed, there has been substantial academic and industrial effort directed toward the accurate prediction of DDIs with the aim of reducing their impact in the clinic by designing out such interactions.

DDIs as a potential source or contributor to drug attrition, either directly or indirectly, has contributed to the industry focus on this area. In the late 1980s poor drug metabolism and pharmacokinetics (DMPK) properties and toxicity were predominantly responsible for the discontinued development of new chemical entities (NCEs) during late stage clinical trials [16, 17]. In response to this, and to increase competitive advantage (e.g., by avoiding product interaction labels), the pharmaceutical industry has increasingly aligned DMPK to the early drug discovery phase. The failure of NCEs at a late stage is a cost the pharmaceutical industry can ill afford; it is estimated that the total preapproval costs for a new drug are in excess of 800 million U.S. dollars [18]. The industry has responded to both the clinical and

economic factors by front-loading DDI screens early in the discovery phase to predict the risk of DDI for NCEs. High throughput automated assays to evaluate the impact of CYP inhibition are now common as early as the hit identification stage [19]. Increased importance is placed on evaluation of the risk for NCEs participating in DDIs, as a victim and/or perpetrator of such interactions. However, despite the focus that DDIs and potentially associated ADRs have received over the last two decades, it was recently reported that there has been little reduction in their clinical impact [6, 17], although with a drug development time in excess of ten years it is perhaps too early to identify the impact of such DDI screens on these clinical statistics.

In the following sections several examples of DDIs are introduced to demonstrate the clinical consequences of CYP inhibition. The kinetics of reversible and irreversible inhibition are presented along with discussion of *in vitro* methodology. Accurate *in vitro* kinetic data is an absolute prerequisite for *in vitro–in vivo* extrapolation (IVIVE), and the current literature models for predicting clinical inhibition are presented. Overall, this chapter aims to summarize the current knowledge base and the complexities of CYP inhibition and to provide a guide for embarking on prediction of clinical DDIs with particular emphasis on the drug discovery setting.

22.2 CYTOCHROME P450 AND ITS ROLE IN DRUG–DRUG INTERACTIONS

The CYP family of enzymes are the primary facilitators of oxidative biotransformation in the liver and are responsible for the metabolism, at least in part, of the majority of human drugs [20]. These heme-containing enzymes are primarily situated in the lipid bilayer of the endoplasmic reticulum of hepatocytes, but are also located in extrahepatic tissues, including the gastrointestinal tract (GIT), kidney, and lung [21]. Fifty-seven different human CYP enzymes have been identified [22] and of these, 23 human isoforms are from the CYP1, CYP2, and CYP3 families that are recognized as important in xenobiotic metabolism [23]. However, it has been estimated that approximately 90% of human drug oxidations can be attributed to just five CYPs, namely, CYP1A2, CYP2C9, CYP2C19, CYP2D6, and CYP3A4/5 [24, 25]. CYP3A4 is the most abundant of these and can constitute up to 50% of total hepatic CYP content [26]. This enzyme is also the most prolific, with approximately 60% of all oxidative biotransformations being attributed to CYP3A4 [27]. The CYP family metabolize a very broad range of substrates, from endogenous steroids and vitamins to small drug molecules of all charge types [28]. For example, CYP3A4 metabolizes large lipophilic molecules including testosterone, erythromycin, and cyclosporine as well as smaller molecules like midazolam and nifedipine. CYP2C9 favors medium sized acidic or neutral molecules such as diclofenac and tienilic acid; CYP2D6 favors basic, lipophilic molecules such as dextromethorphan and metoprolol, while CYP1A2 has affinity for neutral planar molecules such as theophylline and phenacetin [28]. Since CYPs are the major enzyme family in xenobiotic/drug metabolism, they retain a central role in the mediation of clinically relevant DDIs.

22.2.1 Clinical Consequences of Cytochrome P450 Mediated Drug–Drug Interactions

There is a wealth of literature around CYP mediated DDIs. The most documented DDIs resulting in severe clinical adverse reactions are listed in Table 22.1. In the following section examples of drugs as either victims or perpetrators of DDIs will be presented with specific cases exemplifying (1) reversible and irreversible inhibition at the major CYPs and (2) the role of intestinal metabolism and enzyme polymorphisms within the patient population.

The antihistamine terfenadine, a victim of DDI, was withdrawn because of patient fatality following coadministration with ketoconazole [10]. Competitive inhibition of CYP3A4-dependent terfenadine methyl-hydroxylation by ketoconazole resulted in up to a 40-fold increase in the area under the plasma concentration–time curve (*AUC*) of terfenadine. This increased concentration manifested itself clinically as QT prolongation and torsades de pointes [37]. Other victims of DDI are simvastatin and lovastatin. Both are 3-hydroxy-3-methylglutaryl coenzyme A (HMG-CoA) reductase inhibitors, which although exceedingly well tolerated, incur a small risk of myopathy or potentially fatal rhabdomyolysis, particularly when coadministered with medications that increase their systemic exposure [44]. These statins both have a substantial CYP3A4 component to their metabolism, and large (hepatic and intestinal) first-pass metabolism makes them particularly susceptible to interactions via CYP3A4 inhibition. Intestinal metabolism may be effectively abolished in the presence of a potent oral CYP3A4 inhibitor, resulting in an increase in plasma concentration of up to threefold for drugs such as cyclosporine, midazolam, lovastatin, and simvastatin [44–46]. This was elegantly confirmed in clinical studies where midazolam was administered either via the oral or intravenous route alongside the CYP3A4 inhibitors itraconazole and fluconazole [46]. Following an intravenous dose the *AUC* of midazolam was increased 3.5-fold in the presence of itraconazole; however, the *AUC* increased sevenfold when midazolam was administered orally [46]. Clearly, for drugs with a high hepatic extraction, the impact of metabolic inhibition will give rise to large changes in oral exposure, compounded by any effect of inhibition on intestinal metabolism.

Another statin, cerivastatin, was anticipated to have less potential for CYP3A4 mediated DDIs than the other statins due to the additional role of CYP2C8 in its metabolism [47]. Prior to launch it was thought that cerivastatin would provide a safer alternative to simvastatin and lovastatin due to its alternative metabolic pathway. Indeed, interaction studies with erythromycin and itraconazole, two potent inhibitors of CYP3A4, have shown little impact on cerivastatin plasma levels [48–50]. However, coadministration with gemfibrozil increases the *AUC* of cerivastatin about sixfold [33]. This is assumed to be due to inhibition of CYP2C8 by gemfibrozil and its glucuronide metabolite. Interestingly, the glucuronide metabolite demonstrates a 20-fold increase in inhibitory potency at CYP2C8 over its parent (IC_{50} of 80 μM and 4 μM for gemfibrozil and its glucuronide metabolite, respectively [51]) and is actively concentrated in the liver [51, 52]. It is also worth noting that gemfibrozil also inhibits the OATP1B1-mediated hepatic uptake of statins and that this mechanism could well have contributed to this and indeed other gemfibrozil–statin interactions [52, 53]. During cerivastatin monotherapy, the incidence rate of rhabdomyolysis was 10–100 times higher than with the other statins and gemfibrozil

TABLE 22.1 Examples of Marketed Drugs Involved in Clinically Significant Drug–Drug Interactions

Predominant CYP Isoform	Victim Drug	Perpetrator Drug	Maximum Clinical AUC Increase of Victim Drug	Clinical Consequences	References
CYP1A2	Theophylline	Ciprofloxacin	Variable	Theophylline toxicity	29
	Tizanidine	Ciprofloxacin	10-fold	Excess hypotensive and sedative effects	30
	Tacrine	Fluvoxamine	~sixfold	Hepatotoxicity	31, 32
CYP2C8	Cerivastatin[a]	Gemfibrozil	sixfold	Rhabdomylosis	33
CYP2C9	Tolbutamide	Sulfaphenazole	5.3-fold	Hypoglycemia	34
	Warfarin	Fluconazole	50% decrease in clearance	Enhanced hypoprothrombinemic effect	35
CYP2D6	Desipramine	Fluoxetine	~sixfold		31
	Metoprolol	Mibefradil[a]	4–5-fold	Effect on cardioselectivity	36
CYP3A4	Terfenadine[a]	Ketoconazole	~40-fold	Torsades des pointes	2, 10, 37, 38
	Lovastatin	Itraconazole	~20-fold	Rhabdomylosis	39, 40
	Simvastatin	Mibefradil[a]	5–10-fold	Rhabdomylosis	41
	Midazolam	Erythromycin	threefold	Excess sedation	42
	Cisapride[a]	Erythromycin	Variable	QT prolongation	12, 43

[a]Withdrawn from the market between 1990 and 2001.

greatly increased this risk; the number of rhabdomyolysis cases reported to the U.S. Food and Drug Administration with the gemfibrozil–cerivastatin combination was 533 [53]. As a result, cerivastatin was voluntarily withdrawn from the market in 2003.

Adverse events can be manifest without particularly large changes in the *AUC* of the victim drug. In epileptic patients stabilized on carbamazepine therapy, addition of the antidepressant agent viloxazine has resulted in side effects of carbamazepine intoxication (fatigue, dizziness, and ataxia). This is associated with an *AUC* elevation of carbamazepine (approximately twofold) and carbamazepine 10,11-epoxide (approximately 1.3-fold) [54]. The most likely mechanism for this interaction is CYP3A4 inhibition by viloxazine [55]. This example shows how a modest elevation can be detrimental if the therapeutic window of the victim drug is narrow; in this case resulting in an exaggerated pharmacological effect.

Mibefradil, a novel calcium antagonist for the treatment of hypertension and angina and a perpetrator of DDI, was voluntarily withdrawn from the market in 1997, less than a year after its launch [36]. Several severe adverse reactions were observed during mibefradil therapy in combination with various drugs including simvastatin and lovastatin [36, 41]. During its development, mibefradil had been identified as having inhibitory effects on CYP3A4 and CYP2D6, consequently coadministration was contraindicated with terfenadine and metoprolol (a CYP2D6 substrate) and the labeling carried a list of drugs that might require dose adjustment. When mibefradil was withdrawn, an additional complication arose; life-threatening reactions occurred if therapy was replaced with β-blockers or calcium channel antagonists within 5 days of discontinuing mibefradil therapy [36]. This was attributed to the long elimination half-life of mibefradil, but subsequently, it has been observed that mibefradil is a time-dependent inhibitor of CYP3A4 [56, 57] and also inhibits P-gp *in vitro* (K_i of 1.6 μM [58]). The time-dependent nature of its CYP3A4 inhibition could explain the long "wash-out" period of mibefradil mediated inhibition. There are suggestions in the literature that some of the severe interactions observed with mibefradil could have been predicted from the *in vitro* and *in vivo* data available at the time [36, 45, 59].

The extent of DDIs can vary substantially within the population due to variability in enzyme expression. This variation is observed in the ciprofloxacin–theophylline interaction and has implications for the severity of the clinical outcome. The inhibitory effect of ciprofloxacin at CYP1A2 can result in varying changes in theophylline levels across a patient population. In sensitive patients, theophylline clearance can decrease significantly, increasing the risk of theophylline related toxicity [29, 60]. In another case, ciprofloxacin inhibits the CYP1A2 mediated metabolism of tizanidine, resulting in AUC increases of up to 10-fold, dangerously escalating its hypotensive and sedative effects [30]. CYP1A2 is the primary clearance mechanism for both theophylline and tizanidine [61, 62], and there is considerable interindividual variability in the *in vivo* metabolic activity of CYP1A2 (demonstrated by caffeine clearance [63]); therefore, inhibition results in significant changes in plasma levels in sensitive patients only.

As is the case for all polymorphic CYPs, the CYP2D6 related DDIs are complicated by the genetic polymorphisms observed for this enzyme (between 5% and 10% of the Caucasian population are CYP2D6 poor metabolizers). Investigation of potential DDIs observed via CYP2D6 inhibition may be confounded by the pres-

ence of individuals with the poor metabolizer phenotype within the study group [64]. It is evident that poor metabolizers are unlikely to suffer DDIs through CYP2D6 inhibition and therefore will not display the same magnitude of interaction predicted from *in vitro* studies [6]. CYP2D6 is inhibited by antipsychotic drugs and the propensity for interactions is increased for this patient population as psychopharmacologic medications are often taken for long periods of time and commonly coprescribed with other medications [65]. For example, the CYP2D6 inhibitor fluoxetine has been demonstrated to substantially increase the plasma levels of desipramine (between four- and sixfold) [31].

The clinical interactions presented here highlight the need to assess an NCE's involvement in potential DDIs from *both* perspectives of inhibition, either as a victim drug where metabolism is altered by a coadministered inhibitor or as the perpetrator of DDI. The cases also highlight the importance of fully defining the elimination and metabolic profile of an NCE: reaction phenotyping can lend greater understanding to potential interactions as can an understanding of the target patient population and likely coadministered drugs.

22.2.2 Mechanisms of Cytochrome P450 Inhibition

There are different mechanisms through which CYP inhibition may occur, all of which are a function of the metabolic capacity of the enzyme. In nearly all cases of clinically relevant *reversible* inhibition, the perpetrator is a substrate competing for the same CYP mediated metabolism. Simple Michaelis–Menten kinetics often satisfactorily describes CYP metabolism *in vitro*, provided that the enzyme and substrate are in thermodynamic equilibrium.

Enzyme Kinetics In the reaction scheme shown in Fig. 22.1, a steady-state equilibrium is assumed to be reached (the ES complex rapidly reaches a constant value such that $d[ES]/dt = 0$). This assumption is key to the derivation of the Michaelis–Menten equation, which underpins not only prediction of metabolic clearance from *in vitro* data but also prediction of DDIs (since the prediction of DDI magnitude from *in vitro* data always starts with a modification of the Michaelis–Menten equation). The reason that the investigator needs to be aware of this is that experimental conditions are important in making this assumption. For $d[ES]/dt = 0$, the reverse reaction rate should be negligible and the formation of the [ES] complex should not significantly alter the substrate concentration [S]. In other words, the substrate concentration should greatly exceed the enzyme concentration and the substrate concentration should not be significantly depleted during the incubation (less than 20% metabolism). To this end, it is noteworthy that in a typical human liver microsome (HLM) preparation, CYP3A4 concentration may be as much as 0.25 μM when the incubation contains 1 mg/mL HLM.

Equations 22.1 and 22.2 are the Michaelis–Menten equation (22.1) and its rearrangement (22.2), where v is the observed rate of metabolite formation, V_{max} is the maximum rate of this metabolite formation, K_m is the Michaelis–Menten constant representing the enzyme:substrate affinity and is the concentration that supports half the maximum rate of metabolite formation, and [S] is the substrate concentration at the enzyme active site. The derivation of these equations is shown in Appendix A.

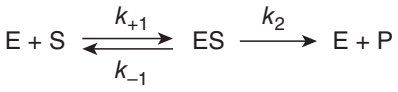

FIGURE 22.1 Schematic representing Michaelis–Menten kinetics, where E is enzyme, S is substrate, k_{+1} is the association rate constant describing ES formation from E + S, k_{-1} is the dissociation rate constant from ES to E + S, ES is substrate-bound enzyme, P is the product of enzyme, and k_2 is the dissociation rate constant from ES to E + P.

$$v = \frac{V_{max} \cdot [S]}{K_m + [S]} \tag{22.1}$$

$$= \frac{V_{max}}{1 + K_m/[S]} \tag{22.2}$$

Only simple one-site binding can be accurately described by hyperbolic Michaelis–Menten kinetics but there is substantial literature evidence that atypical kinetics and multisite binding exist for the CYP enzymes. This is most clear for CYP3A4 [66] but is also observed for CYP2C9 [67, 68]. Positive or negative cooperative effects, where a bound substrate molecule influences the binding of a second molecule, have implications in terms of probe substrate selection and make full kinetic characterizations complex. It must be noted, however, that while cooperativity is clearly demonstrable *in vitro*, there is little evidence of its influence *in vivo* [69, 70]. Only simple one-site models of inhibition will be discussed here and detailed explanation of atypical (or sigmoidal) kinetics in inhibition can be found elsewhere in the scientific literature [14, 66, 71–73].

Reversible Inhibition Having explained the basis of simple CYP kinetics, the details of inhibition can be described. Reversible CYP inhibition can be categorized into three main forms: competitive, noncompetitive, and uncompetitive. Figure 22.2 describes each type of inhibition and the rate equations associated with them are presented below. In competitive inhibition the substrate and inhibitor compete for the same binding site within the enzyme; inhibition therefore decreases as the enzyme becomes saturated with substrate. Competitive inhibitors interfere with substrate binding so as to raise K_m by a factor of $[I]/K_i$ without affecting V_{max} (i.e., the affinity of the substrate for the enzyme, K_m, is decreased by a factor dependent in magnitude on the ratio of inhibitor concentration and the affinity of the inhibitor for the enzyme, K_i (Eq. 22.3)):

$$v = \frac{V_{max} \cdot [S]}{K_m(1 + [I]/K_i) + [S]} \tag{22.3}$$

It is common to relate the potency of competitive inhibition to IC_{50} (the concentration of inhibitor for which the reaction rate is suppressed by 50%). Equation 22.4 is derived from Eq. 22.3 when v becomes $v/2$ and I becomes IC_{50}.

$$IC_{50} = K_i(1 + [S]/K_m) \tag{22.4}$$

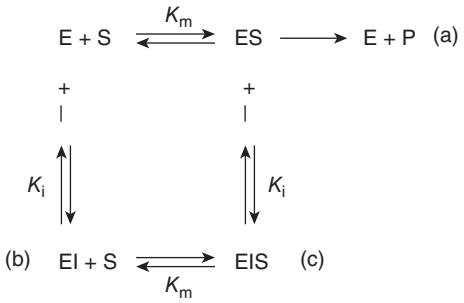

FIGURE 22.2 Schematic of competitive inhibition, representing Michaelis–Menten kinetics. Pathway (a), competitive inhibition; pathway (b), uncompetitive inhibition; pathway (c), noncompetitive inhibition. E is enzyme, S is substrate, ES is substrate-bound enzyme, P is the product of enzyme and substrate, I is inhibitor, EI is inhibitor-bound enzyme, EIS is inhibitor- and substrate-bound enzyme, K_m is the Michaelis–Menten constant, and K_i is the inhibition constant. Note that K_m can be described as $(k_2 + k_{-1}/k_{+1})$—see Appendix A. However, if it is assumed that rapid formation of the ES complex occurs when the enzyme and substrate are mixed; $k_{+1} >> k_2$ and K_m can be described as k_{-1}/k_{+1}.

In noncompetitive inhibition the inhibitor binds at a site distinct from the substrate binding site and can interact with either the substrate-free or the substrate-bound form of the enzyme. It is assumed that the inhibitor binds to both states of the enzyme with the same affinity and so the degree of inhibition is independent of substrate concentration. The binding affinity (K_m) is unaffected but the inhibitor acts to remove active enzyme and consequently the maximal reaction velocity (V_{max}) is decreased. The metabolic rate of noncompetitive inhibition is described by

$$v = \frac{V_{max}/(1+[I]/K_i)\cdot[S]}{K_m+[S]} \tag{22.5}$$

The substrate-independent nature of inhibition is further demonstrated by the IC_{50}, which is equivalent to the inhibitor constant $K_i(IC_{50} = K_i)$, derived from Eq. 22.5 when v becomes $v/2$ and [I] becomes IC_{50}.

In uncompetitive inhibition (which is extremely rare for CYP metabolism [71]), only the substrate-bound form of the enzyme is open to inhibitor binding; the inhibitor cannot bind to free enzyme and so the degree of inhibition will increase with substrate concentration. The metabolic rate in the presence of an uncompetitive inhibitor can be described by Eq. 22.6 and the corresponding IC_{50} by Eq. 22.7:

$$v = \frac{V_{max}/(1+[I]/K_i)\cdot[S]}{K_m(1+[I]/K_i)+[S]} \tag{22.6}$$

$$IC_{50} = K_i(1+K_m/[S]) \tag{22.7}$$

Mechanism-Based Inhibition Irreversible inhibition or mechanism-based inactivation is an unusual occurrence with most enzymes. It is, however, observed in reactions catalyzed by CYP in somewhat higher frequency [74]. In contrast with

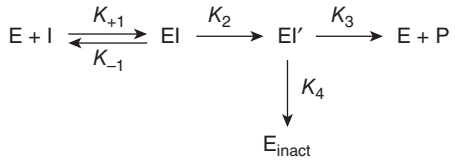

FIGURE 22.3 Schematic of mechanism-based inhibition, where E is enzyme, I is inhibitor, EI is inhibitor-bound enzyme, EI′ is the initial complex formed between metabolic intermediate and enzyme, P is the product of enzyme and inhibitor complex that escapes reactive binding in the active site, $E_{inactive}$ is the inactive enzyme with irreversibly bound metabolic intermediate, k_{+1} is the association rate constant for E + I forming EI, k_2 is the association rate constant for EI forming EI′, k_3 is the dissociation rate constant for EI′ to E + P, and k_4 is the rate constant from EI′ to E_{inact}.

reversible inhibition, the effects of mechanism-based inhibition (MBI) are more profound after multiple dosing and the recovery period, typically several days, is independent of continued exposure to the drug [75, 76]. This MBI transpires when a CYP is quasi-irreversibly or irreversibly inhibited by reactive intermediates formed during the metabolic process. The inhibitory intermediates may form covalently bound adducts to the CYP heme or apoprotein; alternatively, they may form a metabolic inhibitory complex (MIC) in the active site. This MBI is characterized by NADPH-, concentration-, and time-dependent inactivation. Additionally, the inactivation rate is diminished in the presence of a competing substrate, enzyme activity is not restored by dialysis or filtration (as inhibitor is covalently bound), and *de novo* synthesis of protein is required to recover metabolic activity [77]. Figure 22.3 shows a schematic representation of this inhibition [78] and the inhibition for the initial rate of enzyme deactivation can be described as follows.

From Fig. 22.3 it can be seen that the change in concentration over time of inhibitor-bound enzyme, [EI], the initial complex formed between metabolic intermediate and enzyme, [EI′], and the inactive enzyme with irreversibly bound metabolic intermediate, $[E_{inact}]$, respectively can be expressed as

$$d[\mathrm{EI}]/dt = k_{+1}[\mathrm{I}]\cdot[\mathrm{E}] - (k_{-1} + k_2)[\mathrm{EI}] \tag{22.8}$$

$$d[\mathrm{EI}']/dt = k_2[\mathrm{EI}] - (k_3 + k_4)[\mathrm{EI}'] \tag{22.9}$$

$$d[\mathrm{E}_{\mathrm{inact}}]/dt = k_4[\mathrm{EI}'] \tag{22.10}$$

where [E] is the concentration of the unbound active enzyme and [I] is the concentration of the mechanism-based inhibitor.

The parameters k_{inact} (the maximal inactivation rate constant) and K_I (the inhibitor concentration that supports half the maximal rate of inactivation) are described by Eqs. 22.11 and 22.12, respectively, using the association constants shown in Fig. 22.3.

$$k_{\mathrm{inact}} = k_2 k_4/(k_2 + k_3 + k_4) \tag{22.11}$$

$$K_{\mathrm{I}} = \frac{(k_3 + k_4)(k_{-1} + k_2)}{(k_2 + k_3 + k_4)k_1} \tag{22.12}$$

The apparent inactivation rate constant of the enzyme, k_{obs}, is described by

$$k_{obs} = \frac{k_{inact}[I]}{[I] + K_I} \tag{22.13}$$

The derivation of these equations is included in Appendix B to show the mathematical assumptions that must be made to allow such parameters to be defined experimentally.

The partition ratio (r) is a useful additional parameter to k_{inact} and K_I. It is defined as the number of moles of reactive metabolite escaping the enzyme without inactivating it (product) per number of moles of reactive metabolite inactivating the enzyme (trapped product) ($r = k_3/k_4$; Fig. 22.3). As the partition ratio approaches 0, inhibition is more efficient; for every cycle of the enzyme and substrate that results in product, a cycle also results in inactivated enzyme. For a potent inhibitor, the reactive species is less likely to escape the active site without adduct formation. While the partition ratio may be helpful in ranking compounds in order of inhibitory efficiency (as is the k_{inact}/K_I ratio), any use beyond this is limited.

22.3 ASSESSMENT OF CYTOCHROME P450 INHIBITION *IN VITRO*

Over the last decade there have been tremendous advances in the understanding of both the theoretical and technical aspects of generating *in vitro* kinetic data to engender predictions of DDIs [7, 11, 13, 21, 71, 79, 80]. The advantages of using *in vitro* assays to study inhibition include allowing inexpensive and rapid assessment of inhibition potential and consequent evaluation of DDI risk, facilitating detailed kinetic analysis of drugs known to cause DDIs in the clinic, and helping to further develop our understanding of these interactions and ultimately striving toward the avoidance of DDIs for NCEs. However, despite the undoubted usefulness of *in vitro* models, there are limitations, primarily due to the fact that, to date, there is no consensus toward a model that quantitatively predicts interactions in humans from *in vitro* data. Indeed, there is no single method for generating *in vitro* data. Despite the lack of consensus, there are some fundamentally common elements to the existing methodologies and these form the basis of the remainder of this chapter. Prior to modeling data, accurate *in vitro* assessments must be made. There are many parameters to consider when embarking on inhibition studies to generate good *in vitro* data, the key elements of which are discussed here.

22.3.1 Enzyme Systems

Historically, the majority of inhibition studies have been conducted using subcellular fractions of liver. Clear species differences exist in hepatic enzyme content and function [81]. In most cases a homolog of the human enzyme is present in the preclinical species. For example, CYP3A1 and CYP3A2 are the major 3A isoforms in the rat and share substrate crossover to human CYP3A4 and CYP3A5. Likewise CYP2C11 in rodent liver is homologous to CYP2C9 in humans. However, the species-specific isoforms of CYP1A, CYP2C, CYP2D, and CYP3A do show appreciable interspecies differences in terms of catalytic activity [81]. While laboratory

species can be a useful tool for investigating pharmacokinetic species differences and for providing confidence in IVIVE, clinical DDI potential must be investigated *in vitro* using human derived tissues and/or enzymes because of such species differences.

Human liver microsomes (HLMs) are prepared from liver homogenates by differential ultracentrifugation, first removing the cytosolic (S9) fraction, then with further ultracentrifugation collecting the subcellular fraction, which includes membrane-bound enzymes [82]. The utility of HLMs is clear; they can be isolated from a relatively small amount of human liver, can be stored almost indefinitely at –80 °C, contain functional CYPs (and other enzymes such as UDP-glucuronosyltransferases and flavin monooxygenases), and can be used as a single donor or pooled to provide a representation of enzyme expression in the population. However, due to the presence of multiple CYP isoforms with overlapping substrate selectivity, kinetic investigations must be thorough and carefully planned as inhibitors may be substrates for more than one CYP isoform. Consequently, for CYP inhibition studies using HLMs, the use of selective probe reactions is paramount and often relies on careful adjustment of substrate concentration to ensure selectivity.

In the last decade, the use of recombinant human CYP (rCYP) proteins, expressed in yeast, baculovirus-infected insect cells, or *Escherichia coli*, has become widespread and indeed now forms the backbone of screening efforts in the pharmaceutical industry. There are considerable advantages to using a single rCYP enzyme in an assay as it allows manipulation of substrates and inhibitors without the complications of enzyme selectivity. A notable example of this is CYP3A5, which has broad substrate crossover with CYP3A4, making it difficult to characterize reactions that are specific to or of equal affinity at CYP3A5 with respect to CYP3A4 [83]. A sometimes-perceived disadvantage of rCYP is the increased enzyme activity per unit of membrane protein compared to that of HLM. However, the high CYP expression levels give rise to low incubational protein content and low non-specific substrate and inhibitor binding, resulting in more accurate estimations of unbound K_{+1} values. Finally, the utility of rCYP in reaction phenotyping and inhibition studies has been well validated [84–86] and the versatility of rCYPs lends them to enhanced throughput screening.

Isolated human hepatocytes are an alternative *in vitro* tool and can be used to add refinement to data generated using subcellular fractions, as the impact of drug transporter activity on K_i, accounting for intracellular free drug concentrations, can be investigated. As whole cells, hepatocytes express not only all membrane-bound enzymes but also hepatic cytosolic enzymes; moreover, they contain the necessary cofactors. Under the correct conditions, human hepatocytes retain some functionality for many days, express the transcriptional machinery to regulate enzymes, and contain functional proteins for active drug transport across membranes [87]. The utility of hepatocytes for investigation of metabolic stability [88–90] and DDIs mediated by CYP induction [87, 91, 92] is well established. More recently, hepatocytes have been used to describe the impact of reversible [68, 93, 94] and time-dependent CYP inhibition *in vitro* [95, 96]. Primary hepatocytes in culture provide the closest *in vitro* model to human liver and may offer advantages when predicting clinical DDI. Metabolites of one pathway may lead to inhibition of another; this phenomenon is indiscernible using single rCYPs and exemplifies the usefulness of hepatocytes [97].

There is little published comparative data of inhibition constants generated in rCYPs and human hepatocytes. Data generated in this laboratory demonstrates $IC_{50,apparent}$ values generated in human hepatocytes, using probe substrates specific to the CYP isoform, were systematically higher than those determined using the respective rCYP [68]. This was predominantly the result of greater nonspecific binding in hepatocytes compared to rCYPs, as for the majority of compounds tested there was a good concordance between the respective $IC_{50,unbound}$ values (Fig. 22.4a).

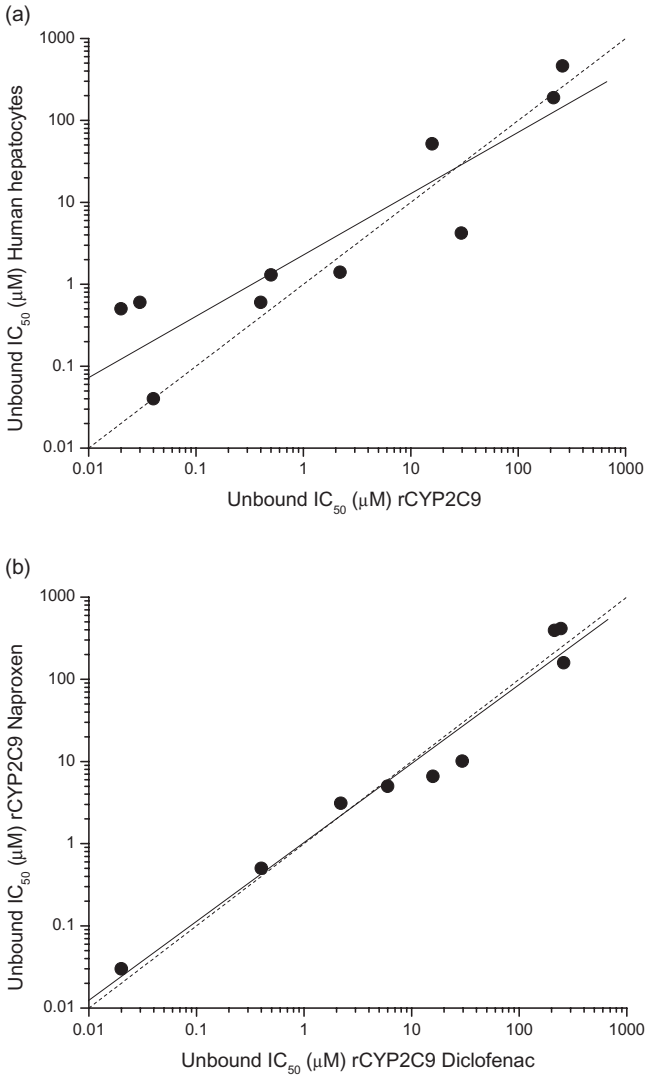

FIGURE 22.4 (a) Relationship between $IC_{50,unbound}$ for CYP2C9 in human hepatocytes and rCYPs. The dotted line is unity. The solid line indicates linear regression of the data ($r^2 = 0.88$, $p < 0.0001$) (b) $IC_{50,unbound}$ comparisons using naproxen and diclofenac as substrates for rCYP2C9. The dotted line is unity. The solid line indicates linear regression of the data ($r^2 = 0.77$, $p < 0.002$). (Part (b) from Ref. 68.)

It can be speculated that the impact of hepatic transporters may explain some discrepancies in $IC_{50,unbound}$ between rCYP and hepatocytes as compound can be actively effluxed from or taken up into the hepatocyte, altering the concentration of drug exposed to the enzyme [97]. Additionally, the impact of time-dependent CYP inhibition in primary cultures of human hepatocytes has been evaluated, again using a cocktail of CYP substrates, which allows the maximum amount of data to be extracted from this limited resource [95]. K_I and k_{inact} values were estimated from nonlinear regression analysis and compared with values obtained from rCYPs and HLMs (Table 22.2). The values generated are also comparable to several literature reports of K_I and k_{inact} estimates using rCYP and HLMs and the results from our laboratory using rCYP, HLMs, and human hepatocytes were consistent with these

TABLE 22.2 Kinetic Parameters of Time-Dependent Inhibitors in Different *In Vitro* Matrices

Compound	CYP Isoform	Enzyme Source	K_I (μM)	k_{inact} (min^{-1})	Reference
Tienilic acid	CYP2C9	rCYP2C9	2	0.19	95
		rCYP2C9 (2C10)	4	0.20	99
		Human hepatocytes	2	0.05	95
AZ1	CYP2C9	rCYP2C9	30	0.02	95
		Human hepatocytes	19	0.02	95
Fluoxetine	CYP2C19	rCYP2C19	0.4	0.5	95
		HLM	8[a] (0.8)	0.03	95
		Human hepatocytes	0.2	0.04	95
	CYP3A4	rCYP3A4	2	0.03	95
		HLM	5[a] (0.5)	0.01	95
		HLM	5[a]	0.02	100
		Human hepatocytes	1	0.01	95
Erythromycin	CYP3A4	rCYP3A4	9	0.12	98
		rCYP3A4	5	0.12	101
		HLM	16[a]	0.07	102
		HLM	82[a]	0.07	103
		HLM	13[a]	0.02	104
		HLM	10[a]	0.08	105
		HLM	11[a]	0.05	106
		HLM	15[a]	0.07	96
		Human hepatocytes	11	0.07	95
Troleandomycin	CYP3A4	rCYP3A4	0.3	0.12	98
		rCYP3A4	0.2	0.15	101
		HLMs	2[a]	0.03	96
		Human hepatocytes	0.4	0.05	95

[a]Apparent K_I values. All other values are *unbound* K_I estimates.

Source: From Ref. 95.

reports. Indeed, the CYP3A4-dependent K_I and k_{inact} values in human hepatocytes are comparable to values determined in rCYP3A4 and HLMs (Table 22.2) when corrected for nonspecific binding in the incubation.

Finally, an element of interlaboratory variability can be expected for different tissue preparations. However, an interlaboratory comparison found the rank order of five HLM preparations was conserved across five laboratories, all using different methodologies, despite differences in absolute values (based on protein content, CYP content, and activity) [107]. Irrespective of the enzyme system used, there are some common factors that must be considered for all *in vitro* inhibition incubations. The assay must be designed such that linear initial rate conditions for the reaction under investigation are assured. To make certain of this, preliminary experiments will be required to ensure product formation is linear with respect to both time and enzyme (protein) concentration [72]. Additionally, protein concentration should be kept as low as reasonably possible to reduce the impact of nonspecific binding [108]. As discussed with respect to hepatocytes and rCYPs, the fraction unbound in the incubation (f_{uinc}) can have a pronounced effect on the apparent K_i, K_I, and IC_{50} determined (Fig. 22.5). This is especially the case for lipophilic inhibitors such as ketoconazole, for which the apparent IC_{50} can vary between 0.005 and 0.3 μM [109]. It is important that such drug binding terms be incorporated by default when making IVIVE to improve the accuracy of *in vitro* data [88], and the importance of considering the fraction unbound in an *in vitro* incubation (f_{uinc}) when relating *in vitro* and *in vivo* data was proposed many years ago by Gillette (1963). The term itself can readily be determined and indeed predicted with accuracy from physiochemical properties [88, 110, 111]. Another important factor is the amount of solvent vehicle, which must be minimized ideally to 1% (or less) of the final incubation volume, as activation or inhibition of CYP activity can be manifest through solvent effects alone (Fig. 22.6). Acetonitrile appears the most favored solvent, having minimal inhibitory effects, despite it being able to activate CYP1A2; although DMSO is commonly used to ensure adequate NCE solubility, it can result in inhibition of metabolism, especially for basic CYP3A4 substrates [88, 112]. Solvent effects

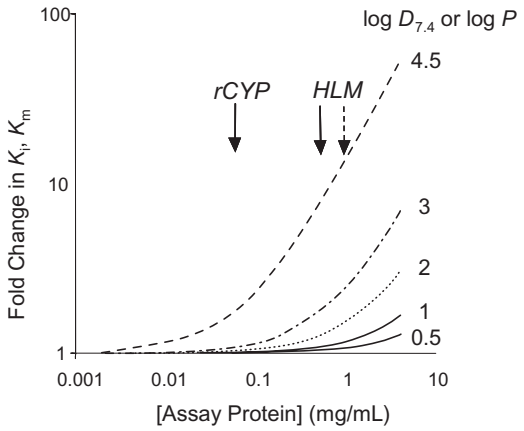

FIGURE 22.5 Simulated effects of microsomal or hepatocyte concentration on K_i or K_m as a function of log P or log $D_{7.4}$-dependent nonspecific binding. (From Ref. 88.)

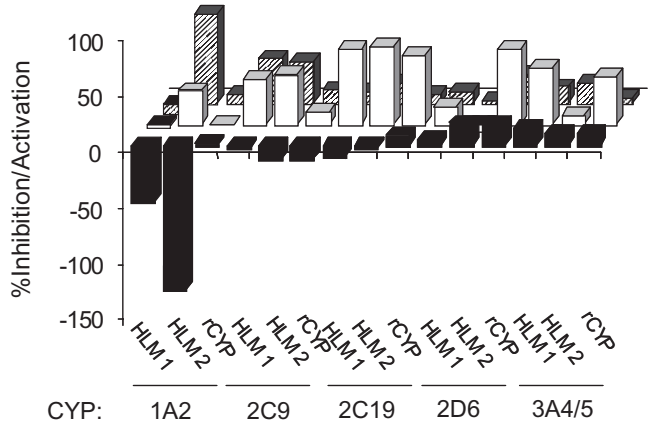

FIGURE 22.6 Overview of potential effects of commonly used organic solvents (1%, v/v) on CYP activities with recombinant proteins and HLMs (solid bars = acetonitrile, open bars = DMSO, hatched bars = methanol). (From Ref. 112.)

can also be selective for probe and enzyme source [113], so it is advisable to check the effects of an alternative solvent for key studies.

22.3.2 Probe Substrate Selection

An important component of *in vitro* inhibition study design is the selection of appropriate probe substrates. Nonselective probes in HLM or human hepatocyte assays can result in hybrid inhibition measurements where multiple enzymes (with varying sensitivity to the inhibitor) can contribute to the reaction under investigation [14]. To avoid such complications, a selective marker substrate is required for each CYP isoform being assessed. These probes should meet the following criteria: possess high affinity for the specific enzyme; be metabolized to a specific product metabolite; provide the ability to detect the product separately from the substrate (using the analytical system of choice); and, finally, the turnover of the probe substrate should be optimized in each enzyme system and be linear with respect to time resulting in less than 20% loss of parent compound to maintain constant reaction velocity throughout the experiment [106, 114]. Industry representatives and regulatory bodies have made recommendations for preferred probe substrates for each CYP isoform (Table 22.3), many of which have the additional benefit of being clinically relevant [117, 120]. These substrates have been rigorously validated for human CYPs [115] and the usefulness and caveats associated with them are well documented [14].

An advantage to the availability of highly selective probes is that, coupled with the improved analytical sensitivity afforded by advances in detection systems such as LC/MS-MS, a cassette of substrates can be used to evaluate the inhibitory potential of a compound upon multiple CYP isoforms in a single incubation. The usefulness of cassette assays derives from increasing the throughput of inhibition screening, although they do require careful optimization and validation to ensure selectivity is maintained [116, 118, 121].

TABLE 22.3 Specific Probe Substrate Reactions for Individual CYP Enzymes

CYP	Substrate	Reaction	Analytical Method	Comments[a]	References
CYP1A2	Phenacetin[b]	O-deethylation	LC/MS-MS	High specificity at <100 μM ($K_m \approx 50$ μM)	115, 116
	Ethoxyresorufin (EROD)	O-deethylation	Fluorescence	$K_m \approx 0.2$ μM; not clinically relevant	117
	Caffeine	N3-demethylation	UV-HPL	Low affinity $K_m \approx 600$ μM	117
CYP2A6	Coumarin	7-Hydroxylation	LC/MS-MS Fluorescence	High specificity $K_m \approx 0.5$ μM	115, 117
CYP2B6	Bupropion[b]	Hydroxylation	LC/MS-MS	High specificity $K_m \approx 90$ μM	115, 118
	S-Mephenytoin	N-demethylation	LC/MS-MS	Not CYP2B6 specific $K_m \approx 2000$ μM (CYP2C9 high affinity $K_m \approx 150$ μM)	14
CYP2C8	Amodiaquine[b]	N-deethylation	LC/MS-MS	High specificity $K_m \approx 2$ μM	115, 118
CYP2C9	Diclofenac[b]	4′-Hydroxylation	LC/MS-MS	Good specificity $K_m \approx 2$ μM (some CYP2C19 $K_m \approx 80$ μM)	115, 116
	Tolbutamide	Hydroxylation	LC/MS-MS Radiometric	$K_m \approx 200$ μM (some CYP2C19 $K_m \approx 500$ μM)	115, 119
CYP2C19	*S*-Mephenytoin[b]	4′-Hydroxylation	LC/MS-MS	High specificity $K_m \approx 40$ μM	115, 116
CYP2D6	Bufuralol[b]	1-Hydroxylation	LC/MS-MS	High affinity component for CYP2D6 $K_m \approx 5$ μM (CYP2C19 and CYP2C9 at high concentrations)	116
	Dextromethorphan	O-demethylation	LC/MS-MS		115
CYP2E1	Chlorzoxazone	7-Hydroxylation	LC/MS-MS	Questionable specificity $K_m \approx 700$ μM	115, 117
CYP3A4	Midazolam[b]	1′-Hydroxylation	LC/MS-MS	High specificity benzodiazepine $K_m \approx 3$ μM	56, 115, 116
	Testosterone	6β-Hydroxylation	UV-HPLC Radiometric	High specificity steroid $K_m \approx 50$ μM	56, 115, 117
	Nifedipine	Oxidations	UV-HPLC	High specificity dihydropyridine $K_m \approx 50$ μM	87

[a]Comments from Ref. 14.

[b]Primary Substrate used in this laboratory.

An additional aspect to be considered for *in vitro* assays is that CYP inhibition can be substrate dependent, particularly for CYP3A4 [122]. CYP3A4 is thought to bind substrates and inhibitors in multiple modes and/or binding sites [66, 123]. As a result, inhibitory interactions observed with one probe substrate may not be representative of those observed with other substrates [19]. This is due to the cooperative nature of substrate–inhibitor interactions within the active site [124]. Kenworthy et al. [122] classified 10 CYP3A4 substrates into three distinct groups: a benzodiazepine group (including diazepam, midazolam, triazolam, and dextromethorphan), a large molecular weight group (including testosterone, erythromycin, and cyclosporine), and finally nifedipine and benzyloxyresorufin (BROD), which fit in neither of the previous groups and are distinct from each other. These substrate groups were classified according to analysis of their behavior as probe reactions for the effect of 34 compounds on CYP3A4 mediated metabolism, with different inhibitor profiles being observed with different substrate groups. For example, the IC_{50} for inhibition of CYP3A4 mediated nifedipine oxidation by haloperidol was 0.1 μM, while for dextromethorphan N-demethylation it was >100 μM [122]. It is postulated that haloperidol is able to inhibit CYP3A4 by binding at more than one site, with the effect being dependent on the substrate, reflecting the cooperative nature of CYP3A4.

There is also increasing evidence that similar multisite kinetics and substrate-dependent interactions are observed for CYP2C9 *in vitro* [67–69]. Therefore, while there is little evidence of auto-/heteroactivation *in vivo* in humans [69, 70, 125], it is good practice to evaluate the inhibitory potential of NCEs against CYP3A4 and CYP2C9 using at least two structurally dissimilar probe substrates, to afford a better predictive quality to the *in vitro* data as *in vivo* effects can be substrate dependent. In our laboratory, routine screens are conducted with drug-like probes for both CYP3A4 (midazolam) and CYP2C9 (diclofenac); for key compounds, a second and potentially a third probe is used to fully evaluate inhibition of these isoforms, for example, erythromycin and naproxen for CYP3A4 and CYP2C9, respectively. Figure 22.4b shows the effect of using either diclofenac or naproxen as probe substrate to measure the IC_{50} for a range of compounds demonstrating CYP2C9 inhibition. On average, it was found that the $IC_{50,apparent}$ generated in an assay using naproxen as a substrate could be approximately 1.5-fold times that using diclofenac. This could be corrected from a consideration of $IC_{50,unbound}$ [68] (see Fig. 22.4b).

22.3.3 Analysis Methods

Several analytical methods are available for determining the impact of inhibition on a probe substrate. The selection of an analytical endpoint depends on the probe under investigation, the availability of the detection system, and the throughput required. LC/MS-MS is probably the system of choice for the pharmaceutical industry due to the selectivity and sensitivity it affords [115, 126]. This, combined with the fact that LC/MS-MS is the backbone of analysis within DMPK laboratories and therefore readily available, has driven its increased use in CYP inhibition assays. There are several LC/MS-MS methods that enable routine analysis of metabolites generated in microsomal and rCYP incubations, and importantly LC/MS-MS facilitates the use of clinically relevant probes. Additionally, the sensitivity afforded by LC/MS-MS has allowed multiple reaction monitoring of substrate cassettes, facilitating the investigation of test inhibitors for multiple CYP isoforms [20, 116, 121]. In

our laboratory we routinely screen for CYP inhibition using a substrate cassette and a rCYP cocktail; the details of this and other assays used are shown in Table 22.4.

An alternative to LC/MS-MS is HPLC-radioflow. This allows separation of metabolites of ^{14}C or ^{3}H labeled probe substrates. It is, however, a time-consuming technique requiring meticulous optimization of conditions and long run times, and LC/MS-MS is a more rapid alternative [115, 116, 118, 126]. A higher throughput radiometric endpoint assay is available and is flexible, sensitive, robust, and free from analytical interference [119, 127]. This laboratory uses a range of automated assays with [*O*- or *N*-methyl-^{14}C]-substrates, which liberate [^{14}C]-formaldehyde as the product of enzyme-specific oxidative demethylation [119]. However, the extra considerations involved with the use of radioactivity, such as the highly regulated disposal of isotopes and additional safety requirements, does constrain their use perhaps to second substrate selection.

Fluorometric assays are commonly used for CYP inhibition studies, especially in early drug discovery, as their speed and cost advantages lend them to enhanced throughput (compared to detailed manual assays) or true HTS (miniaturized assays employing robotics to utilize 96-, 384-, or 1536-well plate formats with rapid endpoints). Indeed, they are widely used throughout the pharmaceutical industry. Fluorescent-based assays are very amenable to multiwell plate assays; but despite their utility in rapidly generating large sets of inhibition data there are drawbacks. There can be fluorescent interference from the test compound or its product and issues with fluorescent quenching as well as lack of probe molecule specificity for an individual CYP [20]. The nonselective nature of fluorescent probes can, of course, be overcome by the use of single rCYPs. A potential concern for these assays is the non-drug-like qualities of most fluorescent probes, particularly in terms of clinically relevant CYP interactions. A detailed study evaluating inhibition data generated using fluorescent probes compared to that of conventional drug probes suggested that in general only a weak correlation between the two endpoints existed, with both endpoints not detecting inhibition by a significant number of compounds [19, 88]. Cohen et al. [19] suggest that concerns over fluorogenic probes not resembling drug molecules are unfounded and that it is the architecture of the CYP active site, permitting binding of structurally diverse molecules, that underlies interprobe differences in IC_{50} values, be they fluorescent or not. In our laboratory, fluorometric assays have been widely replaced by LC/MS-MS-based assays but are still used as an alternative substrate assay to cross-check inhibition data for CYP3A4 and CYP2C9, as it is prudent to assess inhibition in detailed studies using multiple probes and alternative endpoints as least for these enzymes.

Finally, luminescence-based CYP selective probes have recently become commercially available, such as those used in the Promega P450-Glo™ assays. These assays provide a luminescent method for measuring CYP activity from recombinant and native sources. A conventional CYP reaction is performed by incubating the CYP with a luminogenic CYP substrate and NADPH regeneration system. The substrates in the P450-Glo assays are derivatives of beetle luciferin ((4*S*)-4,5-dihydro-2-(6-hydroxybenzothiazolyl)-4-thiazolecarboxylic acid) and are substrates for CYP but not luciferase. The derivatives are converted by CYP to a luciferin product that is detected in a second reaction with a luciferin detection reagent. The amount of light produced in the second reaction is directly proportional to the activity of the CYP (http://www.promega.com). Such assays lend themselves to true

TABLE 22.4 Assay Conditions Used for IC_{50} Generation in the Authors' Laboratory Utilizing Fluorescent or Radiometric Endpoints and a Single rCYP Isoform and LC/MS-MS Endpoint with a Cocktail of rCYPs and Cassette of Substrates[a]

Isoform	Substrate	Final [Substrate] (μM)	[CYP] (pmol/mL)	Incubation Time (min)	Endpoint	Vehicle (1% v/v)	Inhibitor (IC_{50}; μM)
CYP1A2	Ethoxyresorufin	0.7	17	15	λ_{ex} 530 nm; λ_{em} 590 nm	DMSO	Fluvoxamine (0.17)
CYP2C9	7-Methoxy-4-(trifluoromethyl) coumarin	50	50	20	λ_{ex} 410 nm; λ_{em} 535 nm	DMSO	Sulfaphenazole (0.3)
CYP2C19	7-Methoxy-4-(trifluoromethyl) coumarin	50	57	20	λ_{ex} 405 nm; λ_{em} 535 nm	MeCN	Omeprazole (3)
CYP2D6	3-[2-(*N*,*N*-diethyl-*N*-methylammonium)ethyl]-7-methoxy-4-methlycoumarin	10	56	15	λ_{ex} 530 nm; λ_{em} 590 nm	DMSO	Quinidine (0.060)
CYP3A4	7-Benzyloxy-4-(trifluoromethyl) coumarin	10	9	15	λ_{ex} 405 nm; λ_{em} 535 nm	MeOH /MeCN	Ketoconazole (0.007)
CYP2C9	Naproxen	109	70	15	Liquid scintillation counting	DMSO	Sufaphenazole (0.45)
CYP2C19	Diazepam	21	40	15	Liquid scintillation counting	DMSO	Omeprazole (3)
CYP2D6	Dextromethorphan	5	20	15	Liquid scintillation counting	DMSO	Quinidine (0.025)
CYP3A4	Erythromycin	19	25	10	Liquid scintillation counting	DMSO	Ketoconazole (0.035)
5 CYP cocktail	1A2–Phenacetin	26	15				α-Naphthoflavone(0.014)
	2C9–Diclofenac	2	5				Sulfaphenazole (0.26)
	2C19–S-mephenytoin	31	3	10	LC/MS-MS	DMSO	Tranylcypromine (3.60)
	2D6–Bufurolol	9	5				Quinidine (0.018)
	3A4–Midazolam	3	5				Ketoconazole (0.0036)
			Total 33				
3 CYP cocktail	2B6–Bupropion	20	18				Ticlopidine (0.55)
	2C8–Amodiaquine	2	1	10	LC/MS-MS	DMSO	Quercetin (5.12)
	3A5–Midazolam	2	5				Ketoconazole (0.17)
			Total 24				

[a]See Refs. 116, 118, and 119. Data is mean $n > 50$.

TABLE 22.5 Some Considerations in the Selection of CYP Assay Endpoints

	Assay Type			
Consideration	Radiolabeled	Fluorescent	LC/MS-MS	Luminescent
Cost	++	+++	+	++
Throughput	+	+++	++	HTS
Accessibility	++	++	+	++
Interference	+++	+	++	+
Health and safety	+	+++	+++	+++
Published information	++	+++	+++	+
Marketed drug substrates	++	—	+++	—

HTS capabilities, providing quick readouts on multiple well plates. Table 22.5 shows a comparison of LC/MS-MS, fluorometric, radiometric, and luminescent endpoints to aid consideration of assay choice.

Using fluorescent or luminescent assays for enhanced/HTS and rapid generation of IC_{50} data may be invaluable for the development of structure–activity relationships (SARs) for the different CYPs [69, 128]. The utility of high throughput CYP inhibition screens has allowed generation of large datasets, facilitating development of statistical *in silico* approaches. To this end, quantitative *in silico* models now exist for prominent CYPs, often based on physical-chemical properties alone. These models can classify compounds as "noninhibitors" with reasonable accuracy (~80% of compounds were classified correctly for CYP3A4 and CYP2D6 [128]) and can guide medicinal chemistry away from CYP interactions at early stages of drug discovery programs [128, 129]. In theory, these *in silico* models allow predictions of inhibitory potency to be made even before a compound has been synthesized [129].

22.4 GENERATION OF *IN VITRO* CYTOCHROME P450 INHIBITION DATA

Fundamentally, *in vitro* kinetic data must be accurate, meaningful, and relevant. As discussed previously, all assays should be preoptimized for time and protein linearity to ensure the reaction proceeds under linear conditions. The objective is to determine K_i for predicting the likelihood and extent of DDIs. Experimentally, this is achieved by either defining the IC_{50} or by directly determining a K_i. From Eqs. 22.4 and 22.7, it is clear that if $[S] = K_m$, the K_i can be estimated to within twofold from an accurate IC_{50} determination. This may well be less than the error in determining K_i by an extensive (and laborious) fully inhibited Michaelis–Menten study. Furthermore, the mechanism of inhibition must be defined and, if irreversible, generation of K_I and k_{inact} is required for accurate assessment of DDIs.

When generating *in vitro* inhibition data, particularly when evaluating the propensity of NCEs to behave as CYP inhibitors, it is important to include the appropriate positive controls. To this end, known inhibitors should be included in any incubations as markers, and it has been suggested that K_i or IC_{50} values generated

for these standard inhibitors should fall within threefold of the median literature value for an assay to be deemed acceptable [130].

22.4.1 Reversible Inhibition (IC_{50} and K_i)

An IC_{50} is generated using a single concentration of substrate. Inhibitor concentrations should cover at least two log units (e.g., 0, 0.1, 0.3, 1, 3, 10 μM) to ensure a range of measurements from negligible to virtually complete inhibition. The percentage of total enzyme activity remaining (from control incubations) is plotted against log inhibitor concentration [I] to generate an IC_{50} curve. Plotting log [I] results in more accurate confidence intervals when using nonlinear regression, as the data is equally spaced on a log axis, allowing symmetrical confidence intervals to be calculated. In the authors' laboratory, an automated assay to determine IC_{50} is adopted; K_i is estimated to be half the IC_{50} (as [S] = K_m). The automated assay utilizes a pool of recombinant CYPs (CYP1A2, CYP2C9, CYP2C19, CYP2D6, and CYP3A4) to minimize nonspecific binding in the incubation, at protein concentrations and incubation times designed to ensure the selective metabolism of a substrate cassette at concentrations equivalent to the K_m (phenacetin, diclofenac, *S*-mephenytoin, bufuralol, and midazolam, respectively). LC/MS-MS analysis of specific metabolite formation allows comparison of peak area in the presence of increasing concentration of test inhibitor against a DMSO control. Recently, an additional assay was developed for CYP2B6, CYP2C8, and CYP3A5 due to the emerging importance of these enzymes [118]. This second automated assay again uses a pool of rCYPs and a substrate cassette of bupropion, amodiaquine, and midazolam, respectively. Table 22.4 shows the reaction conditions for these assays.

An alternative approach is to experimentally define the inhibition constant K_i. To do this accurately, the inhibitor concentration should span a range around the suspected K_i (based on a prior IC_{50} estimation) using at least five concentrations, for example, $0K_i$, $0.3K_i$, K_i, $3K_i$, and $10K_i$. Typically, 8–10 substrate concentrations should be used to investigate each concentration of inhibitor and these should span from $K_m/3$ to $3K_m$. The range of substrate concentration needs to be expanded for increased inhibitor concentrations, since the K_m shifts up when the substrate's metabolism is competitively inhibited. K_i determinations therefore require large numbers of incubations, as all parts of the velocity–substrate concentration profile need to be defined for each inhibitor concentration. Accurate determinations of any one of the parameters (K_m, V_{max}, K_i) depends on accurate determination of all three.

Once generated, the data can be visually inspected for the mechanism of inhibition; this is commonly achieved using two types of graphical representation—the Eadie–Hofstee plot (v against v/[S]) and the Dixon plot (1/v against [I]). The type of inhibition can be determined from the shape of the linearized data and examples of these plots for each type of reversible inhibition are shown in Fig. 22.7. Kinetic parameters should never be determined from linear transforms such as these as doing so generally leads to inaccurate estimation of K_i (the two-dimensional nature of the data fit does not fully describe the effect of changing inhibitor concentrations on different concentrations of substrate). The plots are solely for the purpose of aiding interpretation of the inhibition type. Consequently, nonlinear regression software is an absolute requirement to facilitate iterative modeling of changing sub-

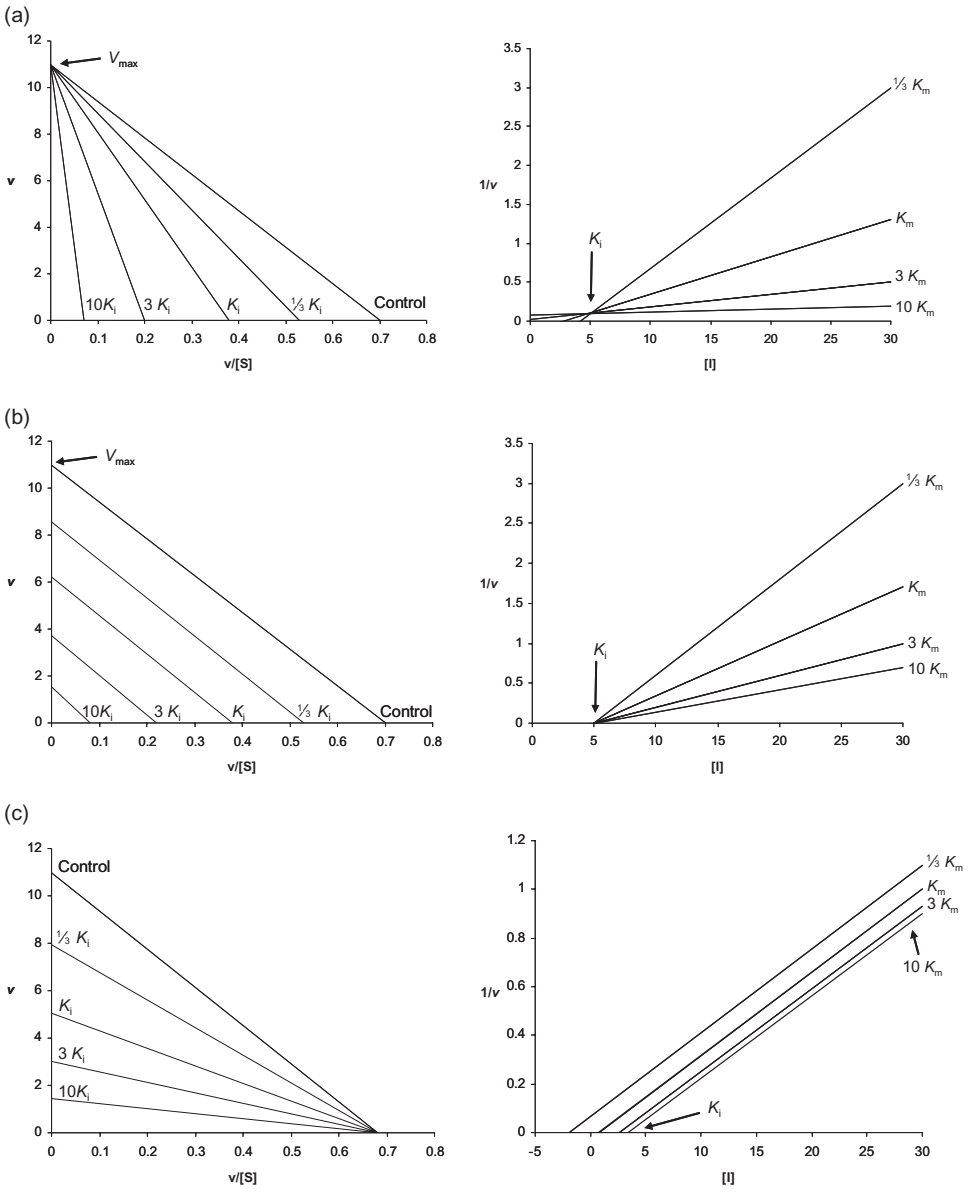

FIGURE 22.7 Graphical representation of inhibition plots: Eadie–Hofstee plots (v against v/[S] on the left) and Dixon plots (1/v against [I] on the right) for (a) competitive inhibition, (b) noncompetitive inhibition, (c) and uncompetitive inhibition.

strate and inhibitor concentrations, fitting the untransformed data to the appropriate rate equation (for competitive, noncompetitive, or uncompetitive inhibition, Eqs. 22.3, 22.5, and 22.6, respectively). In practice, this means nonlinear regression modeling of all the substrate concentration, velocity, and inhibitor concentration data simultaneously using the equation for competitive inhibition (Eq. 22.3). The data

should be weighted by $1/y$, to compensate for unequal experimental variance in the different experimental points. (Velocity–substrate concentration plots tend to have a constant relative error associated such that the residual—the difference between predicted and observed velocity—will be larger at higher reaction velocities. This is true because the error is the same at low and high velocities, giving rise to larger standard deviations from the mean observed velocity at higher velocities.) The same dataset should then be reanalyzed using the equation for noncompetitive inhibition (Eq. 22.5). The two mathematical models can then be discriminated by evaluation of "goodness-of-fit" criteria. For a full explanation, see Mannervik [131]. Generally, goodness-of-fit criteria (e.g., Akaike values) and accuracy of parameter estimates (standard deviation and coefficient of variance) should be compared for both models and the most appropriate model (type of inhibition) chosen.

22.4.2 Mechanism-Based Inhibition (K_I, k_{inact}, and IC_{50})

True irreversible inhibition or mechanism-based inhibition (MBI) of CYPs can only be defined according to the criteria detailed previously and may be established by mechanistic studies such as dialysis of the inhibited CYP or spectral shifts in absorbance [100]. MBI is not readily detected in standard *in vitro* assay formats. Time-dependent inhibition (TDI) is a collective term for a change in potency of CYP inhibitors during an *in vitro* incubation or dosing period *in vivo*. Such changes usually result in an increase in inhibitory potency; potential mechanisms include the formation of more inhibitory metabolites and MBI. In the following assays, it is the time-, concentration-, and/or NADPH-dependent nature of the inhibition under investigation.

In essence, an assay to detect TDI involves a preincubation step, where enzyme is incubated with and without NADPH and in the presence of varying inhibitor concentrations. This reaction is allowed to proceed over a predetermined time course, before dilution of the reaction mixture into a second incubation that includes a probe substrate to assess the degree of enzyme inactivation [77]. To accurately define the inhibitory constants of TDI, the conditions governing the two separate incubations must be carefully chosen. A useful critical evaluation of experimental design, methodology, and data analysis for TDI protocols in published literature highlighted not only the variation between laboratories but the subsequent impact on the predicted effects of TDI *in vivo* if the *in vitro* kinetic parameters are incorrectly defined [79].

The experimental design of a TDI assay must adhere to the same conditions as those for reversible inhibition (linear enzyme reactions, etc.) and protocols have to be adjusted to correctly define the kinetics of different inhibitors. These adjustments are dependent on the potency of the inhibitor under investigation, as potent inhibitors require considerably shorter preincubation times than weaker inhibitors [75, 79]. To this end, the time course of the pre-incubation must be such that the inhibition at each concentration of inhibitor is linear with respect to time—at least over the initial preincubation period. Allowing the preincubation reaction to proceed over a large time course with multiple dilution points into the second assay (0, 0.5, 1, 2, 3, 5, 10, 20, and 30 min) should gauge this; however, this is not necessarily practical due to the large reaction volume required in the preincubation to sustain multiple dilution points. In practice, two separate assays may have to be conducted: an

initial assessment where preincubation occurs over an intermediate time course (such as 5, 10, and 20 min), and a second assay where times are adjusted for more accurate definition of the inhibition profile (based on inspection of the data generated in the initial assessment). In addition to this, it is vital to ensure all the CYP inactivation occurs in this preincubation, to allow accurate measurement of inhibited enzyme with respect to incubation time, without concurrent inhibition and probe substrate metabolism in the second incubation. To this end, the dilution of the preincubation reaction mixture into the second incubation should be as large as possible (in general, 10–50-fold) while still guaranteeing analytical sensitivity for the probe substrate metabolite. Additionally, the concentration of CYP selective substrate in the final incubation should be high relative to its K_m (in general, 5–10-fold), again to minimize further CYP inactivation after the preincubation step, and the final incubation time should be minimized. Finally, since the enzyme can undergo some inactivation in the absence of inhibitor, the enzyme activity remaining following each preincubation time point should be determined by comparison to control (enzyme incubated without inhibitor). In the authors' laboratory, two automated assays with an LC/MS-MS endpoint are used to assess TDI potential [98] and have been modified to allow detection of weaker time-dependent inhibitors [75]. An initial screen generates an IC_{50} value using HLMs and a cassette of CYP specific probe substrates. A single inhibitor concentration is tested using a single preincubation time of 30 min and a 20-fold dilution. If inhibition is detected in this IC_{50} assay, a second assay is then used to generate values for K_I and k_{inact} from rCYPs. This assay adheres to the strict criteria detailed earlier in order to accurately define the kinetic parameters. Five preincubation times (up to 23 min) are used with six inhibitor concentrations and a dilution factor of 20-fold. There is a good correlation between k_{inact}/K_I ratio (a measure of inhibitory efficiency) generated in rCYP and the IC_{50} from the HLM assay, thus allowing NCE evaluation from a reasonable throughput assay [98] (see Fig. 22.8).

The analysis of data generated in TDI assays must be carefully conducted. First, the natural log of the percent control activity remaining is plotted against time. The slope of the linear portion for each inhibitor concentration is equivalent to the inactivation rate constant, k (or k_{obs}). Graphical representations of these plots are shown in Fig. 22.9. Using nonlinear regression, this data can be fitted to Eq. 22.13 to estimate k_{inact} and K_I. A common fault is to use linear Kitz–Wilson plots rather than nonlinear regression, as two-dimensional fitting of the data cannot yield accurate estimations for k_{inact} and K_I. [79]. It is also worth noting that if all the CYP inactivation occurs in the preincubation step, the point where the log-linear fits of each inhibitor concentration cross the y axis (time = 0) represents the reversible inhibition component. However, if the dilution of the preincubation is not sufficient, considerable reversible inhibition may occur during the second incubation, making data interpretation more problematic [98].

Finally, an additional utility of a TDI screen in drug discovery may be as a "flag" for reactive metabolite formation. Electrophilic species are often generated during CYP MBI and there is a high chance that these may escape from the CYP active site and react elsewhere in the body, either via detoxification processes (glutathione deactivation) or more worryingly via reaction with proteins or nucleic acids. It is not at all surprising that the same chemical groups implicated in reactive metabolite formation are also known to inhibit CYPs irreversibly [75]. Perhaps linked to this,

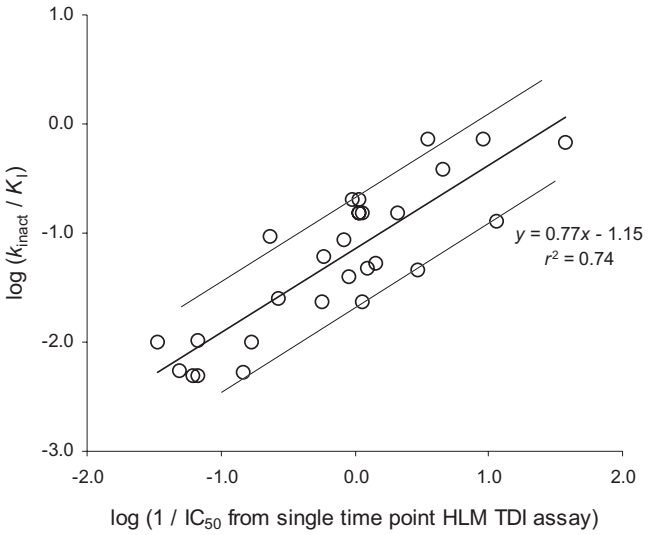

FIGURE 22.8 Plot of log unbound IC_{50} against log (k_{inact}/K_I) for 28 time-dependent inhibitors of CYP3A4. IC_{50} values were generated using the automated single time point, single inhibitor concentration human liver microsomal time-dependent inhibition screen [98]. These values were adjusted for incubational binding to give unbound IC_{50} values (according to the mathematical model of Austin et al. [111]). K_I and k_{inact} were estimated using the 3 time point, 6 inhibitor concentration, recombinant CYP automated time-dependent inhibition assay. The solid line is the line of best fit, with dashed lines representing threefold deviation from the line. (From Ref. 98.)

it is found that many drugs exhibiting TDI are also associated with adverse drug reactions (e.g., erythromycin, diclofenac, tacrine, valproic acid, halothane, suprofen, ticlopidine, tienilic acid, isoniazid, zileuton) [132, 133]. Using TDI screening, alongside cold trapping and/or radiolabeled binding studies, may be advantageous in minimizing the potential for reactive metabolite formation as early as possible in a drug discovery screening cascade.

22.5 *IN VITRO–IN VIVO* EXTRAPOLATION OF CYTOCHROME P450 BASED DRUG–DRUG INTERACTIONS

The clinical implications of DDIs and the importance of generating accurate *in vitro* data have been discussed; from this it follows that IVIVE requires careful data handling using the approach outlined below to generate predictions of clinical impact. Over the last 10–15 years, predicting the extent of DDI in a semiquantitative way has been the subject of many publications and the most effective models are presented here.

22.5.1 Approach for Reversible Inhibitors

If the metabolism of a drug is reversibly inhibited, the magnitude of the effect will be $1 + [I]/K_i$ (sometimes termed the inhibition index, I_i), provided that the concen-

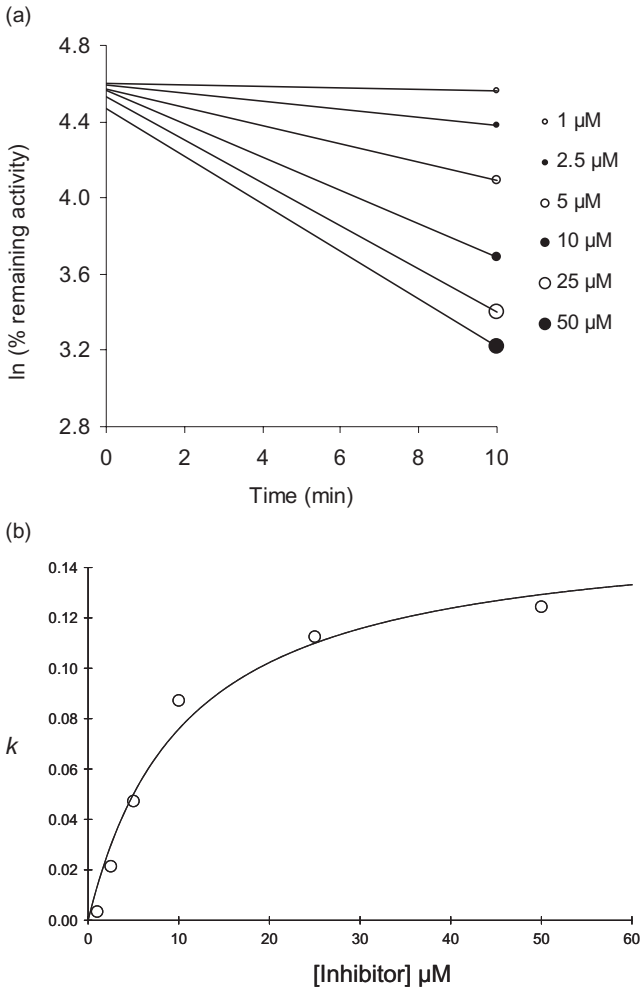

FIGURE 22.9 Graphical representation of irreversible (time-dependent) inhibition. (a) Inhibition of control activity against time for increasing inhibitor concentration; and (b) nonlinear regression of k against inhibitor concentration giving k_{inact} of 0.16 min^{-1} and K_I of 10.6 μM (circles are observed data points and line is predicted data fit).

tration of substrate undergoing inhibition is well below its K_m value and that it is eliminated by the single pathway being inhibited [134]. This is because the magnitude of effect is dependent not only on how much affinity the inhibitor has for the enzyme (K_i) but also on the concentration of inhibitor available. For competitive inhibition, the K_m of the victim drug will be increased to $K_m + K_m\,[I]/K_i$ (or $K_m(1 + [I]/K_i)$) and therefore the intrinsic clearance (CL_{int}) (as $CL_{int} = V_{max}/K_m$) will be decreased to $V_{max}/(K_m(1 + [I]/K_i)$ or $CL_{int}/(1 + [I]/K_i)$.

For an IV administered victim drug, the following is true:

$$CL = \text{Dose}/AUC \tag{22.14}$$

$$CL/CL' = AUC'/AUC \tag{22.15}$$

where CL is the *in vivo* clearance in the absence and CL' in the presence of inhibitor, respectively, and AUC is area under the plasma–concentration time curve in the absence and AUC' in the presence of inhibitor′, respectively.

$$\frac{AUC'}{AUC} = \frac{Q_h \cdot CL_{int} \cdot f_{ub}}{Q_h + CL_{int} \cdot f_{ub}} \cdot \frac{Q_h + CL'_{int} \cdot f_{ub} \cdot 1/I_i}{Q_h \cdot CL'_{int} \cdot f_{ub} \cdot I_i} \tag{22.16}$$

$$= \frac{Q_h^2 \cdot CL_{int} \cdot f_{ub} + Q_h^2 \cdot CL_{int} \cdot f_{ub} \cdot 1/I_i \cdot CL_{int} \cdot f_{ub}}{Q_h^2 \cdot f_{ub} \cdot CL_{int} \cdot 1/I_i + Q_h^2 \cdot f_{ub} \cdot CL_{int} \cdot f_{ub} \cdot CL_{int} \cdot 1/I_i} \tag{22.17}$$

$$= \frac{Q_h + (f_{ub} \cdot CL_{int})/I_i}{Q_h/I_i + (f_{ub} \cdot CL_{int})/I_i} \tag{22.18}$$

$$\frac{AUC'}{AUC} = \frac{Q_h \cdot I_i + f_{ub} \cdot CL_{int}}{Q_h + f_{ub} \cdot CL_{int}} \tag{22.19}$$

where Q_h is hepatic blood flow and I_i is the inhibition index $1 + [I]/K_i$. If $f_{ub} \cdot CL_{int} << Q_h$, there is a high inhibitory effect and the AUC ratio approximates to I_i $(1 + [I]/K_i)$. If $f_{ub} \cdot CL_{int} >> Q_h$, there is little effect since the AUC ratio approximates to 1.

For an orally administered victim drug, the fraction escaping hepatic first-pass extraction in the presence (F') or absence (F) of inhibitor is

$$\frac{F'}{F} = \frac{1 - CL'_h/Q_h}{1 - CL_h/Q_h} \tag{22.20}$$

Rearranging the well stirred model [135],

$$CL_{int} = \frac{CL_h}{f_{ub}(1 - CL_h/Q_h)} \tag{22.21}$$

$$= \frac{CL_h}{F \cdot f_{ub}} \tag{22.22}$$

It follows that

$$F = \frac{CL_h}{CL_{int} \cdot f_{ub}} \tag{22.23}$$

Therefore,

$$F = \frac{CL_{int} \cdot f_{ub} \cdot Q_h}{CL_{int} \cdot f_{ub} + Q_h} \cdot \frac{1}{CL_{int} \cdot f_{ub}} \tag{22.24}$$

$$= \frac{Q_h}{CL_{int} \cdot f_{ub} + Q_h} \tag{22.25}$$

Putting this back into Eq. 22.20, we find

$$\frac{F'}{F} = \frac{Q_h}{CL_{int} \cdot f_{ub}/I_i + Q_h} \cdot \frac{CL_{int} \cdot f_{ub} + Q_h}{Q_h} \tag{22.26}$$

$$\frac{F'}{F} = \frac{CL_{int} \cdot f_{ub} + Q_h}{(CL_{int} \cdot f_{ub}/I_i) + Q_h} \tag{22.27}$$

So, when $f_{ub} \cdot CL_{int} << Q_h$, there is little inhibitor effect since the ratio of the fraction escaping first pass is approximately 1. When $f_{ub} \cdot CL_{int} >> Q_h$, the ratio of the fraction escaping first pass in the presence and absence of inhibitor approximates to $1 + [I]/K_i$.

It is recognized as a "rule of thumb" that inhibitors with $[I]/K_i < 0.1$ represent a low DDI risk, those with $[I]/K_i$ between 0.1 and 1 are moderate risk, and those with $[I]/K_i > 1$ are high risk. The relationship between the *AUC* ratio and $[I]/K_i$ ratio is depicted in Fig. 22.10 and is the most simple model of CYP inhibition [80, 130, 136, 137]. A more detailed approach, that is, the fundamental basis of most IVIVE for CYP inhibition, expands on the inhibition index $(1 + [I]/K_i)$ by including the relative metabolic contribution (*fm*) of each inhibited CYP to the *in vivo* metabolism of the substrate under investigation:

$$\frac{AUC'}{AUC} = \frac{1}{\frac{fm_{CYP}}{1+[I]/K_i} + (1 - fm_{CYP})} \tag{22.28}$$

The impact of *fm* on the magnitude of inhibition can be visualized in Fig. 22.11 [56, 68, 138]. From this plot it is clear that $fm > 0.5$ is required for inhibition to generate significant increases in *AUC* and that predictions are very sensitive to the *fm* used when it approaches 1. Within a population, *fm* will vary and individuals most at risk

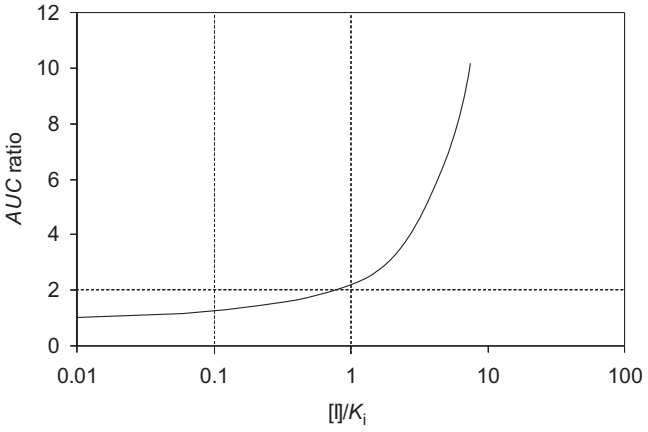

FIGURE 22.10 Qualitative zoning of the prediction of the magnitude and risk of drug–drug interactions mediated by reversible inhibition (*AUC* ratio) using $[I]/K_i$ ratio. Low risk, <0.1; medium risk, 0.1–1; high risk, >1.

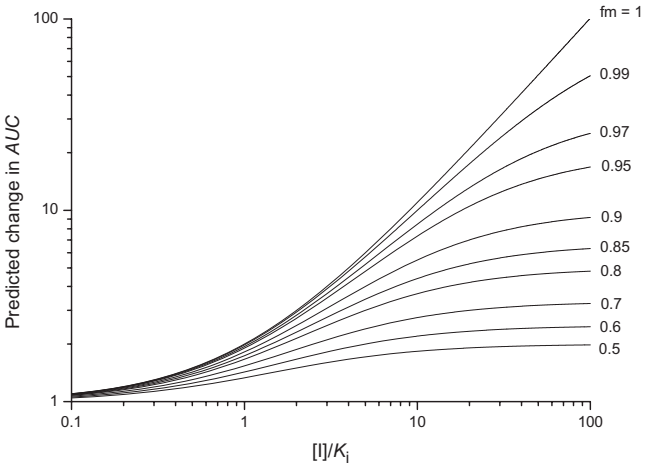

FIGURE 22.11 Simulation of predicted change in *AUC* as a function of $[I]/K_i$ with different *fm* values. The simulation is based on Eq. 22.28, where *fm* is the fraction of substrate clearance mediated by the inhibited metabolic pathway. (Adapted from Ref. 98.)

of DDI will be those with the highest *fm*. The model can be expanded further to include inhibition of multiple CYP isoforms and the effect of each contribution to overall clearance of the victim drug and other routes of elimination need to be considered [136, 138].

The choice of which [I] to use in these predictions has been a source of much debate in the literature [7, 13, 80, 88, 139, 140]. Classical pharmacology states that only the unbound fraction of a drug is able to cross membranes and interact with a target protein; from this it follows that a drug associated with proteins in the plasma or tissue is unavailable for interaction. It follows that the use of unbound drug concentrations and inhibition constants should be the starting point in IVIVE and doing so can give good predictions when other relevant factors are included [88]. Changes in the unbound fraction of a drug in the blood (f_{ub}) is in itself a potential mechanism of DDI; f_{ub} is increased when one drug is displaced by other drugs at the site of plasma protein binding. These interactions rarely cause serious clinical problems [7, 141]. However, despite the rationale for using corrections of unbound drug concentrations to predict clearance [108, 142], the use of drug binding terms in predictive IVIVE models remains controversial [13, 88, 97, 139].

Across the spectrum of literature on the subject, inconsistencies in the use of drug binding terms and the choice of *in vivo* inhibitor concentration may have clouded the general understanding and inadvertently reduced confidence in IVIVE for anything other than *qualitative* DDI predictions (average steady plasma concentration, $[I]_{av}$, peak steady-state plasma concentration, $[I]_{max}$, maximum hepatic input concentration $[I]_{in}$; see Table 22.6) [7, 13, 80, 144]. The suggestion that total blood concentrations can be used with unbound *in vitro* K_i values to achieve good predictivity is less than helpful, since it leaves the reader potentially unsure as to the impact of blood binding *in vivo*. Binding to blood components may not reach equilibrium during the short time period in the portal vein, leading to a greater free-drug concentration than may be predicted and underestimation of DDI [136]. However,

TABLE 22.6 Choice of *In Vivo* Inhibitor Concentration Advocated in the Literature in Recent Years

Which [I]	Equation	K_i Adjusted for f_{uinc}?	Author Comments	References
Maximum *unbound* hepatic input concentration, $[I]_{in}$, where [I] is $[I]\cdot f_{ub}$	$[I]_{av} = \frac{D/\tau}{CL/F}$ $[I]_{in} = [I]_{av} + \frac{k_a \cdot F_a \cdot D}{Q_h}$	No	The incidence of false-negative predictions was largest using $[I_{av}]$ for unbound drug concentration and smallest using $[I_{in}]$ for total drug concentration for each of the CYP enzymes. The use of $[I_{in}]$ is recommended because true negatives can be identified and, in contrast to the use of other [I] values, false negatives eliminated.	137
Maximum *total* hepatic input concentration, $[I]_{in}$	$[I]_{in} = [I]_{av} + \frac{k_a \cdot F_a \cdot D}{Q_h}$	No	True negatives can be identified and, in contrast to the use of other values for [I], false negatives are eliminated. True positives are also predicted well and, although the incidence of false-positive predictions is quite high, the use of hepatic input concentration is recommended.	80
Maximum *total* hepatic input concentration $[I]_{in}$	$[I]_{in} = [I]_{av} + \frac{k_a \cdot F_a \cdot D}{Q_h}$	No	The use of $[I]_{in}$ incorporating both fm_{CYP} and refined k_a values resulted in the most successful prediction overall.	143
Average *total* steady plasma concentration, $[I]_{av}$, or maximum *total* hepatic input concentration, $[I]_{in}$	$[I]_{in} = [I]_{av} + \frac{k_a \cdot F_a \cdot D}{Q_h}$ $[I]_{av} = \frac{D/\tau}{CL/F}$	Yes	Either the average systemic plasma concentration after repeated oral administration ($[I]_{av}$) or the maximum hepatic input concentration ($[I]_{in}$)	56
Average *total* steady plasma concentration, $[I]_{av}$	$[I]_{av} = \frac{D/\tau}{CL/F}$	Yes	The use of $[I]_{av}$ as the [I] surrogate generated the most successful predictions as judged by several criteria. Using $[I]_{av}$ incorporation of either plasma protein binding of inhibitor or gut wall CYP3A4 inhibition did not result in a general improvement of DDI predictions.	13
Maximum *unbound* hepatic input concentration, $[I]_{in,u}$, where [I] is $[I]\cdot f_{ub}$	$[I]_{in} = [I]_{av} + \frac{k_a \cdot F_a \cdot D}{Q_h}$	Yes ([protein] low so f_{uinc} assumed negligible)	The use of estimated unbound hepatic inlet C_{max} during the absorptive phase yielded the most accurate predictions of the magnitudes of DDI.	139

the "free-drug" theory should be regarded as the default situation and if successful predictions cannot be made, the reason(s) should be sought.

Equation 22.29 shows the maximum hepatic input of inhibitor (the sum of the contribution from the systemic circulation and the absorption phase; $[I]_{in}$) calculated using the absorption rate constant (k_a), the fraction absorbed (F_a), and dose [7].

$$[I]_{in} = [I]_{av} + (k_a \cdot F_a \cdot \text{Dose})/Q_h) \tag{22.29}$$

Often it is assumed that the rate of absorption is instantaneous (approaching 0.1 min^{-1}); however, changes in k_a can account for marked differences in $[I]_{in}$ and the value chosen should be carefully considered [143].

In the authors' laboratory, good predictions have been made using unbound maximum hepatic concentration $[I]_{in,u}$ along with correction of K_i for binding in the incubation (f_{uinc}) [88]. Using a published dataset of clinical DDIs [80], an 84% success rate was achieved for prediction of DDI at CYP3A4 and a 91% success rate predicting CYP2D6 interactions (Fig. 22.12) [88]. There were some noticeable outliers in the dataset, however; these highlighted that subtle changes in some parameters (e.g., plasma protein values for a highly bound drug) can result in large discrepancies in calculated unbound concentration and that measured *AUC* changes for drugs with low oral bioavailability are subject to large errors. Additionally, it was apparent that the impact of the $[I]/K_i$ estimate on *AUC* change becomes small once fm_{CYP} falls below 0.85 (Fig. 22.11) [88]. The clinical dataset is substantially smaller for CYP2C9 than for CYP3A4 and CYP2D6, but it was found that using $[I]_{in,u}$ and $K_{i,u}$ to predict changes in *AUC* resulted in 14 correct assignations and 1 false negative [68]. However, the desire to avoid false negatives in a drug discovery screening

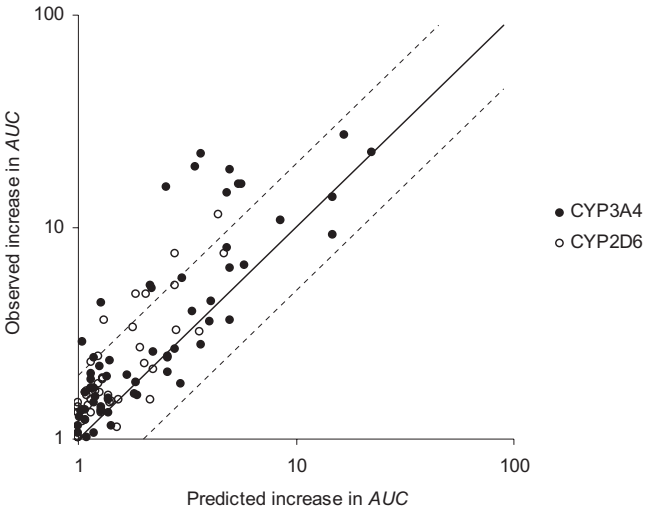

FIGURE 22.12 Observed and predicated *AUC* values for CYP3A4 and CYP2D6 DDIs. The square box represents twofold increase in *AUC*, the solid line is unity and the dashed lines are twofold errors in either direction. (Adapted from Ref. 88.)

cascade perhaps explains the popularity for using *total* concentration terms for [I], despite the decreased accuracy in absolute prediction afforded by doing so.

The multifaceted nature of CYP inhibition *in vivo* requires a great deal of understanding for accurate prediction, and the reasons behind the lack of a unifying model can be appreciated. As the IVIVE field progresses, it is anticipated that prediction accuracy will increase as there is profound interest and utility in such models within the pharmaceutical industry and considerable academic effort being made toward this goal. The ultimate aim is an integrated approach toward CYP inhibition prediction, which encompasses the role of all CYP isoforms and is underpinned by sound pharmacokinetic principles.

22.5.2 Approach for Mechanism-Based Inhibitors

Two models are currently presented in the literature and they rely on some key parameters for accurate predictions of DDI [7, 100]. As for reversible inhibition, the relevant concentration of inhibitor at the target CYP and the fraction of substrate clearance affected by inhibiting the enzyme are fundamental. In addition to this, predictions of MBI also employ the *in vivo* rate of enzyme synthesis (k_{synth}) and of degradation (k_{degrad}), and the *in vitro* inactivation kinetic parameters (K_I and k_{inact}). Where the currently available models differ is in the complexity of predicting the effect of changing inhibitor concentration over a dosing interval and the impact of this on the overall amount of inactivated CYP.

A model first presented by Hall and co-workers and subsequently expanded by the same group [100, 145, 146] is used most widely. This model assumes that the rates of enzyme synthesis and degradation are unaffected by enzyme inactivation and rely on the steady-state concentration of active enzyme being proportional to the ratio of the rate of synthesis and the rate of degradation. In the presence of inhibitor, the rate of degradation is then the sum of the *in vivo* degradation rate constant (k_{degrad}) and the rate constant describing the drug-induced inactivation (λ), where

$$\lambda = ([\mathrm{I}] \cdot k_{inact} / [\mathrm{I}] + K_I) \tag{22.30}$$

The model including inactivation of intestinal CYP and the fraction of drug metabolized by the inhibited pathway in the absence of the inhibitor is given in by

$$\frac{AUC}{AUC'} = \frac{F'}{F} \cdot \left(1 + \frac{fm}{([\mathrm{I}] \cdot k_{inact}) / (k_{degrad} \cdot (K_I + 1))} + (1 - fm) \right)^{-1} \tag{22.31}$$

This model has been shown to predict well for verapamil [145] and other mechanism-based inhibitors [147]. The accuracy of prediction is dependent on the k_{degrad} used, especially for substrates undergoing substantial ($fm > 0.9$) metabolism by the inhibited enzyme [56].

As with reversible CYP inhibition, a nonlinear regression model encompassing the various parameters predicting changing inhibitor and substrate concentrations affords the most sophisticated approach. To that end, an elegant model was proposed by Ito et al. [7], which predicts the effect of macrolide antibiotics on CYP3A4 [104]. A real advantage of this model is that it allows visualization of the plasma concentration–time profiles for the affected substrate and the inhibitor, and more importantly the change in active enzyme concentration over time. This model encompasses not only k_{inact} and K_I and the rate of resynthesis of active enzyme but also the changing concentration of the inhibitor as a function of its own disposition. Three compartments are represented: portal vein, liver, and systemic blood. The rate of change of inhibitor over time is modeled in each compartment with and without coadministered drug and a final compartment describes inactivation of hepatic CYP (Fig. 22.13). The use of this model requires nonlinear regression in a seven-compartment model which, while possible, is not necessarily practicable. Consequently, in the authors' laboratory, an analogous model has been written and implemented using a Microsoft Excel spreadsheet format [75], allowing simple manipulation and interrogation of this complex model.

Alongside the validation of this model presented by Ito et al. [104], where the interaction between erythromycin and clarithromycin with midazolam in humans was accurately predicted, the isolated perfused rat liver model (IPRL) has been used to demonstrate the effect of known mechanism-based inhibitors and NCEs [148]. Using the IPRL allowed ready validation of the predicted impact of TDI *in vivo*. It provides a bridge between the *in vitro* effect and *in vivo* impact for compounds with existing clinical data and NCEs, using pre-clinical species to bring confidence to predicted effect in humans. An adapted five-compartment model was used to fit the data and the *ex vivo* effects, although modest, were well predicted. The interplay between inhibitory potency and pharmacokinetic parameters was demonstrated; a less potent inhibitor with longer PK duration can impact hepatic CYPs to the same extent as a much more potent inhibitor with short duration. This was confirmed for troleandomycin and erythromycin in the IPRL; troleandomycin was found to be over 100-fold more efficient at inhibiting CYP3A2 than erythromycin *in vitro*, yet in the IPRL only a two fold increase over the effect of erythromycin was observed, reflecting the clinical situation for these drugs [149, 150]. This point was further confirmed by a study in cultured human hepatocytes performed in the authors' laboratory [95], where a compound that is a relatively weak time-dependent inhibitor of CYP2C9 was observed to have a dramatic impact on CYP2C9 activity over a prolonged culture period due to the large unbound concentration in the incubation combined with its metabolic stability. However, when the *in vivo* effect was modeled using predicted human PK parameters and dose, only a 5% decrease in *in vivo* CYP2C9 activity was predicted (Fig. 22.14).

22.5.3 Key Concepts

The literature regarding IVIVE of pharmacokinetics and drug interactions is vast, not only in terms of predicting human pharmacokinetic parameters but also the impact of potential DDIs and the correct use of *in vitro* data to engender the most accurate prediction of clinical DDIs. A summary of the underlying key concepts not already covered for CYP mediated DDIs is presented here.

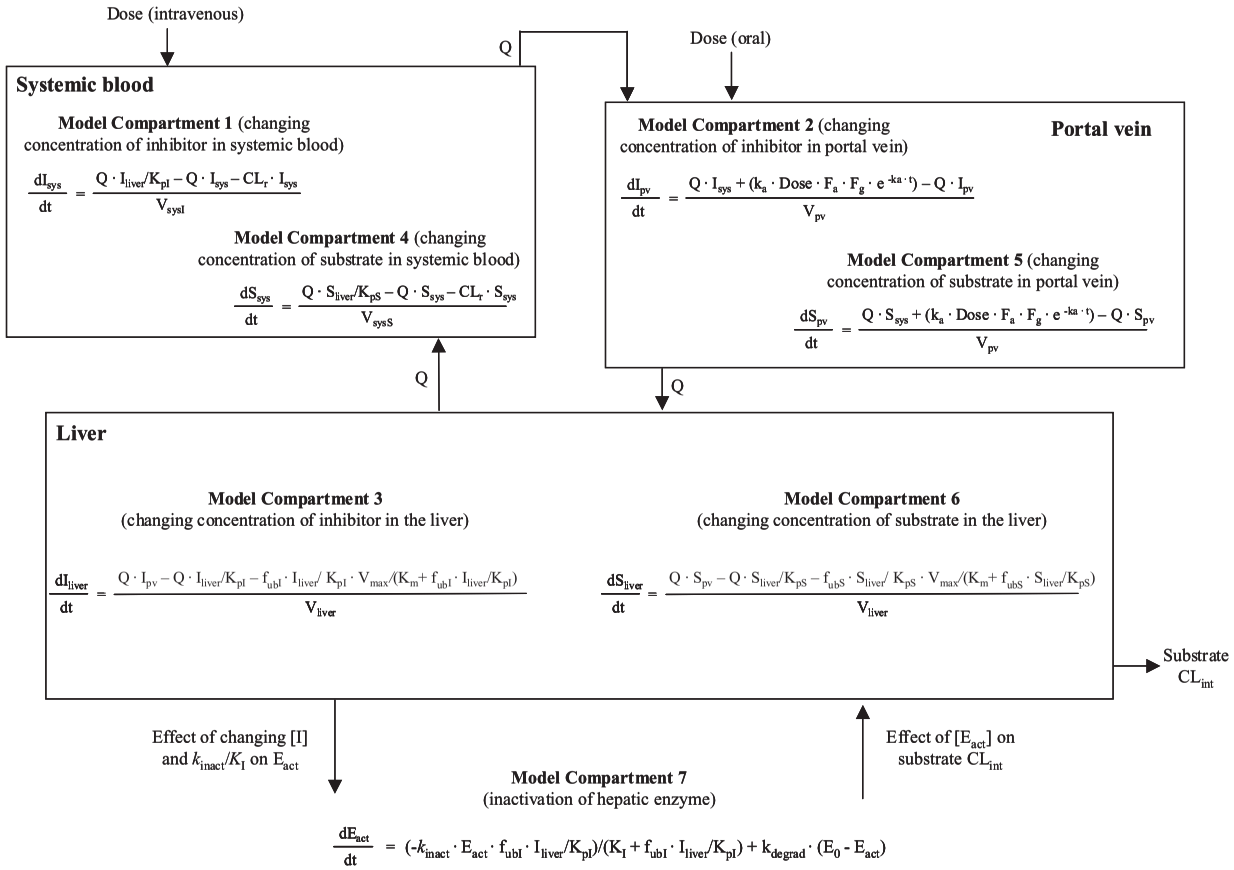

FIGURE 22.13 Model present by Ito et al. [7] for predicting effect of TDI. Seven compartments are described representing the changing inhibitor concentration in systemic blood (compartment 1), the changing inhibitor concentration in the portal vein following an oral dose (compartment 2), the changing inhibitor concentration in the liver (compartment 3), the changing substrate concentration in systemic blood (compartment 4), the changing substrate concentration in the portal vein following an oral dose (compartment 5), the changing substrate concentration in the liver (compartment 6), and the inactivation of hepatic enzyme (compartment 7), where I and S are the concentrations of inhibitor and substrate, respectively; $I_{sys,}$ S_{sys} and I_{liver}, S_{liver} are the concentration in the systemic circulation and liver, respectively; V_{sysI}, V_{sysS} represent the volumes of distribution in the central compartment; K_{pI}, K_{pS} are the liver-to-blood concentration ratios; f_{ubS}, f_{ubI} are the fraction unbound in blood; I_{pv}, S_{pv} represent the concentrations in the portal vein; V_{pv} represents the volume of the portal vein; Q is blood flow, CL_r represents renal clearance; k_a is the absorption rate constant; F_a is fraction absorbed from an oral dose; and F_g represents the intestinal availability.

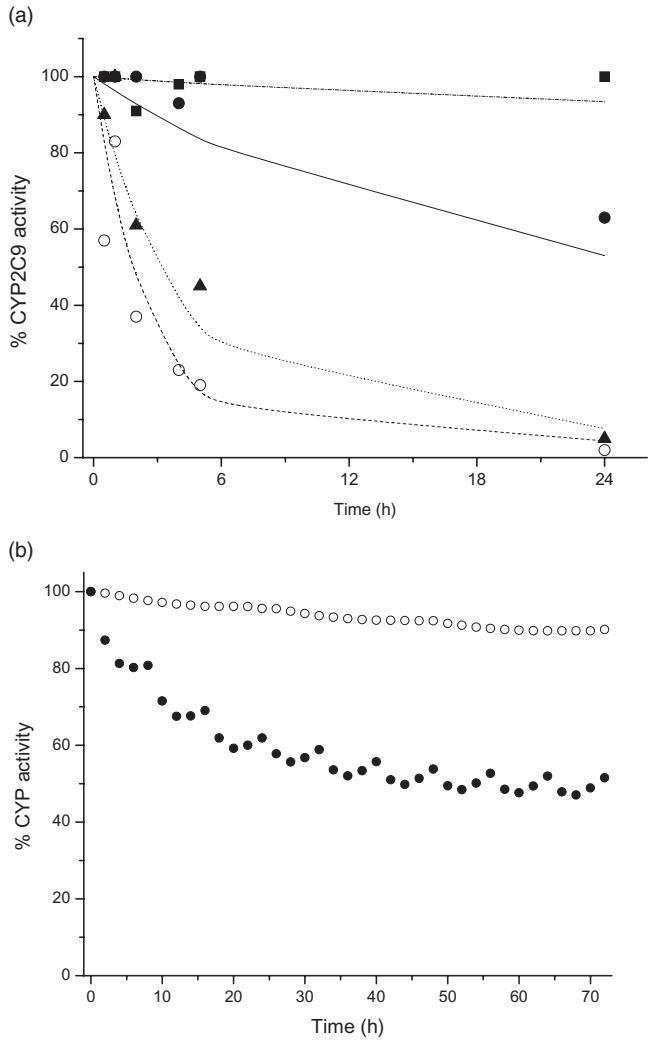

FIGURE 22.14 Effect of CYP2C9 inhibition observed *in vitro* and predicted *in vivo*. (a) CYP2C9 activity in cultured human hepatocytes after incubation with AZ1: CYP2C9-dependent diclofenac 4′-hydroxylation after incubation with AZ1 was determined after incubation with 0.1 μM (solid squares), 1 μM (solid circles), 5 μM (solid triangles), and 10 μM (open circles) AZ1. The dash-dot, solid, dotted, and dashed lines indicate nonlinear regression of the 0.1, 1, 5, and 10 μM AZ1 data, respectively. (b) Simulated profiles of CYP activity in human liver after oral dosing with AZ1 and erythromycin, respectively, using the methodology of Ito et al. [104]: CYP2C9 activity in human liver was simulated after oral dosing with AZ1 (70 mg every 24 h for 72 h open circles) and CYP3A4 activity in human liver after oral dosing with erythromycin (500 mg every 8 h for 72 h closed circles) (From Ref. 95.).

Making quantitative predictions of *in vivo* DDI using *in vitro* data requires consideration not only of inhibitor K_i (or K_I and k_{inact} for mechanism-based inhibition), but also f_{uinc}, $f_{u,b}$, CL, volume, fm_{CYP}, dose, and k_a. Use of such factors has resulted in relatively accurate predictions of DDI for reasonably large datasets [75, 88, 139, 147], with some exceptions (possibly compounds with an active component to their

hepatic uptake/efflux—clearly there is more to learn in this area). For detailed predictions of individual DDIs, computer-modeling software should be used to simulate not only the impact of the scenarios detailed earlier, but also the changing drug concentrations with time as a result of the individual PK parameters; this allows a detailed interrogation of the interaction. If a worst-case scenario is to be provided, the maximum unbound inhibitor concentration at the enzyme site should be used. For this, knowledge of the extent to which the inhibitor concentrates in the hepatocyte is important (if no information is available, 10× the maximum unbound blood concentration has been proposed [7]). Additionally, assuming that elimination of substrate is by a single hepatic CYP predicts a worse-case scenario for the inhibited pathway *in vivo*. These approaches are of utility in a discovery setting when selecting compounds for further progression, but it can be appreciated that it generally leads to an overestimation of the inhibitory effect, especially when combined with the assumption of complete and instantaneous absorption of the inhibitor from an oral dose.

Refinement and improved predictivity is afforded by including the contribution of the inhibited CYP to the total clearance of the substrate (fm_{CYP}) and more realistic estimations of the fraction and rate of absorption for the inhibitor, essentially by estimating not only the concentration of inhibitor in the liver more accurately but also its impact on the metabolic pathway of the substrate. Information on the *in vivo* fm_{CYP} for specific substrates can be found in the literature [68, 138, 151]. As demonstrated by the clinical cases of DDI presented previously, CYP inhibition has greatest impact when a substrate is predominantly cleared by the inhibited pathway; consequently, multiple pathways for drug elimination reduce the chance of clinically significant DDI. However, consideration must be given to the target patient population as, for example, renal impairment can dramatically affect the elimination pathway of a drug.

Recently, an *in vitro* approach aimed at overcoming the difficultly of assessing inhibitor concentration at the enzyme was presented [152]. It involves using human hepatocytes suspended in human plasma to generate K_i without the need for correction for free concentration at the active site (with the caveat that active transport in hepatocytes *in vitro* may not fully represent that *in vivo*). Using this method, the authors claim accurate prediction of several clinically relevant CYP DDIs by including the CYP phenotypic metabolism for each substrate. This method requires a large range of inhibitor concentrations in the *in vitro* incubations and relies heavily on acute analytical sensitivity. A limitation of this and other methods utilizing fm_{CYP} is the level of understanding required for each substrate under investigation (optimal concentration range for determining K_i and an accurate estimation of the contribution of different CYPs to the substrates' *in vivo* metabolism). This method is one approach to minimizing the difficulty of predicting [I] at the active site.

Other points of consideration for IVIVE of DDI include using appropriate substrate–inhibitor combinations *in vitro* so the *in vivo* interaction is correctly assessed; this further emphasizes the importance of using clinically relevant probe substrates in the *in vitro* determinations. Consideration must also be given to the metabolites of an inhibitor, which can often have a significant inhibitory effect in their own right. If they persist in the systemic circulation or are actively concentrated in the liver, their influence can lead to underprediction of the magnitude of the interaction if they are discounted.

There are several pharmacokinetic parameters to be considered for both substrate and inhibitor when making predictions of DDIs. These considerations essentially require estimating levels of drug within the body, be it in the circulating plasma, liver, portal vein, or gastrointestinal tract. Dose and clearance are the primary determinants for these parameters. For drugs in preclinical development, accurate prediction of the relative impact of DDI relies on reasonable assessment of dose level, frequency, and route. It follows that by minimizing dose the potential of DDI will also be minimized. The route of administration of the victim drug must also be considered. A compound with high (intestinal and hepatic) first-pass extraction will behave very differently in the presence of an inhibitor when administered orally as opposed to intravenously. For a drug with a high extraction ratio, the C_{max} will be significantly increased in the presence of an inhibitor but the elimination half-life will be quite similar in the presence and absence of inhibitor. Conversely, for a compound with a low extraction ratio, the same inhibitor will have limited effect on C_{max} following an oral dose but the elimination half-life may be considerably larger; this will also be the case following an IV dose [130].

Predictions of CYP inhibition made in isolation of other contributing factors, albeit sometimes unknown, may only result in an approximation of *in vivo* effect. The ultimate goal is to be able to predict *in vivo* disposition by encompassing not only multiple mechanisms of CYP (and indeed other enzyme) inhibition but also the potential inductive capacity and transporter interactions for the compound under evaluation. Many drugs exhibit numerous interactive attributes, one such example is the antiviral protease inhibitor ritonavir. *In vitro* ritonavir has been demonstrated to induce CYP3A4 expression through activation of the Pregnane X receptor [153]; it is also a potent mechanism-based inhibitor of CYP3A4 [154] and a substrate and inducer of the P-glycoprotein transporter [155]. Despite accurate *in vitro* assessment of its inhibitory capacity, predictions of the *in vivo* effect of ritonavir are often erroneous due to varying contribution of all these factors and also are dependent on the time course of drug exposure. Initially, ritonavir exerts an inhibitory effect on CYP3A4 mediated metabolism *in vivo* but with prolonged exposure the inductive capacity of the drug predominates. For example, short-term low-dose administration of ritonavir produces a large and significant impairment of triazolam clearance and enhancement of clinical effects [156] with the AUC of triazolam increasing from 13.6 to 553 ng/mL·h following 1 day of ritonavir treatment but following 10 days of treatment falling to 287 ng/mL·h [157]. Accurate prediction of such situations becomes difficult. A unifying model allowing all factors to be encompassed, although complex, would be beneficial.

As discussed, a comprehensive, integrated, and systematic approach is required for IVIVE of CYP mediated DDIs. To this end there exists Simcyp® (http://www.simcyp.com), a population-based prediction software tool that offers such an evaluation for CYP mediated DDIs. This software incorporates physiological, genetic, and epidemiological information, which, together with *in vitro* data, facilitates the modeling and simulation of the time course and fate of drugs in representative virtual patient populations. Simcyp uses information from routine *in vitro* studies generated in most drug discovery departments and with this information predicts individual pharmacokinetic parameters (such as F_{abs}, CL, and V_{ss}) and simulates CYP mediated drug interactions and the likely associated population variability. This allows prediction of outcomes in relevant patient populations, identifying those

individuals at most risk from a DDI, not just a single value in an average individual. The software has the potential to simulate the effect of combined CYP induction and inhibition and can also be applied to DDIs involving time-dependent inhibition. Simcyp may assist in the evaluation and optimization of candidate drugs, in the estimation of early human doses and exposures in the clinic, and the prioritization and planning of suitable *in vitro* and clinical interaction studies in the development phase. Tools such as Simcyp are attracting a lot of interest in the pharmaceutical industry and may facilitate a more aligned strategy and as such are worthy of further investment and validation.

22.5.4 FDA Guidelines

The FDA defines a significant DDI as a two fold (or more) increase in the *AUC* of the substrate drug in the presence of an inhibitor. The two fold threshold is given as inter-individual variation and polymorphisms in CYP expression within the population could account for changes less than this [158]. If a risk of DDI is predicted from *in vitro* data, a clinical study evaluating the risk and a thorough investigation of the mechanism of CYP inhibition (along with understanding of the potential coadministered drugs in the target patient population) may make it possible to launch a candidate drug, providing it carries a product label stating possible risk of DDI. For example, if a drug has been determined to be a "strong" inhibitor of CYP3A, a warning about an interaction with "sensitive CYP3A substrates" and CYP3A substrates with narrow therapeutic range may be required [158].

The FDA has released guidance documents, which reflect current thinking in the field specifically aimed at industry evaluating metabolism-based drug interactions; *Guidance for Industry: Drug Metabolism/Drug Interaction Studies in the Drug Development Process—Studies in Vitro*; and *Guidance for Industry: In Vivo Drug Metabolism/Drug Interaction Studies—Study Design, Data Analysis and Recommendations for Dosing and Labelling* [159]. The *in vitro* studies guide, as well as providing a summary of drug metabolism and relevant concepts, describes *in vitro* techniques for evaluating the potential of metabolism-based interactions, the correlation of *in vitro* and *in vivo* findings, and the timing of *in vitro* studies and subsequent product labeling. It defines the goals of evaluating *in vitro* drug metabolism as: (1) to identify all of the major metabolic pathways that affect the test drug and its metabolites, including the specific enzymes responsible for elimination and the intermediates formed; and (2) to explore and anticipate the effects of the test drug on the metabolism of other drugs and the effects of other drugs on its metabolism.

22.6 CONCLUSION

Undoubtedly, using *in vitro* data to make accurate predictions of clinical DDIs involving inhibition of CYP is possible providing that there is understanding of the various processes involved. The availability of clinical data is central to building predictive models and is required for feedback on their accuracy and further iteration of these algorithms. Misinterpretation of the risk of CYP inhibition can be

costly both in terms of patient safety and pharmaceutical resources; in a drug discovery setting predicting the worst-case scenario is a prudent approach.

In brief, CYP inhibition may/can result in serious clinical adverse reactions, the prediction of which is a maturing science. Accurate predictions are possible and the pitfalls and progress in using *in vitro* inhibition data to project clinical drug–drug interactions have been presented. Clearly, accurate predictions start with the production of high quality *in vitro* data, require rational examination of the kinetics of inhibition, and, finally, require the application of sound pharmacokinetic theory. The approaches discussed here should guide the researcher in implementing this best practice.

REFERENCES

1. Pirmohamed M, James S, Meakin S, Green C, Scott AK, Walley TJ, Farrar K, Park BK, Breckenridge AM. Adverse drug reactions as cause of admission to hospital: prospective analysis of 18,820 patients. *Br Med J* 2004;329(7456):15–19.
2. Lazarou J, Pomeranz BH, Corey PN. Incidence of adverse drug reactions in hospitalised patients. *JAMA* 1998;279(15):1200–1205.
3. Frankfort SV, Tulner LR, van Campen JPCM, Koks CHW, Beijnen JH. Evaluation of pharmacotherapy in geriatric patients after performing complete geriatric assessment at a diagnostic day clinic. *Clin Drug Invest* 2006;26(3):169–174.
4. Jankel C, Fitterman LK. Epidemiology of drug–drug interactions as a cause of hospital admissions. *Drug Safety* 1993;9:51–59.
5. Howard RL, Avery AJ, Slavenburg S, Royal S, Pipe G, Lucassen P, Pirmohamed M. Which drugs cause preventable admissions to hospital? A systematic review. *Br J Clin Pharmacol* 2007;63(2):136–147.
6. Shah RR. Mechanistic basis of adverse drug reactions: the perils of inappropriate dose schedules. *Expert Opin Drug Safety* 2005;4(1):103–128.
7. Ito K, Iwatsubo T, Kanamutsu S, Ueda K, Suzuki H, Sugiyama Y. Prediction of pharmacokinetic alterations caused by drug–drug interactions: metabolic interaction in the liver. *Pharmacol Rev* 1998;50(3):387–411.
8. Kumar V, Wahlstrom JL, Rock DA, Warren CJ, Gorman LA, Tracy TS. CYP2C9 inhibition: impact of probe selection and pharmacogenetics on *in vitro* inhibition profiles. *Drug Metab Dispos* 2006;34(12):1966–1075.
9. Shou M. Prediction of pharmacokinetics and drug–drug interactions from *in vitro* metabolic data. *Curr Opin Drug Discov Dev* 2005;8(1):66–77.
10. Zimmermann M, Duruz H, Guinand O, Broccard O, Levy P, Lacatis D, Bloch A. Torsades de pointes after treatment with terfenadine and ketoconazole. *Eur Heart J* 1992; 13(7):1002–1003.
11. Backmann KA, Lewis JD. Predicting inhibitory drug–drug interactions and evaluating interaction reports using inhibition constants. *Ann Pharmacother* 2005;39:1064–1072.
12. Wysowsk DK, Bacsanyi J. Cisapride and fatal arrhythmia. *N Engl J Med* 1996; 335(4):290–291.
13. Brown HS, Galetin A, Halifax D, Houston JB. Prediction of *in vivo* drug–drug interactions from *in vitro* data: factors affecting prototypic drug–drug interactions involving CYP2C9, CYP2D6 and CYP3A4. *Clin Pharmacokinet* 2006;45(10):1035–1050.

14. Venkatakrishnan K, von Moltke LL, Obach RS, Greenblatt DJ. Drug metabolism and drug interactions: application and clinical value of *in vitro* models. *Curr Drug Metab* 2003;4:423–459.
15. Lin JH, Lu AYH. Interindividual variability in inhibition and induction of cytochrome P450 enzymes. *Annu Rev Pharmacol Toxicol* 2001;41:535–567.
16. Prentis RA, Lis Y, Walker SR. Pharmaceutical innovation by the seven UK-owned pharmaceutical companies (1964–1985). *Br J Clin Pharmacol* 1988;25:387–396.
17. Schuster D, Laggner C, Langer T. Why drugs fail—a study on side effects in new chemical entities. *Curr Pharm Des* 2005;11:3545–3559.
18. DiMasi JA, Hansen RW, Grabowski HG. The price of innovation: new estimates of drug development costs. *J Health Econ* 2003;22:151–185.
19. Cohen LH, Remley MJ, Raunig D, Vaz ADN. *In vitro* drug interactions of cytochrome P450: an evaluation of fluorogenic to conventional substrates. *Drug Metab Dispos* 2003;31:1005–1015.
20. Wienkers LC, Heath TG. Predicting *in vivo* drug interactions from *in vitro* drug discovery data. *Nat Rev (Drug Disco)* 2005;4:825–833.
21. Donato MT, Gomez-Lechón MJ. Inhibition of P450 enzymes: an *in vitro* approach. *Curr Enzyme Inhib* 2006;2:281–304.
22. Lewis DFV. 57 varieties: the human cytochromes P450. *Pharmacogenomics* 2004; 5(3):305–318.
23. Girault I, Rougier N, Chesné C, Lideraue R, Beaune P, Biéche I, De Waziers I. Simultaneous measurement of 23 isoforms from the human cytochrome P450 families 1 to 3 by quantitative reverse transcriptase-polymerase chain reaction. *Drug Metab Dispos* 2005;33:1803–1810.
24. Tanaka E. Clinically important pharmacokinetic drug–drug interactions: role of cytochrome P450 enzymes. *J Clin Pharm Ther* 1998;23:403–416.
25. Bertz RJ, Granneman GR. Use of *in vitro* and *in vivo* data to estimate the likelihood of metabolic pharmacokinetic interactions. *Clin Pharmacokin* 1997;32(3):210–258.
26. Shimada T, Yamazaki H, Mimura M, Yukiharu I, Guengerich FP. Interindividual variations in human liver cytochrome P450 enzymes involved in oxidation of drugs, carcinogens and toxic chemicals; studies with liver microsomes of 30 Japanese and 30 Caucasians. *J Pharmacol Exp Ther* 1994;270:414–423.
27. Dresser GK, Spence JD, Bailey DG. Pharmacokinetic–pharmacodynamic consequences and clinical relevance of cytochrome P450 inhibition. *Clin Pharmacokinet* 2000; 38(1):41–57.
28. Lewis JD, Bachmann KA. Cytochrome P450 enzymes and drug–drug interactions: an update on the superfamily. *J Pharm Technol* 2006;22:22–31.
29. Batty KT, Davis TME, Ilett KF, Dusci LJ, Langton SR. The effect of ciprofloxacin on theophylline pharmacokinetics in healthy subjects. *Br J Clin Pharmacol* 1995; 39(3):305–311.
30. Granfors MT, Backman JT, Neuvonen M, Neuvonen PJ. Ciprofloxacin greatly increases concentrations and hypotensive effect of tizanidine by inhibiting its cytochrome P450 1A2-mediated presystemic metabolism. *Clin Pharmacol Ther* 2004;76(6):598–606.
31. Hemeryck A, Belpaire FM. Selective serotonin reuptake inhibitors and cytochrome P-450 mediated drug–drug interactions: an update. *Curr Drug Metab* 2002;3:13–37.
32. Becquemont L, Bot MA, Le Riche C, Beaune P. Influence of fluvoxamine on tacrine metabolism *in vitro*: potential implication for hepatotoxicity *in vivo*. *Fundam Clin Pharmacol* 1996;10(2):156–157.

33. Backman JT, Kyrklund C, Neuvonen M, Neuvonen PJ. Gemfibrozil greatly increases plasma concentrations of cerivastatin. *Clin Pharmacol Ther* 2002;72:685–691.
34. Veronese ME, Miners JO, Randles D, Gregov D, Birkett DJ. Validation of the tolbutamide metabolic ratio for population screening with use of sulfaphenazole to produce model phenotypic poor metabolizers. *Clin Pharmacol Ther* 1990;47:403–411.
35. Crussell-Porter LL, Rindone JP, Ford MA, Jaskar DW. Low-dose fluconazole therapy potentiates the hypoprothrombinemic response of warfarin sodium. *Arch Intern Med* 1993;153(1):102–104.
36. Krayenbühl JC, Vozeh S, Kondo-Oestreicher M, Dayer P. Drug–drug interactions of new active substances: mibefradil example. *Eur J Clin Pharmacol* 1999;55:559–565.
37. Boxenbaum H. Cytochrome P450 3A4 *in vivo* ketoconazole competitive inhibition: determination of K_i and dangers associated with high clearance drugs in general. *J Pharm Pharm Sci* 1999;2(2):47–52.
38. Honig PK, Woosley RL, Zamani K, Conner DP, Cantilena LR, Jr. Changes in the pharmacokinetics and electrocardiograph pharmacodynamics of terfenadine with concomitant administration of erythromycin. *Clin Pharmacol Ther* 1992;52(3):231–238.
39. Ishigam M, Uchiyama M, Kondo T, Iwabuchi H, Inoue SI, Takasaki W, Ikeda T, Komai T, Ito K, Sugiyama Y. Inhibition of *in vitro* metabolism of simvastatin by itraconazole in humans and prediction of *in vivo* drug–drug interactions. *Pharm Res* 2001;18(5):622–631.
40. Corpier CL, Jones PH, Suki WN, Lederer ED, Quinones MA, Schmidt SW, Young JB. Rhabdomyolysis and renal injury with lovastatin use. Report of two cases in cardiac transplant recipients. *JAMA* 1998;260(2):239–241.
41. Schmassmann-Suhijar D, Bullingham R, Gasser R, Schmutz J, Haefeli WE. Rhabdomyolysis due to interaction of simvastatin with mibefradil [letter]. *Lancet* 1998;351:1929–1930.
42. Kantola T, Kivisto KT, Neuvonen PJ. Erythromycin and verapamil considerably increase serum simvastatin and simvastatin acid concentrations. *Clin Pharmacol Ther* 1998;64(2):177–182.
43. Michalets EL, Williams CR. Drug interactions with cisapride: clinical implications. *Clin Pharmacokinet* 2000;39(1):49–75.
44. Jacobsen W, Kirchner G, Hallensleben K, Mancinelli L, Deters M, Hackbarth I, Baner K, Benet LZ, Sewing K, Christians U. Small intestinal metabolism of the 3-hydroxy-3-methylglutaryl-coenzyme A reductase inhibitor lovastatin and comparison with pravastatin. *J Pharmacol Exp Ther* 1999;291(1):131–139.
45. Spoendlin M, Peters J, Welker H, Bock A, Thiel G. Pharmacokinetic interaction between oral cyclosporin and mibefradil in stabilized post-renal-transplant patients. *Nephrol Dial Transplant* 1998;13:1787–1791.
46. Olkkola KT, Ahonen J, Neuvonen PJ. The effect of the systemic antimycotics, itraconazole and fluconazole, on the pharmacokinetics and pharmacodynamics of intravenous and oral midazolam. *Anesth Analg* 1996;82(3):511–516.
47. Muck W. Rational assessment of the interaction profile of cerivastatin supports its low propensity for drug interactions. *Drugs* 1998;56(1s):15–23.
48. Muck W, Ochmann K, Rohde G, Unger S, Kuhlmann J. Influence of erythromycin pre- and co-treatment on single-dose pharmacokinetics of the HMG-CoA reductase inhibitor cerivastatin. *Eur J Clin Pharmacol* 1998;53:469–473.
49. Kantola T, Kivisto KT, Neuvonen PJ. Effect of itraconazole on cerivastatin pharmacokinetics. *Eur J Clin Pharmacol* 1999;54:851–855.

50. Mazzu AL, Lasseter KC, Shamblen EC, Agarwal V, Lettieri J, Sundaresen P. Itraconazole alters the pharmacokinetics of atorvastatin to a greater extent than either cerivastatin or pravastatin. *Clin Pharmacol Ther* 2000;68:391–400.
51. Shitara Y, Sugiyama Y. Pharmacokinetic and pharmacodynamic alterations of 3-hydroxy-3-methylglutaryl coenzyme A (HMG-CoA) reductase inhibitors: drug–drug interactions and interindividual differences in transporter and metabolic enzyme functions. *Pharmacol Ther* 2006;112(1):71–105.
52. Shitara Y, Hirano M, Sato H, Sugiyama Y. Gemfibrozil and its glucuronide inhibit the organic anion transporting polypeptide 2 (OATP2/OATP1B1:SLC21A6)-mediated hepatic uptake and CYP2C8-mediated metabolism of cerivastatin: analysis of the mechanism of the clinically relevant drug–drug interaction between cerivastatin and gemfibrozil. *J Pharmacol Exp Ther* 2004;311:228–236.
53. Neuvonen PJ, Mikko Niemi M, Backman JT. Drug interactions with lipid-lowering drugs: mechanisms and clinical relevance. *Clin Pharmacol Ther* 2006;80(6):565–581.
54. Pisani F, Narbone MC, Fazio A, Crisafulli P, Primerano G, D'Agostino AA, Oteri G, Di Perri R. Increased serum carbamazepine levels by viloxazine in epileptic patients. *Epilepsia* 1986;25:482–285.
55. Rotzinger S, Bourin M, Akimoto Y, Coutts RT, Bake GB. Metabolism of some "second"– and "fourth"–generation antidepressants: iprindole, viloxazine, bupropion, mianserin, maprotiline, trazodone, nefazodone, and venlafaxine. *Cell Mol Neurobiol* 1999;19(4): 427–442.
56. Galetin A, Ito K, Halifax D, Houston JB. CYP3A4 substrate selection and substitution in the prediction of potential drug–drug interactions. *J Pharmacol Exp Ther* 2005; 314(1):180–190.
57. Prueksaritanont T, Ma B, Tang C, Meng Y, Assang C, Lu P, Reider PJ, Lin JH, Baillie TA. Metabolic interactions between mibefradil and HMG-CoA reductase inhibitors: an *in vitro* investigation with human liver preparations. *Br J Clin Pharmacol* 1999;47(3):291–298.
58. Wandel C, Kim RB, Guengerich PF, Wood AJJ. Mibefradil is a P-glycoprotein substrate and a potent inhibitor of P-glycoprotein and CYP3A4 *in vitro*. *Drug Metab Dispos* 2000;28:895–898.
59. Reynolds KS. Drug interactions: regulatory perspective. In Piscitelle S, Rodvold K, Eds. *Drug Interactions in Infectious Diseases*, 2nd eds. Totowa, NJ: Humana Press; 2005.
60. Venkatakrishnan K, von Moltke LL, Greenblatt DJ. Effects of the antifungal agents on oxidative drug metabolism: clinical relevance. *Clin Pharmacokinet* 2000;8(2): 111–180.
61. Granfors MT, Backman JT, Jouko L, Neuvonen PJ. Tizanidine is mainly metabolized by cytochrome P450 1A2 *in vitro*. *Br J Clin Pharmacol* 2004;57(3):349–353.
62. Ha HR, Chen J, Freiburghaus AU, Follath F. Metabolism of theophylline by cDNA-expressed human cytochromes P-450. *Br J Clin Pharmacol* 1995;39(3):321–326.
63. Ilett KF, Castleden WM, Vandongen YK, Stacey MC, Butler MA, Kadlubar FF. Acetylation phenotype and cytochrome P450IA2 phenotype are unlikely to be associated with peripheral arterial disease. *Clin Pharmacol Ther* 1993;54(3):317–322.
64. Dorado P, Berecz R, Penas-Lledo EM, Caceres MC, Llerena A. Clinical implications of CYP2D6 genetic polymorphism during treatment with antipsychotic drugs. *Curr Drug Targets* 2006;7(12):1671–1680.
65. Preskorn SH, Harvey AT. Cytochrome P450 enzymes and psychopharmacology. In Bloom FE, Kupfer DJ, Eds. *Psychopharmacology—The Fourth Generation of Progress*, 4threv ed. Philadelphia: Raven Press; 1995.

66. Kenworthy KE, Clarke SE, Andrews J, Houston JB. Multisite kinetic models for CYP3A4: simultaneous activation and inhibition of diazepam and testosterone metabolism. *Drug Metab Dispos* 2001;29(12):1644–1651.
67. Hutzler JM, Hauer MJ, Tracy TS. Dapsone activation of CYP2C9-mediated metabolism: evidence for activation of multiple substrates and a two-site model. *Drug Metab Dispos* 2001;29(7):1029–1034.
68. McGinnity DF, Tucker J, Trigg S, Riley RJ. Prediction of CYP2C9-mediated drug–drug interactions: a comparison using data from recombinant enzymes and human hepatocytes. *Drug Metab Dispos* 2005;33(11):1700–1707.
69. Egnell A-C, Eriksson C, Albertson N, Houston B, Boyer S. Generation and evaluation of a CYP2C9 heteroactivation pharmacophore. *J Pharmacol Exp Ther* 2003;307:878–887.
70. Egnell A-C, Houston B, Boyer S. *In vivo* CYP3A4 heteroactivation is a possible mechanism for the drug interaction between felbamate and carbamazepine. *J Pharmacol Exp Ther* 2003;305(3):1251–1262.
71. Zhang Z, Wong YN. Enzyme kinetics for clinically relevant CYP inhibition. *Curr Drug Metab* 2005;6:241–257.
72. Tracy TS, Hummell MA. Modelling kinetic data from *in vitro* drug metabolising enzyme experiments. *Drug Metab Rev* 2004;26(2):231–242.
73. Houston JB, Kenworthy KE, Galetin A. Typical and atypical enzyme kinetics. In Lee JS, Obach RS, Fisher MB, Eds. *Drug Metabolising Enzymes, Cytochrome P450 and Other Enzymes in Drug Discovery and Development*. New York: Marcel Dekker; 2003, pp 211–254.
74. Hollenberg PF. Characteristics and common properties of inhibitors, inducers, and activators of CYP enzymes. *Drug Metab Rev* 2002;34(1–2):17–35.
75. Riley RJ, Grime K, Weaver R. Time-dependent CYP inhibition. *Expert Opin Drug Metab Toxicol* 2007;3(1):51–66.
76. Zhou S, Yung Chan S, Cher Goh B, Chan E, Duan W, Huang M, McLeod HL. Mechanism-based inhibition of cytochrome P450 3A4 by therapeutic drugs. *Clin Pharmacokinet* 2005;44(3):279–304.
77. Silverman RB. Mechanism-based enzyme inactivation. In *Chemistry and Enzymology*, Vol 1. Boca Raton, FL: CRC Press; 1988, pp 3–30.
78. Waley SG. Kinetics of suicide substrates: practical procedures for determining parameters. *Biochem J* 1985;227:843–849.
79. Ghanbari F, Rowland-Yeo K, Bloomer JC, Clarke SE, Lennard MS, Tucker GT, Rostami-Hodjegan A. A critical evaluation of the experimental design of studies of mechanism-based enzyme inhibition, with implications for *in vitro–in vivo* extrapolation. *Curr Drug Metab* 2006;7:315–334.
80. Ito K, Brown HS, Houston JB. Database analyses for the prediction of *in vivo* drug–drug interactions from *in vitro* data. *Br J Clin Pharmacol* 2004;57(4):473–486.
81. Martignoni M, Groothuis GMM, de Kanter R. Species differences between mouse, rat, dog, monkey and human CYP-mediated drug metabolism, inhibition and induction. *Expert Opin Drug Metab Toxicol* 2006;2(6):875–894.
82. Gill HJ, Tingle MD, Park BK. N-Hydroxylation of dapsone by multiple enzymes of cytochrome P450: implications for inhibition of hemotoxicity. *Br J Clin Pharmacol* 1995;40(6):531–538.
83. Soars MG, Grime K, Riely RJ. Comparative analysis of substrate and inhibitor interactions with CYP3A4 and CYP3A5. *Xenobiotica* 2006;36(4):287–299.
84. Tang W, Wang WW, Lu AYH. Utility of recombinant cytochrome P450 enzymes: a drug metabolism perspective. *Curr Drug Metab* 2005;6:503–517.

85. Proctor NJ, Tucker GT, Rostami-Hodjegan A. Predicting drug clearance from recombinantly expressed CYPs: intersystem extrapolation factors. *Xenobiotica* 2004;34(2):151–178.

86. McGinnity DF, Riley RJ. Predicting drug pharmacokinetics in humans from *in vitro* metabolism studies. *Biochem Soc Transact* 2001;29(2):135–139.

87. Gomez-Lechón MJ, Donato MT, Castell JV, Jover R. Human hepatocytes in primary culture: the choice to investigated drug metabolism in man. *Curr Drug Metab* 2004;5:443–462.

88. Grime K, Riley RJ. The impact of *in vitro* binding on *in vitro–in vivo* extrapolations, projections of metabolic clearance and clinical drug–drug interactions. *Curr Drug Metab* 2006;7(3):251–264.

89. Griffin SJ, Houston JB. Comparison of fresh and cryopreserved rat hepatocyte suspensions for the prediction of *in vitro* intrinsic clearance. *Drug Metab Dispos* 2004;32:552–558.

90. Houston JB, Carlile DJ. Prediction of hepatic clearance from microsomes, hepatocytes and liver slices. *Drug Metab Rev* 1997;29:891–922.

91. Dickins M. Induction of cytochromes P450. *Curr Top Med Chem* 2004;4(16): 1745–1766.

92. LeCluyse EL. Human hepatocyte culture systems for the *in vitro* evaluation of cytochrome P450 expression and regulation. *Eur J Pharm Sci* 2001;13(4):343–368.

93. Oleson FB, Berman CL, Li AP. An evaluation of the P450 inhibition and induction potential of daptomycin in primary human hepatocytes. *Chem Biol Interact* 2004; 150:137–147.

94. Li AP, Lu C, Brent JA, Pham C, Fackett A, Ruegg CE, Silber PM. Cryopreserved human hepatocytes: characterization of drug-metabolizing enzyme activities and applications in higher throughput screening assays for hepatotoxicity, metabolic stability, and drug–drug interaction potential. *Chem Biol Interact* 1999;121:17–35.

95. McGinnity DF, Berry AJ, Kenny JR, Grime K, Riley RJ. Evaluation of time-dependent cytochrome P450 inhibition using cultured human hepatocytes. *Drug Metab Dispos* 2006;34:1291–1300.

96. Zhao P, Kunze KL, Lee CA. Evaluation of time-dependent inactivation of CYP3A in cryopreserved human hepatocytes. *Drug Metab Dispos* 2005;33:853–861.

97. Soars MG, McGinnity DF, Grime K, Riely RJ. The pivotal role of hepatocytes in drug discovery. *Chem-Biol Interact* 2007;168(1):2–15.

98. Atkinson A, Kenny JR, Grime K. Automated assessment of time-dependent inhibition of human cytochrome P450 enzymes using liquid chromatography-tandem mass spectrometry analysis. *Drug Metab Dispos* 2005;33:1637–1647.

99. Lopez-Garcia MP, Dansette PM, Mansuy D. Thiophene derivatives as new mechanism-based inhibitors of cytochromes P-450: inactivation of yeast-expressed human liver cytochrome P-450 2C9 by tienilic acid. *Biochemistry* 1994;33(1):166–175.

100. Mayhew BS, Jones DR, Hall SD. An *in vitro* model for predicting *in vivo* inhibition of cytochrome P450 3A4 by metabolic intermediate complex formation. *Drug Metab Dispos* 2000;28:1031–1037.

101. Chan WK, Delucchi AB. Resveratrol, a red wine constituent, is a mechanism-based inactivator of cytochrome P450 3A4. *Life Sci* 2000;67(25):3103–3112.

102. Kanamitsu S, Ito K, Green CE, Tyson CA, Shimada N, Sugiyama Y. Prediction of *in vivo* interaction between triazolam and erythromycin based on *in vitro* studies using human liver microsomes and recombinant human CYP3A4. *Pharm Res* 2000;17(4):419–426.

103. Yamano K, Yamamoto K, Katashima M, Kotaki H, Takedomi S, Matsuo H, Ohtani H, Sawada Y, Iga T. Prediction of midazolam-CYP3A inhibitors interaction in the human liver from *in vivo*/*in vitro* absorption, distribution, and metabolism data. *Drug Metab Dispos* 2001;29(4):443–452.

104. Ito K, Ogihara K, Kanamitsu S, Itoh T. Prediction of the *in vivo* interaction between midazolam and macrolides based on *in vitro* studies using human liver microsomes. *Drug Metab Dispos* 2003;31(7):945–954.

105. Dai R, Wei X, Luo G, Sinz M, Marathe P. Metabolism-dependent P450 3A4 inactivation with multiple substrates. Abstract from 12th North American ISSX Meeting, Providence, RI. *Drug Metab Rev* 2003;35:341.

106. McConn DJ, Zhao Z. Integrating *in vitro* kinetic data from compounds exhibiting induction, reversible inhibition and mechanism-based inactivation: *in vitro* study design. *Curr Drug Metab* 2004;5:141–146.

107. Boobis AR, McKillop D, Robinson DT, Adams DA, McCormick DJ. Interlaboratory comparison of the assessment of P450 activities in human hepatic microsomal samples. *Xenobiotica* 1998;28(5):493–506.

108. Obach RS. Prediction of human clearance of twenty-nine drugs from hepatic microsomal intrinsic clearance data: an examination of *in vitro* half-life approach and nonspecific binding to microsomes. *Drug Metab Dispos* 1999;27:1350–1359.

109. Riley RJ. The potential pharmacological and toxicological impact of P450 screening. *Curr Opin Drug Discov Dev* 2001;4:45–54.

110. Austin RP, Barton P, Mohmed S, Riley RJ. The binding of drugs to hepatocytes and its relastionship to physicochemical properties. *Drug Metab Dispos* 2005;33(3):419–425.

111. Austin RP, Barton P, Cockroft SL, Wenlock MC, Riley RJ. The influence of nonspecific microsomal binding on apparent intrinsic clearance, and its prediction from physicochemical properties. *Drug Metab Dispos* 2002;30(12):1497–1503.

112. Riley RJ, Grime K. Metabolic screening *in vitro*: metabolic stability, CYP inhibition and induction. *Drug Discov Today* 2004;1(4):365–372.

113. Tang C, Shou M, Rodrigues AD. Substrate-dependent effect of acetronitrile on human liver microsomal cytochrome P450 2C9 (CYP2C9) activity. *Drug Metab Dispos* 2000;28:567–572.

114. Baranczewski P, Stanczak A, Sundberg K, Svensson R, Wallin A, Jansson J, Garberg P, Postlind H. Introduction to *in vitro* estimation of metabolic stability and drug interactions of new chemical entities in drug discovery and development. *Pharmacol Rep* 2006;58:453–472.

115. Walsky RL, Obach RS. Validated assays for human cytochrome P450 activities. *Drug Metab Dispos* 2004;32:647–660.

116. Weaver R, Grime K, Beatie IG, Riley RJ. Cytochrome P450 inhibition using recombinant proteins and mass spectrometry/multiple reaction monitoring technology in a cassette incubation. *Drug Metab Dispos* 2003;31:955–966.

117. Tucker GT, Houston JB, Huang S. Optimising drug development: strategies to assess drug metabolism/transport interaction potential—towards a consensus. *Pharm Res* 2001;18(8):1071–1080.

118. O'Donnell CJ, Grime K, Courtney P, Slee D, Riley RJ. The development of a cocktail CYP2B6, CYP2C8 and CYP3A5 inhibition assay and a preliminary assessment of utiliy in a drug discovery setting. *Drug Metab Dispos* 2007;35(3):381–385.

119. Moody GC, Griffin SJ, Mather AN, McGinnity DF, Riley RJ. Fully automated analysis of activities catalysed by the major human liver cytochrome P450 (CYP) enzymes: assessment of human CYP inhibition potential. *Xenobiotica* 1999;29(1):53–75.

120. US Food and Drug Administration, Center for Drug Evaluation and Research website. Drug Development And Drug Interactions information page. http://www.fda.gov/cder/drug/drugInteractions/.

121. Bu H-Z, Magis L, Knuth K, Teitelbaum P. High-throughput cytochrome P450 (CYP) inhibition screening via a cassette probe-dosing strategy. VI. Simultaneous evaluation of inhibition potential of drugs on human hepatic isozymes CYP2A6, 3A4, 2C9, 2D6 and 2E1. *Rapid Commun Mass Spectrom* 2001;15(10):741–748.

122. Kenworthy KE, Bloomer JC, Clarke SE, Houston JB. CYP3A4 drug interactions: correlation of 10 *in vitro* probe substrates. *Br J Clin Pharmacol* 1999;48(5):716–727.

123. Shou M, Lin Y, Lu P, Tang C, Mei Q, Cui D, Tang W, Ngui JS, Lin CC, Singh R, Wong BK, Yergey JA, Lin JH, Pearson PG, Baillie TA, Rodrigues AD, Rushmore TH. Enzyme kinetics of cytochrome P450-mediated reactions. *Curr Drug Metab* 2001;2(1):17–36.

124. Ueng YF, Kuwabara T, Chun YJ, Guengerich FP. Cooperativity in oxidations catalyzed by cytochrome P450 3A4. *Biochemistry* 1997;36(2):370–381.

125. Zhang Z, Li Y, Shou M, Zhang Y, Ngui JS, Stearns RA, Evans DC, Baillie TA, Tang W. Influence of different recombinant systems on the cooperativity exhibited by cytochrome P4503A4. *Xenobiotica* 2004;34(5):473–486.

126. Janiszewski JS, Rogers KJ, Whalen KM, Cole MJ, Liston TE, Duchosiav E, Fouda HG. A high-capacity LC-MS system for the bioanalysis of samples generated from plate based metabolic screening. *Anal Chem* 2001;73(7):1495–1501.

127. DiMarco A, Marcucci I, Verdirame M, Perez J, Sanchez M, Pelaez F, Chaudhary A, Laufer R. Development and validation of a high throughput radiometric CYP3A4 inhibition assay using tritiated testosterone. *Drug Metab Dispos* 2005;33:349–358.

128. Jensen BF, Vind C, Padkjr SB, Brockhoff PB, Refsgaard HHF. *In silico* prediction of cytochrome P450 2D6 and 3A4 inhibition using Gaussian kernel weighted k-nearest neighbor and extended connectivity fingerprints, including structural fragment analysis of inhibitors versus noninhibitors. *J Med Chem* 2007;50(3):501–511.

129. Refsgaard HHF, Jensen BF, Christensen IT, Hagen N, Brockhoff PB. *In silico* prediction of cytochrome P450 inhibitors. *Drug Dev Res* 2006;67:417–429.

130. Bachmann KA. Inhibition constants, inhibitor concentrations and the prediction of inhibitory drug drug interactions: pitfalls, progress and promise. *Curr Drug Metab* 2006;7:1–14.

131. Mannervik B. Regression analysis in design and analysis. In Purich DL, Ed. *Contemporary Enzyme Kinetics and Mechanism*, 2nd ed. San Diego, CA: Academic Press; 1996.

132. Kalgutkar AS, Gardner I, Obach RS, Shaffer CL, Callegari E, Henne KR, Mutlib AE, Dalvie DK, Lee JS, Nakai Y, O'Donnell JP, Boer J, Harriman SP. A comprehensive listing of bioactivation pathways of organic functional groups. *Curr Drug Metab* 2005; 6(3):161–225.

133. Li AP. A review of the common properties of drugs with idiosyncratic hepatotoxicity and the "multiple determinant hypothesis" for the manifestation of idiosyncratic drug toxicity. *Chem Biol Interact* 2002;142(1–2):7–23.

134. Segel IH. Simple inhibition systems. In *Enzyme Kinetics: Behaviour and Analysis of Rapid Equilibrium and Steady-State Enzyme Systems*. Hoboken, NJ: Wiley; 1975.

135. Wilkinson GR, Shand DG. A physiological approach to hepatic drug clearance. *Clin Pharmacol Ther* 1975;18:377–390.

136. Rostami-Hodjegan A, Tucker G. *In silico* simulations to assess the *in vivo* consequences of *in vitro* metabolic drug–drug interactions. *Drug Discov Today* 2004;1(4):441–448.

137. Houston JB, Galetin A. Progress towards prediction of human pharmacokinetic parameters from *in vitro* technologies. *Drug Metab Rev* 2003;35(4):393–415.

138. Ito K, Halifax D, Obach RS, Houston JB. Impact of parallel pathways of drug elimination and multiple cytochrome P450 involvement on drug–drug interactions: CYP2D6 paradigm. *Drug Metab Dispos* 2005;33(6):837–844.

139. Obach RS, Walsky RL, Venkatakrishnan K, Gaman EA, Houston JB, Termaine LM. The utility of *in vitro* cytochrome P450 inhibition data in the prediction of drug–drug interactions. *J Pharmacol Exp Ther* 2006;316:336–348.

140. Kato M, Tachibana T, Ito K, Sugiyama Y. Evaluation of methods for predicting drug–drug interactions by Monte Carlo simulation. *Drug Metab Pharmacokinet* 2003;18(2): 121–127.

141. Rowland M, Tozer TN. Interacting drugs. In Rowland M, Tozer TN, Eds. *Clinical Pharmacokinetics: Concepts and Applications*. Philadelphia: Williams & Wilkins; 1995, pp 267–289.

142. Riley RJ, McGinnity DF, Austin RP. A unified model for predicting human hepatic, metabolic clearance from *in vitro* intrinsic clearance data in hepatocytes and microsomes. *Drug Metab Dispos* 2005;33(9):1304–1311.

143. Brown HS, Ito K, Galetin A, Houston JB. Prediction of *in vivo* drug–drug interactions from *in vitro* data: impact of incorporating parallel pathways of drug elimination and inhibitor absorption rate constant. *Br J Clin Pharmacol* 2005;60(5):508–518.

144. Blanchard N, Richert L, Coassolo P, Lave T. Qualitative and quantitative assessment of drug–drug interaction potential in man, based on K_i, IC_{50} and inhibitor concentration. *Curr Drug Metab* 2006;5(2):147–156.

145. Wang YH, Jones DR, Hall SD. Prediction of cytochrome P450 3A inhibition by verapamil enantiomers and their metabolites. *Drug Metab Dispos* 2004;32(2):259–266.

146. Ernest CS, Hall SD, Jones DR. Mechanism-based inactivation of CYP3A by HIV protease inhibitors. *J Pharmacol Exp Ther* 2005;312(2):583–591.

147. Obach RS, Walsky RL, Venkatakrishnan K. Mechanism based inactivation of human cytochrome P450 enzymes and the prediction of drug–drug interactions. *Drug Metab Dispos* 2007;35(2):246–255.

148. Kenny JR, Grime K. Pharmacokinetic consequences of time-dependent inhibition using the isolated perfused rat liver model. *Xenobiotica* 2006;36(5):351–365.

149. Warot D, Bergougnan L, Lamiable D, Berlin I, Bensimon G, Danjou P, Puech AJ. TroleandomycIn–triazolam interaction in healthy volunteers: pharmacokinetic and psychometric evaluation. *Eur J Clin Pharmacol* 1987;32:389–393.

150. Phillips JP, Antal EJ, Smith RB. A pharmacokinetic drug interaction between erythromycin and triazolam. *J Clin Psychopharmacol* 1986;6:297–299.

151. Galetin A, Burt H, Gibbons L, Houston JB. Prediction of time-dependent CYP3A4 drug–drug interactions: impact of enzyme degradation, parallel elimination pathways, and intestinal inhibition. *Drug Metab Dispos* 2006;34(1):166–175.

152. Lu C, Miwa GT, Prakash SR, Gan L, Balani SK. A novel method for the prediction of drug–drug interactions in humans based on *in vitro* CYP phenotypic data. *Drug Metab Dispos* 2007;35(1):79–85.

153. Luo G, Cunningham M, Kim S, Burn T, Lin J, Sinz M, Hamilton G, Rizzo C, Jolley S, Gilbert D, Downey A, Mudra D, Graham R, Carroll K, Xie J, Madan A, Parkinson A, Christ D, Selling B, Lecluyse E, Gan L. CYP3A4 induction by drugs: correlation between a pregnane X receptor reporter gene assay and CYP3A4 expression in human hepatocytes. *Drug Metab Dispos* 2002;30(7):795–804.

154. von Moltke LL, Durol ALB, Duan SX, Greenblatt DJ. Potent mechanism-based inhibition of human CYP3A *in vitro* by amprenavir and ritonavir: comparison with ketoconazole. *Eur J Clin Pharmacol* 2000;56(3):259–261.

155. Perloff MD, Stoermer E, von Moltke LL, Greenblatt DJ. Rapid assessment of P-glycoprotein inhibition and induction *in vitro*. *Pharm Res* 2003;20(8):1177–1183.
156. Greenblatt DJ, von Moltke LL, Harmatz JS, Durol ALB, Daily JP, Graf JA, Mertzanis P, Hoffman JL, Shader RI. Differential impairment of triazolam and zolpidem clearance by ritonavir. *J Acquir Immune Defic Syndr Hum Retrovirol* 2000;24(2):129–136.
157. Culm-Merdek KE, von Moltke LL, Gan L, Horan KA, Reynolds R, Harmatz JS, Court MH, Greenblatt DJ. Effect of extended exposure to grapefruit juice on cytochrome P450 3A activity in humans: comparison with ritonavir. *Clin Pharmacol Ther* 2006;79(3):243–254.
158. US Food and Drug Administration, Center for Drug Evaluation and Research website. http://www.fda.gov/CDER.
159. US Food and Drug Administration, Center for Drug Evaluation and Research website. Guidance web page. http://www.fda.gov/CDER/guidance.

APPENDIX A

From Fig. 22.1 it can be seen that

$$d[\mathrm{ES}]/dt = k_1 \cdot [\mathrm{E}] \cdot [\mathrm{S}] - k_{-1} \cdot [\mathrm{ES}] - k_2 \cdot [\mathrm{ES}] \tag{A.1}$$

But at steady state, $d[\mathrm{ES}]/dt = 0$; therefore,

$$k_1 \cdot [\mathrm{E}] \cdot [\mathrm{S}] = k_{-1} \cdot [\mathrm{ES}] + k_2 \cdot [\mathrm{ES}] \tag{A.2}$$

The total enzyme concentration is

$$[\mathrm{E}]_0 = [\mathrm{E}] + [\mathrm{ES}] \tag{A.3}$$

and the total substrate concentration is

$$[\mathrm{S}]_0 = [\mathrm{S}] + [\mathrm{ES}] \tag{A.4}$$

and therefore

$$[\mathrm{E}] = [\mathrm{E}]_0 - [\mathrm{ES}] \tag{A.5}$$

and

$$[\mathrm{S}] = [\mathrm{S}]_0 - [\mathrm{ES}] \tag{A.6}$$

Therefore, substituting Eqs. A.5 and A.6 into Eq. A.2 gives

$$k_1 \cdot [\mathrm{S}]([\mathrm{E}]_0 - [\mathrm{ES}]) = (k_{-1} + k_2) \cdot [\mathrm{ES}] \tag{A.7}$$

Dividing through by [ES] gives

$$\frac{k_1 \cdot [\mathrm{E}]_0 \cdot [\mathrm{S}]}{[\mathrm{ES}]} - k_1 \cdot [\mathrm{S}] = k_{-1} + k_2 \tag{A.8}$$

and therefore

$$k_{-1} + k_2 + k_1 \cdot [\mathrm{S}] = k_1 \cdot \frac{[\mathrm{E}]_0 \cdot [\mathrm{S}]}{[\mathrm{ES}]} \tag{A.9}$$

and

$$[\mathrm{ES}] = \frac{k_1 \cdot [\mathrm{E}]_0 \cdot [\mathrm{S}]}{k_1 \cdot [\mathrm{S}] + k_{-1} + k_2} \tag{A.10}$$

Dividing through by k_1 gives

$$[\mathrm{ES}] = \frac{[\mathrm{E}]_0 \cdot [\mathrm{S}]}{[\mathrm{S}] + (k_{-1} + k_2/k_1)} \tag{A.11}$$

since from the reaction scheme in Fig. 22.1 the overall dissociation rate constant for enzyme–substrate complex, $[\mathrm{ES}] = (k_{-1} + k_2)/k_1$. This is referred to as the Michaelis–Menten constant K_m. Therefore, Eq. A.11 becomes

$$[\mathrm{ES}] = \frac{[\mathrm{E}]_0 \cdot [\mathrm{S}]}{[\mathrm{S}] + K_\mathrm{m}} \tag{A.12}$$

Referring again to the reaction scheme in Fig. 22.1, the rate of reaction, v, or product formation, $d[\mathrm{P}]/dt = k_2 \cdot [\mathrm{ES}]$. Substituting this into Eq. A.12 gives

$$\frac{d[\mathrm{P}]}{dt} = v = \frac{k_2 \cdot [\mathrm{E}]_0 \cdot [\mathrm{S}]}{[\mathrm{S}] + K_\mathrm{m}} \tag{A.13}$$

where $[\mathrm{S}] >> K_\mathrm{m}$ and v tends to $k_2 \cdot [\mathrm{E}]_0$ such that the maximal reaction rate can be described as $V_\mathrm{max} = k_2 \cdot [\mathrm{E}]_0$. Equation A.13 therefore becomes

$$v = \frac{V_\mathrm{max} \cdot [\mathrm{S}]}{K_\mathrm{m} + [\mathrm{S}]} \tag{A.14}$$

$$= \frac{V_\mathrm{max}}{1 + K_\mathrm{m}/[\mathrm{S}]} \tag{A.15}$$

APPENDIX B

$$d[\mathrm{EI}]/dt = k_{+1} \cdot [\mathrm{I}] \cdot [\mathrm{E}] - (k_{-1} + k_2) \cdot [\mathrm{EI}] \tag{B.1}$$

$$d[\mathrm{EI}']/dt = k_2 \cdot [\mathrm{EI}] - (k_3 + k_4) \cdot [\mathrm{EI}'] \tag{B.2}$$

$$d[\mathrm{E}_\mathrm{inact}]/dt = k_4 \cdot [\mathrm{EI}'] \tag{B.3}$$

The *initial* rate of enzyme degradation, v_{inact}, is described by Eq. B.1, where k_{obs} is the apparent inactivation rate constant of the enzyme

$$v_{inact} = d[E_{inact}]/dt = k_4 \cdot [EI'] = k_{obs} \cdot [E]_0 \tag{B.4}$$

It is assumed that $[E_{inact}]$ is negligible before [EI′] reaches steady state; therefore, the total enzyme concentration, $[E]_0$, remains the same whether it is free, in complex with inhibitor, [EI], or inactivated [EI′]:

$$[E]_0 = [E] + [EI] + [EI'] \tag{B.5}$$

Referring to Fig. 22.3, when the levels of the inhibitor-bound enzyme are at steady state, $d[EI]/dt = 0$,

$$k_1 \cdot [E] \cdot [I] = (k_{-1} + k_2) \cdot [EI] \tag{B.6}$$

therefore,

$$[EI] = \frac{k_1 \cdot [E] \cdot [I]}{k_{-1} + k_2} \tag{B.7}$$

and when the levels of the initial complex formed between metabolic intermediate and enzyme are at steady state, $d[EI']/dt = 0$,

$$k_2 \cdot [EI] = (k_3 + k_4) \cdot [EI'] \tag{B.8}$$

therefore,

$$[EI'] = \frac{k_2 \cdot [EI]}{k_3 + k_4} \tag{B.9}$$

Substituting Eq. B.4 into Eq. B.6 gives

$$[EI'] = \frac{k_2 \cdot k_1 \cdot [I] \cdot [E]}{(k_3 + k_4) \cdot (k_{-1} + k_2)} \tag{B.10}$$

Substituting Eqs. B.8 and B.9 into Eq. B.5 gives

$$[E]_0 = [E] + \frac{k_1 \cdot [I] \cdot [E]}{(k_{-1} + k_2)} + \frac{k_2 \cdot k_1 \cdot [I] \cdot [E]}{(k_3 + k_4) \cdot (k_{-1} + k_2)} \tag{B.11}$$

To simplify Eq. B.11, the common denominator $(k_3 + k_4) \cdot (k_{-1} + k_2)$ is used:

$$[E]_0 = \frac{(k_3 + k_4) \cdot (k_{-1} + k_2)}{(k_3 + k_4) \cdot (k_{-1} + k_2)} \cdot [E] + \frac{(k_3 + k_4) \cdot k_1 \cdot [I] \cdot [E]}{(k_3 + k_4) \cdot (k_{-1} + k_2)} + \frac{k_2 \cdot k_1 \cdot [I] \cdot [E]}{(k_3 + k_4) \cdot (k_{-1} + k_2)} \tag{B.12}$$

$$= [\mathrm{E}] \cdot \frac{(k_3 + k_4) \cdot (k_{-1} + k_2) + (k_3 + k_4) \cdot k_1 \cdot [\mathrm{I}] + k_2 \cdot k_1 \cdot [\mathrm{I}]}{(k_3 + k_4) \cdot (k_{-1} + k_2)} \tag{B.13}$$

Therefore,

$$[\mathrm{E}] = \frac{(k_3 + k_4) \cdot (k_{-1} + k_2) \cdot [\mathrm{E}]_0}{k_2 \cdot k_1 \cdot [\mathrm{I}] + (k_3 + k_4) \cdot k_1 \cdot [\mathrm{I}] + (k_3 + k_4) \cdot (k_{-1} + k_2)} \tag{B.14}$$

Substituting Eq. B.13 into Eq. B.10 gives

$$[\mathrm{EI}'] = \frac{k_2 \cdot k_1 \cdot [\mathrm{I}] \cdot [\mathrm{E}]}{(k_3 + k_4) \cdot (k_{-1} + k_2)} \cdot \frac{(k_3 + k_4) \cdot (k_{-1} + k_2) \cdot [\mathrm{E}]_0}{k_2 \cdot k_1 \cdot [\mathrm{I}] + (k_3 + k_4) \cdot k_1 \cdot [\mathrm{I}] + (k_3 + k_4) \cdot (k_{-1} + k_2)} \tag{B.15}$$

$$= \frac{k_2 \cdot k_1 \cdot [\mathrm{I}] \cdot [\mathrm{E}]_0}{k_2 \cdot k_1 \cdot [\mathrm{I}] + (k_3 + k_4) \cdot k_1 \cdot [\mathrm{I}] + (k_3 + k_4) \cdot (k_{-1} + k_2)} \tag{B.16}$$

Dividing through by k_1 gives

$$[\mathrm{EI}'] = \frac{k_2 \cdot [\mathrm{I}] \cdot [\mathrm{E}]_0}{k_2 \cdot [\mathrm{I}] + (k_3 + k_4) \cdot [\mathrm{I}] + ((k_3 + k_4) \cdot (k_{-1} + k_2)/k_1)} \tag{B.17}$$

Then dividing through by $(k_2 + k_3 + k_4)$ gives

$$[\mathrm{EI}'] = \frac{(k_2/(k_2 + k_3 + k_4)) \cdot [\mathrm{I}] \cdot [\mathrm{E}]_0}{[\mathrm{I}] + \dfrac{(k_3 + k_4) \cdot (k_{-1} + k_2)}{(k_2 + k_3 + k_4) \cdot k_1}} \tag{B.18}$$

From Eq. B.18, we have

$$k_4 \cdot [\mathrm{EI}'] = \frac{(k_2 \cdot k_4/(k_2 + k_3 + k_4)) \cdot [\mathrm{I}] \cdot [\mathrm{E}]_0}{[\mathrm{I}] + \dfrac{(k_3 + k_4) \cdot (k_{-1} + k_2)}{(k_2 + k_3 + k_4) \cdot k_1}} \tag{B.19}$$

Substituting Eq. B.17 into Eq. B.3 gives

$$k_{\mathrm{obs}} = \frac{(k_2 \cdot k_4/(k_2 + k_3 + k_4)) \cdot [\mathrm{I}]}{[\mathrm{I}] + \dfrac{(k_3 + k_4) \cdot (k_{-1} + k_2)}{(k_2 + k_3 + k_4) \cdot k_1}} \tag{B.20}$$

$$k_{\mathrm{obs}} = \frac{k_{\mathrm{inact}} \cdot [\mathrm{I}]}{[\mathrm{I}] + K_{\mathrm{I}}} \tag{B.21}$$

where k_{inact} is the maximal inactivation rate constant and K_I is the inhibitor concentration that supports half the maximal rate of inactivation and, referring to Fig. 22.3, can be described by

$$k_{inact} = k_2 \cdot k_4/(k_2 + k_3 + k_4) \tag{B.22}$$

$$K_I = \frac{(k_3 + k_4)\cdot(k_{-1} + k_2)}{(k_2 + k_3 + k_4)\cdot k_1} \tag{B.23}$$

23

IN VIVO METABOLISM IN PRECLINICAL DRUG DEVELOPMENT

SEVIM ROLLAS
Marmara University, Istanbul, Turkey

Contents

23.1 INTRODUCTION

Drug biotransformation plays an important role in the absorption, distribution, metabolism, excretion, and toxicology (ADMET) properties. Undesirable ADMET properties are the cause of many drug development failures [1–3]. Many toxic side effects (carcinogenicity, tissue necrosis, apoptosis, hypersensitivity, teratogenicity) of

Preclinical Development Handbook: ADME and Biopharmaceutical Properties,
edited by Shayne Cox Gad

drugs are directly attributable to the formation of chemically reactive metabolites [4–6]. The liver is a major site for the metabolism of xenobiotics (drugs and other exogenous compounds) and endogenous compounds. Other tissues such as kidney, lungs, adrenals, placenta, brain, intestinal mucosa, and skin have some degree of drug-metabolizing capability. Drug metabolism reactions have been divided into two main classes, phase I (functionalization) includes oxidation, reduction, and enzymatic hydrolysis reactions and phase II (conjugation) includes glucuronidation, sulfation, acetylation, methylation, amino acid and glutation conjugation, and mercapturic acid formation reactions. In phase I reactions, the cytochrome P450 (CYP) enzymes are responsible for oxidative biotransformation of many organic compounds [7]. Other drug-metabolizing enzymes, flavin-containing monooxygenase, monoamine oxidase, epoxide hydrolase, UDP-glucuronosyltransferase, glutation *S*-transferase, sulfotransferase, methyltransferase, and *N*-acetyltransferase may also be important when the drug is primarily metabolized by a non-P450 enzyme [8]. Glucuronidation is a well known major drug-metabolizing reaction (pathway) in humans and changes the structure of the parent drug, and thus its chemical and biological reactivity.

Individual differences in drug biotransformation exist. Some people metabolize a drug rapidly so that therapeutically effective blood and tissue levels are not achieved; others metabolize the same drug slowly so that toxicity results. Most CYP enzymes that belong to the CYP 1, 2, or 3 families are polymorphic [9]; so it may be diffucult to predict a clinical response to a particular dose of a drug. Genetic polymorphisms have played an important role in these differences [10].

Metabolites can be obtained from plasma, urine, and bile after administration of compounds to laboratory animals and are used in preclinical *in vivo* studies as a reference standard [11–13]. The synthesis of metabolites is mostly done with parent compounds or is performed by total synthesis [14]. In addition, microbial methods can be used to obtain metabolites. The last two methods are very important for active metabolite synthesis.

Prodrug approches are very valuable in drug development. The goal of prodrug development is to solve specific pharmaceutical or pharmacological problems. The prodrug itself is inactive and is converted to the active drug *in vivo*. Early screening of their *in vitro* and/or *in vivo* plasma stability provides vital information for a stability profile of prodrug candidates [15, 16].

The application of well established preclinical *in vitro* and *in vivo* methodologies, such as gas chromatography–mass spectrometry (GC-MS) and liquid chromatography–mass spectrometry (LC-MS), is essential for drug discovery. Sensitive and specific analytical methods—for example liquid chromatography–high resolution nuclear magnetic resonance spectrometry [17, 18], LC-MS/MS (tandem mass spectrometry) [19–22], liquid chromatography–nuclear magnetic resonance/mass spectrometry (LC-NMR/MS) [23], and quadrupole time-of-flight mass spectrometry [24]—provide the identification and quantitation of metabolites. In general, this chapter is devoted to the preclinical *in vivo* metabolism of drug candidates. In the first part of this chapter, isolation, identification, synthesis, protein binding, and preclinical experimental studies are discussed, while in the following parts, *in vivo* metabolism of prodrugs, acyl glucuronides, and the role of active metabolites are covered.

23.2 *IN VIVO* METABOLISM OF DRUG CANDIDATES

In preclinical drug discovery, investigation of the *in vitro, in vivo* metabolism and toxicity screening of a drug candidate together play a very important role in the drug's success before entering into clinical use [25]. Rapid metabolism is one of the most important problems in achieving therapeutic drug levels [26]. Liver microsomal incubation has routinely been carried out by pharmaceutical companies to survey the metabolisim of potential drugs. Phase I and phase II drug-metabolizing enzymes affect the overall therapeutic and toxicity profiles of a drug. Several *in vitro* models, such as isolated perfused livers, liver tissue slices, freshly isolated hepatocytes in suspension, primary hepatocyte cultures, cell lines, microsomes, mitochondria, and expression systems, in particular, have been developed to profile human metabolism [1]. *In silico* (computational) techniques are tools that are used to predict the metabolic profiles of drugs that are in the design phase, but there is still insufficient data on the efficacy of *in silico* techniques. That is why *in vivo* metabolism studies should be performed on pharmacophore groups for an *in silico* database. *In vivo* metabolism is still being studied for conventional drugs in humans or animals for the detection of unknown metabolites [27–31]. During drug development, *in vivo* drug absorption, metabolic fate, and hepatic first-pass metabolism studies generally are performed in rats, dogs, and/or monkeys [32–34]. Indeed, the results of *in vitro* metabolism may not be the same as results of *in vivo* metabolism in animals and humans. Reliable human tests should be carried out. Human hepatocytes are used to model biotransformation in the human liver to predict human clearance [35–37]. Dog hepatocytes have also been used. However, the most successful results have been provided using human hepatocytes [38, 39]. Investigating the stereoselective metabolism of optical isomers of drugs is crucial in distinguishing their pharmacokinetic behaviors. The formation of sulfone, hydroxy, and 5-*O*-demethyl metabolites from *S*- and *R*-omeprazole using liver microsomes has been reported [40]. The metabolism of the optical isomers of omeprazole exhibits a significant stereoselectivity. Current strategies in high throughput chemistry are focused on high quality lead compounds [41]. Therefore animal testing is the most important step for lead identification and *in vitro–in vivo* correlation. The preclinical evaluation of selected lead compounds is represented in Fig. 23.1.

23.2.1 Isolation and Identification of Metabolites

Metabolite isolation and identification are important processes in discovery and development of new drugs. In many cases, the isolation and identification of metabolites are diffucult because of the low concentration or instability of these compounds in biological matrix. Therefore metabolites are synthesized and characterized by spectroscopic methods. The drug metabolism methodologies may be divided into isolation technologies (e.g., extraction, fractioning, chromatography) and chemical characterization (by means of spectroscopic techniques). For *in vivo* characterization of metabolites, biological samples are collected and it is determined what extraction methods (e.g., preparative solid phase extraction, solid phase extraction, liquid–liquid extraction, or protein precipitation (deproteination)) are necessary for analysis of the samples. Several studies reported use of extraction processes [13, 14,

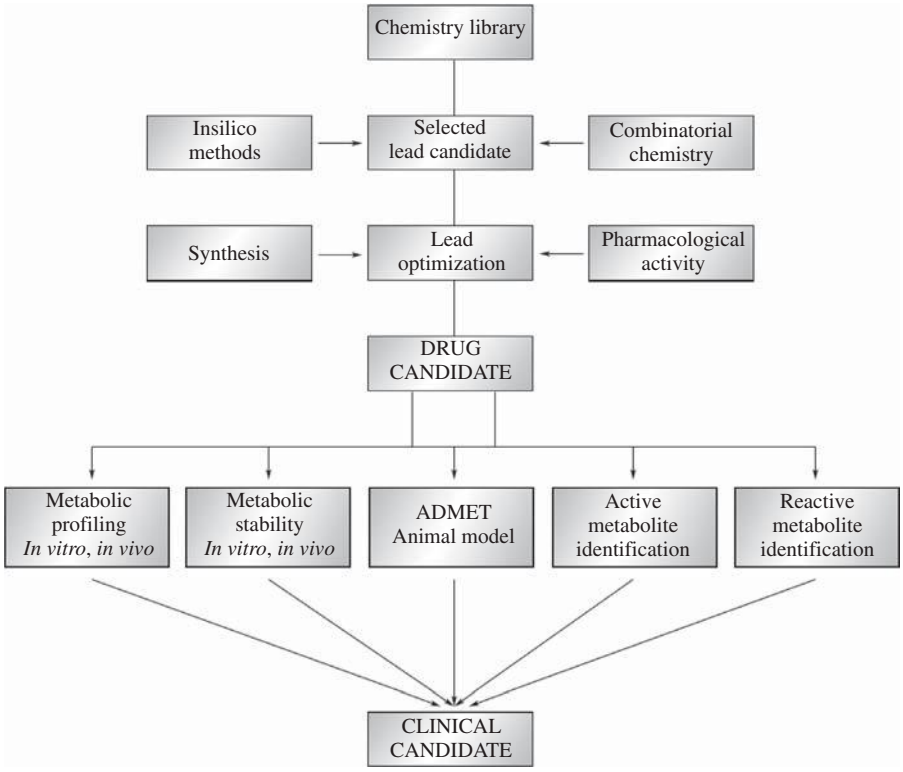

FIGURE 23.1 Preclinical evaluation of selected lead candidates.

19, 34, 42–46]. Recently, the use of turbulent flow chromatography with online solid phase extraction and column switching for sample preparation has been reported by Ong et al. [47]. Development of an analytical methodology suitable for accurate determination of both drug and metabolite in biological fluids is an advantange for the examination of the metabolic profile of a drug. The well known technique of liquid chromatography–tandem mass spectrometry (LC-MS/MS), can provide information for the identification for drug metabolites [25, 48]. High resolution nuclear magnetic resonance (NMR) spectroscopy is widely used for structure elucidation of organic compounds and their metabolites in biological samples [49–51]. The most high throughput analytical method for substrate and metabolite analysis is liquid chromatography with parallel NMR and mass spectrometry (LC-NMR/MS) [23, 49]. Timm and colleagues [42] reported another method for the analysis of oral platelet aggregation inhibitor, a double protected prodrug, and its metabolites by using HPLC—column switching combined with turbo ion spray single quadrupole mass spectrometry after precipitation of plasma protein by 0.5 M perchloric acid. Deproteination is a suitable method for sample preparation. Acetonitrile, methanol, perchloric acid, and trichloroacetic acid are used as deproteination agents [52–56]. Hydrophilic glucuronide conjugates may be hydrolyzed by β-glucuronidase in acetate buffer [28, 29, 57] or by acid or alkali [46, 58, 59] before being analyzed. In recent years, ultra performance liquid chromatography (UPLC) [60] has been used

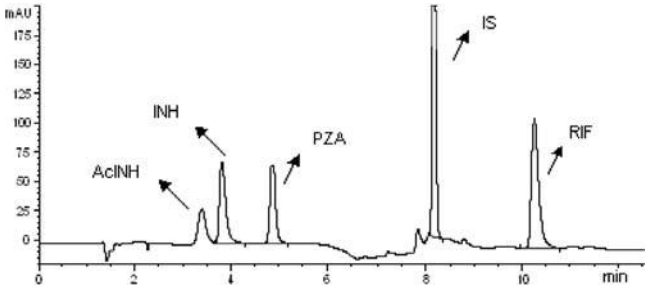

FIGURE 23.2 HPLC chromatogram of AcINH (acetylisoniazide), INH (isoniazide), PZA (pyrazinamide), IS (internal standard), and RIF (rifampin). Pore size is 4 μm Pore 3.9 × 150 mm long Nova-Pak C_{18} column. Signals were monitored by diode array detector. Gradient elution was used.

for drug and metabolite identification in biological fluids [61, 62]. Johnson and Plump [62] reported human metabolism of acetaminophen using UPLC with quadrupole time-of-flight mass analysis. Dear et al. [52] also reported a new approach by using UPLC for *in vivo* metabolite identification. These novel fast and successful methods may be applied to preclinical *in vivo* metabolite identification of drug candidates.

Metabolites alter the quantity of drug during pharmacokinetic or drug monitoring studies if an efficient separation is not provided. In our study on the monitoring of isoniazide, pyrazinamide, and rifampicin, for the separation of isoniazid and its major metabolite acetylisoniazid, we developed an HPLC analysis method represented in Fig. 23.2 for the drug monitoring study [55].

23.2.2 Synthesis of Metabolites

Metabolite identification and synthesis are important processes in the development of new lead candidates for drug metabolite profiling, pharmacokinetic studies (interference of metabolite), pharmacological activity testing (for active metabolite), metabolite quantification, CYP identification, and toxicity testing. Therefore a synthesis of methods are needed to obtain authentic metabolites. The synthesis of metabolites that are not easily obtained by chemistry methods may be produced by microbial biotransformation of the drugs. Chemical synthesis [14, 63] and microbial methods [64–66] are reported in the literature. Sulfadimethoxine *N*-glucuronide was prepared by Bridges et al. [67] starting from sodium sulfadimethoxine and methyl 2,3,4-tri-*O*-acetyl-1-bromoglucuronate. Ketotifen [68] and soraprazam [69] glucuronides have also been prepared synthetically. The N-oxide metabolite of the model compound *N*-benzyl-*N*-methylaniline was prepared by oxidizing with hydrogen peroxide [70]. Sulfinpyrazone sulfide metabolite was prepared by He et al. [71] by the reduction of sulfinpyrazone with iron powder. The hydroxamic acid metabolites are usually obtained from molecules containing an ester functional group [72].

The use of microbial models is a suitable method to produce a sufficient quantity of metabolites [73, 74]. Most bacterial species have P450 enzymes [75]. Enantiomeri-

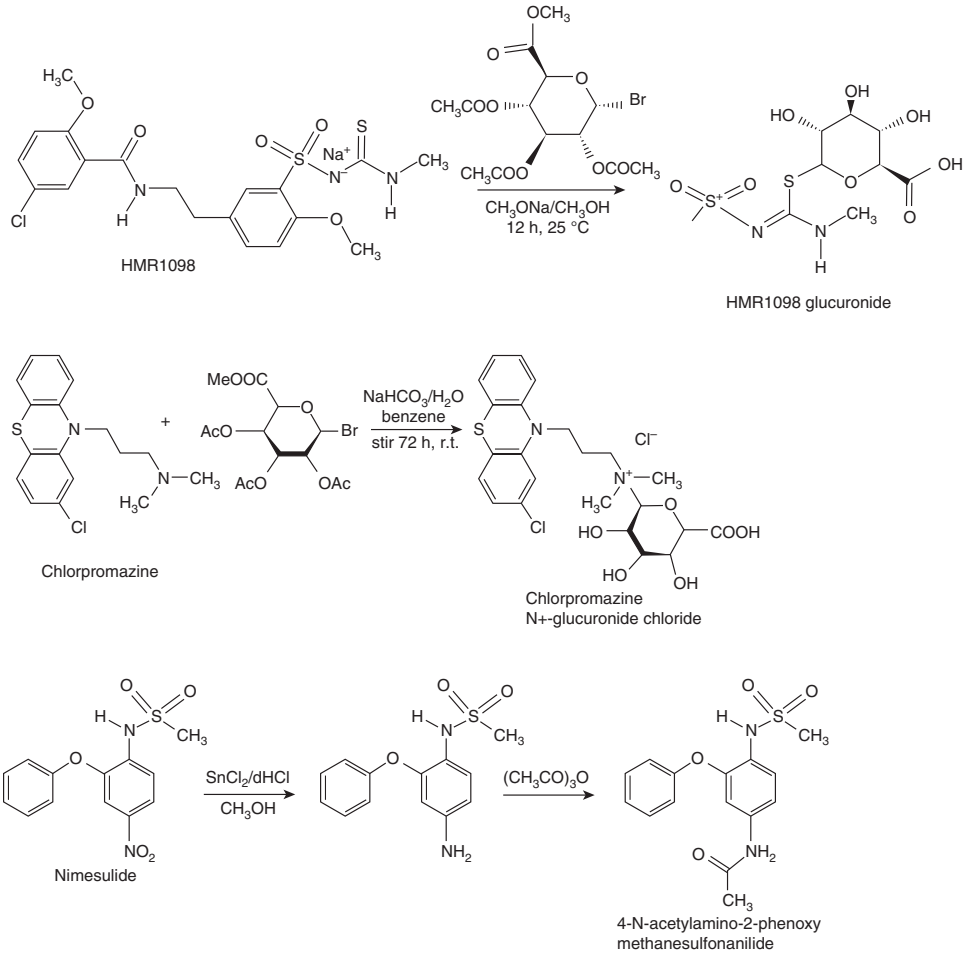

FIGURE 23.3 Examples for synthesis of some metabolites.

cally pure sulfoxides may be synthesized by biocatalytic methods using microorganisms or isolated enzymes. Ricci et al. [76] prepared aromatic sulfoxides from sulfides employing Basidiomycetes. Zhang et al. [77] reported biotransformation of amitriptyline by the filamentous fungus *Cunninghamella elegans*. The amitriptyline N-oxide metabolite that is produced from fungus can also be obtained by the oxidation of amitriptyline with 3-chloroperoxybenzoic acid to compare with the microbial product. The biosynthesis of drug glucuronides may be performed using suitable animal microsomes to obtain glucuronide metabolites [78]. The synthesis route of some metabolites is shown in Fig. 23.3 [20, 79, 80].

23.2.3 Protein Binding of Metabolites

Most drugs and/or their metabolites bind to plasma proteins and other blood components such as red blood cells [81–84]. Generally, free drug molecules can arrive

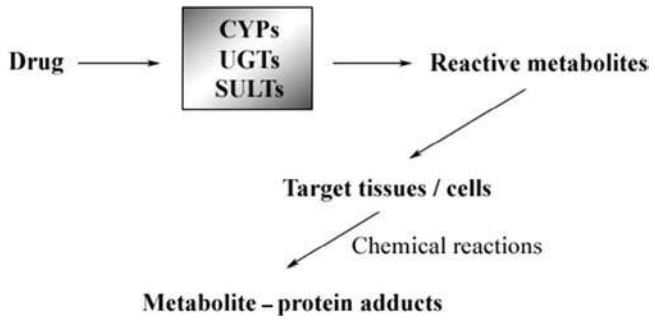

FIGURE 23.4 Formation of metabolite–protein adducts of drugs.

at the site of action. They are distributed into tissues for direct binding to tissue proteins [85]. Binding of a drug to plasma protein influences the drug's ADME processes. Yamazaki and Kanaoka [86] have developed a computational method that can provide precise and useful prediction of plasma protein binding for new drug candidates. However, preclinically, the *in vivo* studies must also be performed on drug candidates. The binding of drugs and/or their metabolites to plasma and tissue proteins is reversible. In some cases, they may covalently bind to plasma and tissue proteins, resulting of drug–protein or metabolite–protein adducts [87–89]. In most cases, the covalent binding by drugs is via their reactive metabolites [90–93]. Covalent binding to tissue proteins has been demonstrated for several metabolites such as acetaminophen–quinoneimine metabolite [94], carbamazepine–10,11-epoxide metabolite [95], furosemide–epoxide metabolite [88], ibuprofen–glucuronide metabolite [96], clozapine–nitrenium ion derived from clozapine N-oxide metabolite [97], and valproic acid–4-ene metabolite [98]. Formation of metabolite–protein adducts of drugs is represented in Fig. 23.4.

23.2.4 Preclinical Experimental Studies

The application of human-based preclinical *in vitro* hepatic metabolism (hepatocyte or liver microsome) is a must for the evaluation of drug metabolism and the selection of drug candidates with a probability of clinical success. However, *in vitro* metabolic stability and metabolite profiling studies should be correlated with *in vivo* experiments with relevant laboratory animal species for prediction of *in vivo* human drug properties [99]. Sample preparation is the most important element in *in vivo* metabolism studies. Conventional solid phase extraction is performed with a C_{18} cartridge [82, 100, 101]. Recently, Oasis HLB (hydrophilic–lipophilic balance), MCX (mixed mode, cation-exchange), and MAX (mixed mode, anion-exchange) cartridges have been developed to prepare samples [102–104]. Cleanup of the samples by means of solid phase extraction is shown Fig. 23.5.

Examples of *in vivo* metabolism studies are given next. The metabolite profile of 5-(2-ethyl-2*H*-tetrazol-5-yl)-1-methyl-1,2,3,6-tetrahydropyridine (Lu 25-109), a muscarine agonist, has been reported in mice, rats, dogs, and humans in plasma and

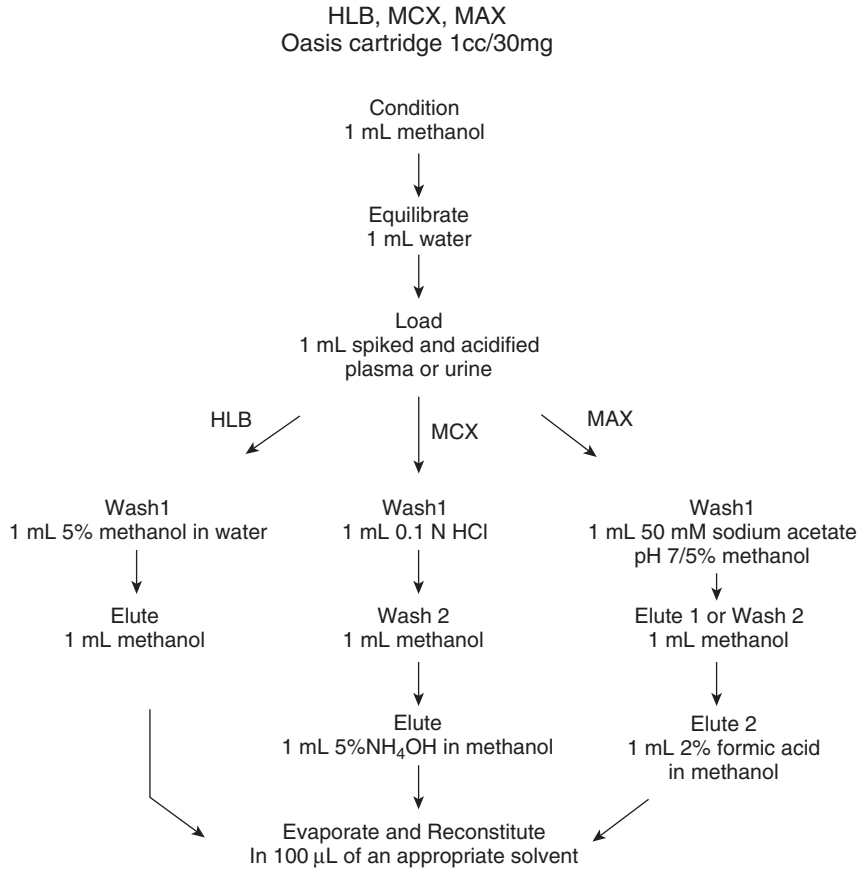

FIGURE 23.5 Cleanup of the samples by HLB, MCX, and MAX cartridges.

urine after oral administration of [^{14}C]Lu 25-109. The *N*-deethyl metabolite is a major metabolite in human plasma. The formation of a pyridine derivative has only been shown in rats [105].

The myocardial binding of the high potency antipsychotic benzisoxazol derivative risperidone and its active metabolite, 9-hydroxyrisperidone, was studied by using equilibrium dialysis *in vitro* and using intraperitoneal administration *in vivo* on plasma and tissue samples of guinea pig by Titier et al [106]. Risperidone and its metabolite concentrations have been determined by the HPLC method with UV detection. The plasma protein and tissue binding of 9-hydroxyrisperidone was lower than that of the more lipophilic risperidone. This method can be applied for other drugs and for therapeutic drug monitoring [106].

In our laboratory, *in vivo* metabolic pathway selected model compounds—1,2,4-triazole-3-thiones [82, 107], hydrazide [108], thiourea derivative [109], azo compounds [110, 111], and quinazolinone [112] and pyridazine [113] rings compounds—were investigated in rats (Fig. 23.6). The potential metabolites of substrate, which cannot be provided, were synthesized. Unknown metabolites were

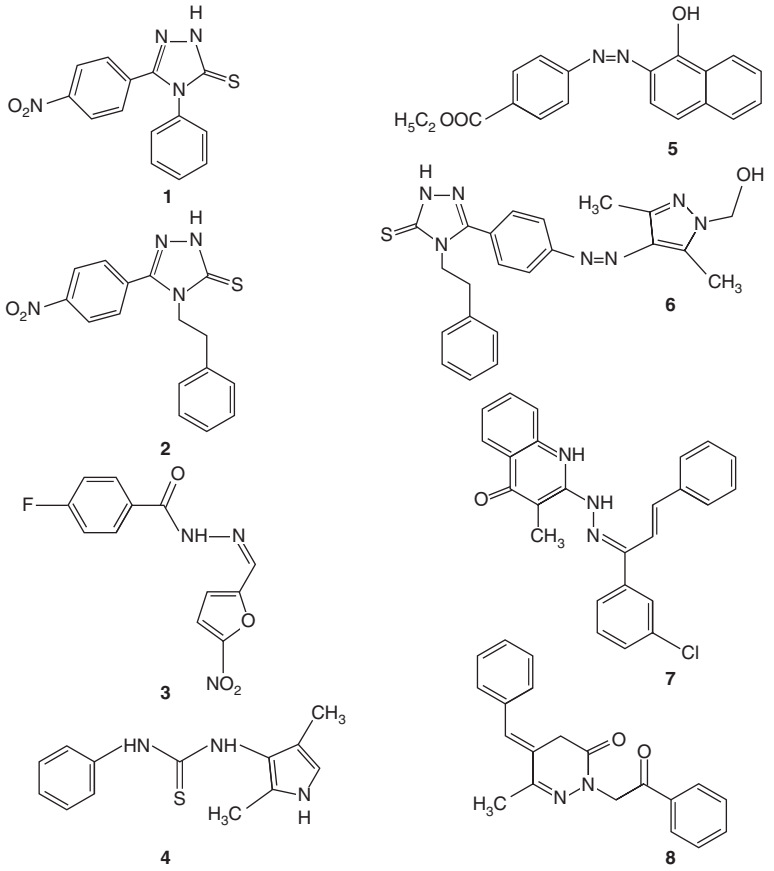

FIGURE 23.6 Examples of model compounds investigated for their *in vivo* meta-bolism: (**1**) 5-(4-nitrophenyl)-4-phenyl-2,4-dihydro-3*H*-1,2,4-triazole-3-thione [82]; (**2**) 5-(4-nitrophenyl)-4-(2-phenylethyl)-2,4-dihydro-3*H*-1,2,4-triazole-3-thione [107]; (**3**) 4-fluorobenzoic acid [(5-nitro-2-furanyl)methylene]hydrazide [108]; (**4**) *N*-phenyl-*N*′-(3,5-dimethyl-pyrazole-4-yl)thiourea [109]; (**5**) ethyl 4-[(2-hydroxy-1-naphthyl)azo]benzoate [110]; (**6**) 4-phenylethyl-5-[4-(1-(2-hydroxy-ethyl)-3,5-dimethyl-4-pyrazolylazo)-phenyl]-2,4-dihydro-3*H*-1,2,4-triazole-3-thione [111]; (**7**) 2-[1′-phenyl-3′-(3-chlorophenyl)-2′-propenylyden]hydrazino-3-methyl-4(3*H*)-quinazolinone [112]; (**8**) 3-oxo-5-benzylidene-6-methyl-(4*H*)-2-(benzoylmethyl)pyridazine [113].

collected during HPLC studies for mass analysis. Desulfurization reaction did not occur in the 1,2,4-triazole-3-thiones model compounds. Their oxygen analogues were synthesized and used as a reference standard in these studies. Examples of model compounds investigated for their *in vivo* metabolism are shown in Fig. 23.6.

4-Fluorobenzoic acid [(5-nitro-2-furanyl)methylene]hydrazide (substrate) is active against *Staphylococcus aureus* ATCC 29213 (MIC value 3.25 μg/mL) [114]. It was administered intraperitoneally in doses of 50 or 100 mg/kg. Blood samples were collected after administration. The substrate and its potential metabolites were synthesized and separated using HPLC [108]. The substrate and its potential metabolites were not detected in plasma. After plasma proteins were denaturated, 4-

fluorobenzoic acid (1.5 h) was detected. However, it rapidly metabolizes via a hydrolytic reaction in rats and shows poor metabolic stability *in vivo*.

23.3 *IN VIVO* METABOLISM OF PRODRUGS

Drug activation has been known since the identification of prontosil as a bioreductive prodrug of sulfanylamide. The aim of prodrug development is to solve specific pharmaceutical or pharmacological problems. Various drugs with groups that can be modified by chemical reactions can be converted into prodrugs. They can be synthesized to improve drug stability and absorption, to reduce diverse effects, to extend the duration of action, to increase water solubility or other desirable properties, and to allow site-specific delivery [115]. Generally, synthetic or natural compounds with therapeutic potential as bioactive agents contain alcohol, phenol, ester, thioether, amino, or nitro groups in their structure. In the synthesis of prodrugs, mainly esters, amides, ethers, phosphamides, hydroxamic acids, imines, N-oxides, Mannich bases, azo groups, glycosides, peptides, salts, polymers, and complexes from the parent drug are obtained. The anti-inflammatory drug sulindac is a prodrug and its two active metabolites—sulindac sulfide and sulindac sulfone—result from reduction and oxidation, respectively [116]. This type of prodrug is called a *bioprecursor*. Examples of other bioprecursors are diazepam, primidone, and clofibrate. Quantitative prediction of the effect of a prodrug's enzymatic catalysis *in vivo* is diffucult due to the variety and complexity of enzyme systems [117]. The conversion of a prodrug into a parent drug is represented schematically in Fig. 23.7.

23.3.1 Ester and Amide Prodrugs

Esterification and amidation are two important reactions for the synthesis of prodrugs. Many drugs contain free carboxylic acid and/or an amine group. Chandrasekaran et al. [118] reported that the nonsteroidal anti-inflammatory drug indomethacin conjugated with triethylene glycol at the carboxylic acid to obtain its ester and amide prodrugs. Sriram et al. [119] synthesized the amino acid ester prodrug of stavudine for the effective treatment of HIV/AIDS. Wu et al. [120] synthesized lipophilic metronidazol esters using enzymes as catalyst. The best enzymatic transesterfication is provided by *Candida antarctica* lipase acrylic resin.

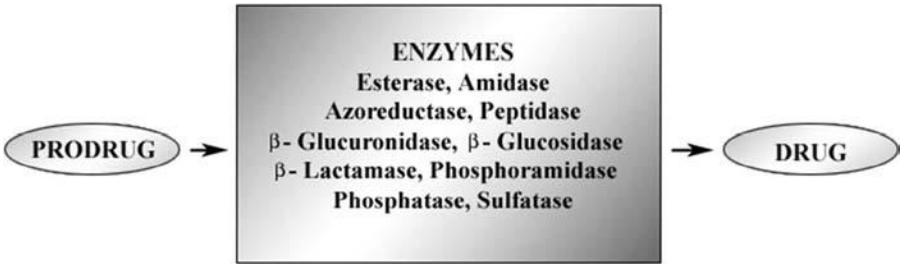

FIGURE 23.7 Conversion of prodrug to parent drug.

23.3.2 Other Prodrugs

Generally, prodrugs are designed for dealing with problems like rapid metabolism or poor absorption or reducing diverse effects seen with conventional drugs. In recent years, tumor-activated prodrug (TAP) strategies have become a very important approach in cancer therapy [121]. These prodrugs can be selectively activated in tumor tissue. The aromatic and aliphatic N-oxides, quinones, aromatic nitro groups, and cobalt complexes are the most important structures in developing hypoxia-selective TAPs [122]. Monoclonal antibody–enzyme conjugates (antibody-directed enzyme prodrugs) have recently been developed and rituximab, cetuximab, and trastuzumab are being used in the clinical setting [123,124]. β-Lactamase-dependent prodrugs have also been developed for antibody-directed enzyme therapy [125].

Another class of prodrugs is the dendritic prodrugs, which can improve drug delivery and solubility: thus decreasing dosages and prolonging drug release [126–128]. Najlah et al. [129] reported that the design, synthesis, and characterization of polyamidoamine (PAMAM) dendrimer-based prodrugs are described by selecting as the model compound naproxen, a poorly water-soluble drug. Propranolol-G_3 PAMAM dendrimer conjugates were also synthesized to increase propranolol solubility [130]. Salamonczyk [131] prepared phosphorus-based dendrimers of acyclovir.

23.3.3 Metabolic Stability of Prodrugs

The metabolic stability of a drug candidate in liver microsomes of different animal species is determined in order to assess the potential of this drug to form undesired, potentially toxic, or pharmacologically inactive/active metabolites. In the determination of metabolic stability, *in vitro* models were widely used in order to investigate the metabolic fate of drug candidates. Liver microsomes and S9 (cytosolic and mitochondrial) fractions as drug-metabolizing enzyme sources are used for metabolic stability studies [132]. Di et al. [133] have suggested a single time-point microsomal stability assay and incubation time of 15 min for metabolic stability profiling at the early stage of drug discovery. The duration and/or the intensity of action of most drugs are determined by their rate of metabolism by hepatic enzymes [134]. The metabolic stability procedure involves the following [15, 16, 135]:

- Preparation of buffers
- Preparation of stock solution of test compound (in DMSO or water)
- Incubation (at 37 °C)
- Sample preparation
- Determination of loss of parent compound (using LC-MS, LC-MS/MS)

Screening of plasma stability of the prodrugs is very important for rapid conversion in plasma [136]. However, *in vitro* hydrolysis rates of prodrugs of ester or amide must be correlated with *in vivo* hydrolysis rates [137]. Lai and Khojasteh-Bakht [138] reported a new method for prodrug stability—an automated online liquid chromatographic–mass spectrometric method.

23.4 ACYL GLUCURONIDES

Glucuronidation reaction represents the major route for elimination and detoxification of drugs. The biosynthesis of glucuronides is catalyzed by the uridine diphosphate glucuronosyltransferases, which are localized in hepatic endoplasmic reticulum. However, the glucuronidation of some drugs has been observed in human kidney microsomes [135]. Seventeen human UDP-glucuronosyltransferases have been identified to date [139]. The mechanism of glucuronidation is a nucleophilic substitution reaction and the resulting glucuronide has the 1β-glycosidic configuration.

The rate of glucuronidation is dependent on the nucleophilic character of the substrate and enzyme concentration. The most systematic investigations were initiated in the 1930s by R. T. Williams and collaborators [140, 141]. Acyl glucuronide metabolites of carboxylic acid may be hydrolyzed under physiological conditions. Therefore the glucuronides produced can potentially interfere with the pharmacokinetics of the parent drug. In this case, early pharmacokinetic study is important in animal models to regulate dosing and duration of action.

On the other hand, glucuronide conjugates are capable of cellular injury (e.g., hepatotoxicity, carcinogenesis) by facilitating the formation of reactive electrophilic intermediates and their transport into target tissues [87]. Acyl glucuronides are chemically unstable in aqueous solution and undergo the intramolecular acyl migration. The acyl group may migrate to the C-2, C-3, or C-4 position of the glucuronic acid from the 1β position [142]. In addition, unstable acyl glucuronides have also been shown to form covalent adducts with proteins under *in vivo* conditions. The existence of genetic polymorphism in the rate of drug acylation has important consequences in drug therapy. Chen et al. [143] developed a rapid *in vitro* method for the assessment of the stability of acyl glucuronides. Many nonsteroidal anti-inflammatory drugs, such as diclofenac, diflunisal, zomepirac, and naproxen, and other drugs, such as valproic acid, citalopram, and furosemide, which bear the carboxylic functional group, have been metabolized to form acy lglucuronides [49, 144, 145].

23.5 ROLE OF ACTIVE METABOLITES IN PRECLINICAL DRUG DEVELOPMENT

Drugs can metabolize inactive, reactive, or pharmacologically active molecules [146, 147]. Fura et al. [148] and Guengerich et al. [149] define an active metabolite as the active metabolic product possessing the same pharmacological activity as the parent drug. Pharmacologically active metabolites should be recognized at the drug discovery stage, because the potential contribution of an active metabolite to total activity is an important factor for pharmacokinetic properties of a drug candidate. Therefore active metabolite kinetics should be studied in animal models. Klein et al. [150] reported a population pharmacokinetic model for irinotecan and two of its metabolites, SN-38 and SN-38 glucuronide. The active metabolite 7-hydroxycamptothecin (SN-38) is 300–1000 times more potent than its parent molecule irinotecan. Therefore it is important to develop dosing strategies for irinotecan. Mak and Weglicki [151] reported on the antioxidant properties of 4-hydroxypropranolol, a major metabolite of propranolol. It is four- to eightfold more potent than vitamin E. As a result, 4-hydroxypropranolol may contribute to the cardiovascular therapeutic

benefits of propranolol because of its endothelial cytoprotective efficacy against cell injury.

Active metabolites play a role as lead candidates during lead optimization [148, 152]. For example, ezetimibe was found during the lead optimization phase [152]. During drug development, it is sometimes impossible to characterize the pharmacological activity of active metabolites because of the difficulties in their synthesis by common methods. They may be more active than their respective parent molecules. However, a number of active metabolites have been marketed as drugs: for example, acetaminophen, cetirizine, imipramine, desloratadine, fexofenadine, mesoridazone, nortriptyline, and oxazepam [148].

Metabolism of the antifungal drug itraconazole (ITZ) involves both phase I (oxidative) and phase II (conjugative) pathways. One of these metabolites, hydroxy-itraconazole (OH-ITZ), possesses antifungal activity similar to that of ITZ [153]. Therefore, the pharmacokinetic behavior of ITZ may be affected by its active metabolites. Gasparro et al. [154] reported that the active metabolite *R*-desmethyl-deprenyl of *R*-deprenyl has been shown to be more active than R-deprenyl. Ciclesonide, an inhaled corticosteroid with prolonged anti-inflammatory activity, is being developed for the treatment of asthma. Nave et al. [155] reported ciclesonide is converted to an active metabolite, desisobutyryl-ciclesonide, which undergoes reversible fatty acid conjugation in *in vitro* studies. Cannell et al. [144] demostrated that nonsteroidal anti-inflammatory drugs (diflunisal, zomepirac, and diclofenac), acyl glucuronides, and their rearrangement isomers had antiproliferative activity on human adenocarcinoma HT-29 cells in culture.

In conclusion, active metabolites may:

- Alter pharmacokinetic properties of parent compounds.
- Cause enzyme induction or inhibition.
- Alter pharmacokinetics of drugs when used together.
- Show different pharmacological activity.
- Be toxic.

23.6 CURRENT APPROACHES FOR EVALUATING PRECLINICAL *IN VIVO* METABOLISM

Metabolism is one of the most important steps in ADMET studies. Metabolites affect pharmacokinetic results [156]. *In vivo* pharmacokinetic behavior involves permeability, metabolic stability, inhibition, and induction of CYP isoenzymes and plasma protein binding. A new approach may be the use of ultra performance liquid chromatography [52], online hyphenated LC-NMR/MS [48], and an integrated high capacity solid phase extraction–MS/MS system [157] for *in vivo* metabolite identification in the future. Metabolism is also one of the most complicated of the pharmacokinetic properties. Genetic, environmental, and physiological factors may affect drug metabolism. Computational approaches for predicting CYP-related metabolism is very important for the evaulation of a successful new drug [158]. Therefore, CYP inhibitors, CYP inducers, CYP regioselectivity, and CYP substrates have been studied for the development of a reliable predictive model.

Computational or virtual ADME [2, 26, 159–162] and metabolism models derived from past *in vitro* and *in vivo* data have been developed to contribute to new drug discovery in the pharmaceutical industry [163, 164]. Klopman et al. [165] evaluated a computer model for prediction of intestinal absorption in humans. This model may be applied to particularly active metabolites. Recent studies have shown that one of the current trends will be drug-induced autoimmunity. Idiosyncratic drug reactions that do not occur in most patients are an important clinical problem [166]. Most of these reactions appear to be immune-mediated reactions. It is nessesary to develop new animal models, in addition to the present models, for preclinical studies. However, the newest approaches of drug discovery may be the mechanism-based, the function-based, and the physiology-based approaches [167].

23.7 CONCLUSION

In the last few years, much effort in drug discovery and development has focused on defining the metabolic profile, toxicity, stereoselective metabolism, and pharmacokinetics of new drug candidates. Understanding the role of drug–metabolizing enzymes in drug metabolism is an important area of research for human toxicology testing. *In vitro* and *in vivo* models have been used as part of high throughput screening programs to characterize lead identification, drug metabolic profiling, metabolic stability, drug permeability, drug solubility, and drug safety. *In vitro* studies generally provide a valuable insight into a drug's metabolic profile in humans; however, sometimes there are discrepancies between *in vitro* results and *in vivo* findings. In the future, the use of *in silico* predictive models and ultra developed analysis techniques for preclinical *in vivo* studies will be an essential requirement for the discovery and development of successful new drugs.

REFERENCES

1. Sivaraman A, Leach JK, Townsend S, Iida T, Hogan BJ, Stolz DB, Fry R, Samson LD, Tannenbaum SR, Griffith LG. A microscale *in vitro* physiological model of the liver: predictive screens for drug metabolism and enzyme induction. *Curr Drug Metabolism* 2005;6:569–591.
2. Bugrim A, Nikolskaya T, Nikolsky Y. Early prediction of drug metabolism and toxicity: systems biology approach and modeling. *Drug Discov Today* 2004;9:127–135.
3. Ekins S, Ring BJ, Grace J, McRobie-Belle DJ, Wrighton SA. Present and future *in vitro* approaches for drug metabolism. *Pharmacol Toxicol Methods* 2000;44:313–324.
4. Wells PG, Kim PM, Laposa RR, Nicol CJ, Parman T, Winn LM. Oxidative damage in chemical teratogenesis. *Mutat Res* 1997;396:65–78.
5. Williams DP. Toxicophores: investigations in drug safety. *Toxicology* 2006;226:1–11.
6. Park KB, Dalton-Brown E, Hirst C, Williams DP. Selection of new chemical entities with decreased potential for adverse drug reactions. *Eur J Pharmacol* 2006;549:1–8.
7. Rendic S. Summary of information on human CYP enzymes: human P450 metabolism data. *Drug Metab Rev* 2002;34:438–448.
8. Lu AYH, Wang RW, Lin JH. Cytochrome P450 *in vitro* reaction phenotyping: a re-evaluation of approaches used for P450 isoform identification. *Drug Metab Dispos* 2003;31:345–350.

9. Agundez JAG. Cytochrome P450 gene polymorphism and cancer. *Curr Drug Metab* 2004;5:211–224.
10. Dorne JLCM, Walton K, Renwick AG. Human variability in xenobiotic metabolism and pathway-related uncertainty factors for chemical risk assessment: a review. *Food Chem Toxicol* 2005;43:203–216.
11. Williams RT. Studies in detoxification 13. The biosynthesis of aminophenyl- and sulphonamidoaminophenyl- glucuronides in the rabbit and their action on haemoglobin *in vitro*. *Biochem J* 1943;37:329–333.
12. Turgeon J, Pare JRJ, Lalande M, Grech-Belanger O, Belanger PM. Isolation and structural characterization by spectroscopic methods of two glucuronide metabolites of mexiletine after N-oxidation and deamination. *Drug Metab Dispos* 1992;20:762–769.
13. Sidelman UG, Christiansen E, Krogh L, Cornett C, Tjornelund J, Hansen SH. Prufication and ^{1}H NMR spectroscopic characterization of phase II metabolites of tolfenamic acid. *Drug Metab Dispos* 1997;25:725–731.
14. Lantz RJ, Gillespie TA, Rash TJ, Kuo F, Skinner M, Kuan HY, Knadler MP. Metabolism, excretion, and pharmacokinetics of duloxetine in healthy human subjects. *Drug Metab Dispos* 2003;31:1142–1150.
15. Di L, Kerns EH, Hong Y, Chen H. Develoment and application of high throughput plasma stability assay for drug discovery. *Int J Pharm* 2005;297:110–119.
16. Kerns EH, Di L. Pharmaceutical profiling in drug discovery. *Drug Discov Today* 2003; 8:316–323.
17. Mutlib AE, Chen H, Nemeth GA, Markwalder JA, Seitz SP, Gan LS, Christ DD. Identification and characterization of efavirenz metabolites by liquid chromatography/mass spectrometry and high field NMR: species differences in the metabolism of efavirenz. *Drug Metab Dispos* 1999;27:1319–1333.
18. Zhang KE, Hee B, Lee CA, Liang B, Potts BCM. Liquid chromatography–mass spectrometry and liquid chromatography–NMR characterization of *in vitro* metabolites of a potent and irreversible peptidomimetic inhibitor or rhinovirus 3C protease. *Drug Metab Dispos* 2001;29:729–734.
19. Bramer SL, Tata PNV, Vengurlekar SS, Brisson JH. Method for the quantitative analysis of cilostazol using LC/MS/MS. *J Pharm Biomed Anal* 2001;26:637–650.
20. Kucukguzel SG, Kucukguzel I, Oral B, Sezen S, Rollas S. Detection of nimesulide metabolites in rat plasma and hepatic subcellular fractions by HPLC-UV/DAD and LC-MS/MS studies. *Eur J Drug Metab Pharmacokinet* 2005;30:127–134.
21. Lampinen-Salomonsson M, Beckman E, Bondesson U, Hedeland M. Detection of altrenogest and its metabolites in post administration horse urine using liquid chromatography tandem mass spectrometry—increased sensitivity by chemical derivatization of glucuronic acid conjugate. *J Chromatogr B* 2006;833:245–256.
22. Guo L, Qi M, Jin X, Wang P, Zhao H. Determination of active metabolite of prulifloxacin in human plasma by liquid chromatography–tandem mass spectrometry. *J Chromatogr B* 2006;832:280–285.
23. Corcoran O, Spraul M. LC-NMR-MS in drug discovery. *Drug Discov Today* 2003; 8:624–631.
24. Ishigai M, Langridge JI, Bordoli RS. A new approach for dynamics of enzyme-catalyzed glutation conjugation by electrospray quadrupole/time–of-flight mass spectrometry. *Anal Biochem* 2001;298:83–92.
25. Lee M-Y, Dordick JS. High-throughput human metabolism and toxicity analysis. *Curr Opin Biotechnol* 2006;17:1–9.

26. Tarbit MH, Berman J. High-throughput approaches for evaluating absorption, distribution, metabolism and excretion properties of lead compounds. *Curr Opin Chem Biol* 1998;2:411–416.
27. Schaber G, Wiatr G, Wachsmuth H, Dachtler M, Albert K, Gaertner I, Breyer-Pfaff U. Isolation and identification of clozapine metabolites in patient urine. *Drug Metab Dispos* 2001;29:923–931.
28. Strickmann DB, Blaschke G. Isolation of an unknown metabolite of non-steroidal anti-inflammatory drug etodolac and its identification as 5-hydroxy etodolac. *J Pharm Biomed Anal* 2001;25:977–984.
29. Desmoulin F, Gilard V, Martino R, Malet-Martino M. Isolation of an unknown metabolite of capecitabine, an oral 5-fluorouracil prodrug, and its identification by nuclear magnetic resonance and liquid chromatography–tandem mass spectrometry as a glucuroconjugate of 5′-deoxy-5-fluorocytidine, namely 2′-(β-D-glucuronic acid)-5′-deoxy-5-fluorocytidine. *J Chromatogr B* 2003;792:323–332.
30. Walles M, Thum T, Levsen K, Borlak J. Metabolism of verapamil: 24 new phase I and phase II metabolites identified in cell cultures of rat hepatocytes by liquid chromatography–tandem mass spectrometry. *J Chromatogr B* 2003;798:265–274.
31. Aresta A, Carbonara T, Palmisano F, Zambonin CG. Profiling urinary metabolites of naproxen by liquid chromatography–electrospray mass spectrometry. *J Pharm Biomed Anal* 2006;41:1312–1316.
32. Bertrand M, Jackson P, Walther B. Rapid assessment of drug metabolism in the drug discovery process. *Eur J Pharm Sci* 2000;11(Suppl 2):S61–S62.
33. Ward KW, Smith BR. A comprehensive quantitative and qualitative evaluation of extrapolation of intravenous pharmacokinetic parameters from rat, dog and monkey to humans. I. Clearance. *Drug Metab Dispos* 2004;32:603–611.
34. Mattiuz EL, Ponsler GD, Barbuch RJ, Wood PG, Mullen JH, Shugert RL, Li Q, Wheeler WJ, Kuo F, Conrad PC, Sauer J-M. Disposition and metabolic fate of atomoxetine hydrocloride: pharmacokinetics, metabolism, and excretion in the Fischer 344 rats and beagle dog. *Drug Metab Dispos* 2003;31:88–97.
35. Wilkening S, Stahl F, Bader A. Comparison of primary human hepatocytes and hepatoma cell line HEPG2 with regard to their biotransformation properties. *Drug Metab Dispos* 2003;31:1035–1042.
36. Naritomi Y, Terashita S, Kagayama A, Sugiyama Y. Utility of hepatocytes in predicting drug metabolism: comparison of hepatic intrinsic clearance in rats and humans *in vivo* and *in vitro*. *Drug Metab Dispos* 2003;31:580–588.
37. Soars MG, Burchell B, Riley RJ. *In vitro* analysis of human drug glucoronidation and prediction of *in vivo* metabolic clearance. *J Pharmacol Exp Ther* 2001;301:382–390.
38. McGinnity DF, Soars MG, Urbanowicz RA, Riley RJ. Evaluation of fresh and cryopreserved hepatocytes as *in vitro* drug metabolism tools for the prediction of metabolic clearance. *Drug Metab Dispos* 2004;32:1247–1253.
39. Iwatsubo T, Hirota N, Ooide T, Suzuki H, Shimada N, Chiba K, Ishizaki T, Green CE, Tyson CA, Sugiyama Y. Prediction of *in vivo* drug metabolism in the human liver from *in vitro* metabolism data. *Pharmacol Ther* 1997;73:147–171.
40. Abelo A, Anderson TB, Antonsson M, Naudot AK, Skanberg I, Weidolf L. Stereoselective metabolism of omeprazole by human cytochrome P450 enzymes. *Drug Metab Dispos* 2000;28:966–972.
41. Steinmeyer A. The hit-to-lead process at Schering AG: strategic aspects. *ChemMedChem* 2006;1:31–36.
42. Timm U, Birnböck H, Erdin R, Hopfgartner G., Zumbrunnen R. Determination of oral platelet aggregation inhibitor Sibrafiban® in rat, dog and human plasma utilising

HPLC–column switching with turbo ion spray single quadrupole mass spectrometry. *J Pharm Biomed Anal* 1999;21:151–163.

43. Wang XJ, Jin YX, Ying JY, Zeng S, Yao TW. Determination of rutin deca(H-) sulfate sodium in rat plasma using ion-pairing liquid chromatography after ion-pairing solid-phase extraction. *J Chromatogr B* 2006;833:231–235.
44. Wang PG, Wei JS, Kim G, Chang M, El-Shourbagy T. Validation and application of a high-performance liquid chromatography–tandem mass spectrometric method for simultaneous quantification of lopinavir and ritonavir in human plasma using semi-automated 96-well liquid–liquid extraction. *J Chromatogr A* 2006;1130:302–307.
45. Dumasia MC. *In vivo* biotransformation of metoprolol in the horse and on-column esterification of the aminocarboxylic acid metabolite by alcohols during solid phase extraction using mixed mode columns. *J Pharm Biomed Anal* 2006;40:75–81.
46. Oruc EE, Kocyigit-Kaymakcioglu B, Yilmaz-Demircan F, Gurbuz Y, Kalaca S, Kucukguzel SG, Ulgen M, Rollas S. An high performance liquid chromatographic method for the quantification of cotinine in the urine of preschool children. *Pharmazie* 2006; 61:823–827.
47. Ong VS, Cook KL, Kosora CM, Brubaker WF. Quantitative bioanalysis: an integrated approach for drug discovery and development. *Int J Mass Spectrom* 2004;238:139–152.
48. Constanzer ML, Chavez-Eng CM, Fu I, Woolf EJ, Matuszewski BK. Determination of dextromethorphan and its metabolite dextrorphan in human urine using high performance liquid chromatography with atmospheric pressure chemical ionization tandem mass spectrometry: a study of selectivity of a tandem mass spectrometric assay. *J Chromatogr B* 2005;816:297–308.
49. Yang Z. Online hyphenated liquid chromatography–nuclear magnetic resonance spectroscopy–mass-spectrometry for drug metabolite and nature product analysis. *J Pharm Biomed Anal* 2006;40:516–527.
50. Sidelmann UG, Bjornsdottir I, Shockcor JC, Hansen SH, Lindon JC, Nicholson JK. Directly coupled HPLC-NMR and HPLC-MS approaches for the rapid characterisation of drug metabolites in urine: application to the human metabolism of naproxen. *J Pharm Biomed Anal* 2001;24:569–579.
51. Vanderhoeven SJ, Lindon JC, Troke J, Nicholson JK, Wilson ID. NMR spectroscopic studies of the transacylation reactivity 1-β-*O*-acyl glucuronide. *J Pharm Biomed Anal* 2006;41:1002–1006.
52. Dear GJ, Patel N, Kelly PJ, Webber L, Yung M. TopCount coupled to ultra-performance liquid chromatography for the profiling of radiolabeled drug metabolites in complex biological samples. *J Chromatogr B* 2006;844:96–103.
53. Gemesi LI, Kapas M, Szeberenyi SZ. Application of LC-MS analysis to the characterisation of the *in vitro* and *in vivo* metabolite profiles of RGH-1756 in the rat. *J Pharm Biomed Anal* 2001;24:877–885.
54. Mohri K, Okoda K, Benet LZ. Stereoselective metabolism of benoxaprofen in rats. Biliary excretion of benoxaprofen taurine conjugate and glucuronide. *Drug Metab Dispos* 1998;26:332–337.
55. Unsalan S, Sancar M, Bekce B, Clark PM, Karagoz T, Izzettin FV, Rollas S. Therapeutic monitoring of isoniazid, pyrazinamide and rifampicin in tuberculosis patients using LC. *Chromatographia* 2005;61:595–598.
56. Nobilis M, Vybiralova Z, Sladkova K, Lisa M, Holcapek M, Kvetina J. High-performance liquid-chromatographic determination of 5-aminosalicylic acid and its metabolites in bood plasma. *J Chromatogr A* 2006;1119:299–308.
57. Zhang JY, Yuan JJ, Wang YF, Roy H, Bible JR, Breau AP. Pharmacokinetics and metabolism of a COX-2 inhibitor, valdecoxib in mice. *Drug Metab Dispos* 2003;31:491–501.

58. Kamata T, Nishikawa M, Katagi M, Tsuchihashi H. Optimized glucuronide hydrolysis for the detection of psilocin in human urine samples. *J Chromatogr B* 2003; 796:421–427.
59. Groff M, Riffel K, Song H, Lo M-W. Stabilization and determination of a PPAR agonist in human urine using automated 96-well liquid–liquid extraction and liquid chromatography/tandem mass spectrometry. *J Chromatogr B* 2006;842:122–130.
60. Wren SAC. Peak capacity in gradient ultra performance liquid chromatography (UPLC). *J Pharm Biomed Anal* 2005;38:337–343.
61. Li R, Dong L, Huang J. Ultra performance liquid chromatography–tandem mass spectrometry for the determination of epirubicin in human plasma. *Anal Chim Acta* 2005;546:167–173.
62. Johnson KA, Plumb R. Investigation of the human metabolism of acetaminophen using UPLC and exact mass oa-TOF MS. *J Pharm Biomed Anal* 2005;39:805–810.
63. Yu W, Dener JM, Dickman DA, Grothaus P, Ling Y, Liu L, Havel C, Malesky K, Mahajan T, O'Brain C, Shelton EJ, Sperandio D, Tong Z, Yee R, Mordenti JJ. Identification of metabolites of the tryptase inhibitor CRA-9249: observation of a metabolite derived from an unexpected hydroxylation pathway. *Bioorg Med Chem Lett* 2006;16:4053–4058.
64. Funhoff EG, Salzmann J, Bauer U, Witholt B, Blein JB. Hydroxylation and epoxidation reactions catalyzed by CYP153 enzymes. *Enzyme Microbial Technol* 2007;40:806–812.
65. Medici R, Lewkowicz ES, Iribarren AM. Microbial synthesis of 2,6-diaminopurine nucleosides. *J Mol Catal B: Enzymatic* 2006;39:40–44.
66. Keppler AF, Porto ALM, Schoenlein-Crusius IH, Comasseto JV, Andrade LH. Enzymatic evaluation of different *Aspergillus* strains by biotransformation of cyclic ketones. *Enzyme Microbial Technol* 2005;36:967–975.
67. Bridges JW, Kibby MR, Williams RT. The structure of the glucuronide of sulphadimethoxine formed in man. *Biochem J* 1965;96:829–836.
68. Mey U, Wachsmuth H, Breyer-Pfaff U. Conjugation of the enantiomers of ketotifen to four isomeric quarternary ammonium glucuronides in humans *in vivo* and in liver microsomes. *Drug Metab Dispos* 1999;27:1281–1292.
69. Senn-Bilfinger J, Ferguson JR, Holmes MA, Lumbard KW, Huber R, Zech K, Hummel RP, Zimmermann PJ. Glucuronide conjugates of Soraprazan (BY359), a new potassium-competitive acid blocker (P-CAB) for the treatment of acid-related diseases. *Tetrahedron Lett* 2006;47:3321–3323.
70. Kucukguzel I, Ulgen M, Gorrod JW. *In vitro* hepatic metabolism of *N*-benzyl-*N*-methylaniline. *Il Farmaco* 1999;54:331–337.
71. He M, Rettie AE, Neal J, Trager WF. Metabolism of sulfinpyrazone sulfide and sulfinpyrazone by human liver microsomes and cDNA-expressed cytochrome p450s. *Drug Metab Dispos* 2001;29:701–711.
72. Mshvidobadze EV, Vasilevsky SF, Elguero J. A new route to pyrazolo[3,4-c] and [4,3-c]pyridinones via heterocyclization of *vic*-substituted hydroxamic acids of acetylenylpyrazoles. *Tetrahedron* 2004;60:11875–11878.
73. Duhart BT, Zhang JD, Deck J, Freeman JP, Cerniglia CE. Biotransformation of protriptyline by filamentous fungi and yeasts. *Xenobiotica* 1999;29:733–746.
74. Li L, Liu R, Ye M, Hu X, Wang Q, Bi K, Guo D. Microbial, metabolism of evodiamine by *Penicillium janthinellum* and its application for metabolite identification in rat urine. *Enzyme Microbial Technol* 2006;39:561–567.
75. Lewis DFV, Wiseman A. A selective review of bacterial forms of cytochrome P450 enzymes. *Enzyme Microbial Technol* 2005;36:377–384.

76. Ricci LC, Commasseto JV, Andrabe LH, Capelari M, Cass QB, Porto ALM. Biotransformations of aryl alkyl sulfides by whole cells of white-rot Basidiomycetes. *Enzyme Microbial Technol* 2005;36:937–946.
77. Zhang D, Evans FE, Freeman JP, Duhart B Jr, Cerniglia CE. Biotransformation of amitriptyline by Cunninghamella elegans. *Drug Metab Dispos* 1995;23:1417–1425.
78. Soars MG, Mattiuz ED, Jackson DA, Kulanthaivel P, Ehlhardt WJ, Wrighton SA. Biosynthesis of drug glucuronides for use as authentic standards. *J Pharmacol Toxicol Methods* 2002;47:161–168.
79. Ethell BT, Riedel J, Englert H, Jantz H, Oekonomopulos R, Burchell B. Glucuronidation of HMR-1098 in human microsomes: evidence for the involvement of UGT1A1 in the formation of *S*-glucuronides. *Drug Metab Dispos* 2003;31:1027–1034.
80. Luo H, Hawes EM., McKay G, Midha KK. Synthesis and charecterization of quaternary ammonium-linked glucuronide metabolites of drugs with an aliphatic tertiary amine group. *J Pharm Sci* 1992;81:1079–1083.
81. Tonn GR, Kerr CR, Axelson JE. *In vitro* protein binding of propafenone and 5-hydroxypropafenone in serum, in solutions of isolated serum proteins, and to red blood cells. *J Pharm Sci* 1992;81:1098–1103.
82. Oruc EE, Rollas S, Kabasakal L, Uysal MK. The *in vivo* metabolism of 5-(4-nitrophenyl)-4-phenyl-2,4-dihydro-3*H*-1,2,4-triazole-3-thione in rats. *Drug Metab Drug Interact* 1999;15:127–140.
83. Degelman CJ, Ebner T, Ludwig E, Happich S, Schildberg FW, Koebe HG. Protein binding capacity *in vitro* changes metabolism of substrates and influences the predictability of metabolic patways *in vivo*. *Toxicol In Vitro* 2004;18:835–840.
84. Acharya MR, Sparreboom A, Sausville EA, Conley BA, Doroshow JH, Venitz J, Figg WD. Interspecies differences in plasma protein binding of MS-275, a novel histon deacetylase inhibitor. *Cancer Chemother Pharmacol* 2006;57:275–281.
85. Yang XX, Hu ZP, Chan SY, Zhou SF. Monitoring drug–protein interaction. *Clin Chim Acta* 2006;365:9–29.
86. Yamazaki K, Kanaoka M. Computational prediction of the plasma protein-binding present in diverse pharmaceutical compounds. *J Pharm Sci* 2004;93:1480–1494.
87. Bailey MJ, Dickinson RG. Acyl glucuronide reactivity in perspective: biological consequences. *Chem-Biol Interact* 2003;145:117–137.
88. Park K, Williams DP, Naisbitt DJ, Kitteringham NR, Pirmohamed M. Investigation of toxic metabolites during drug development. *Toxicol Appl Pharmacol* 2005;207: 425–434.
89. Day SH, Mao A, White R, Schulz-Utermoehl T, Miller R, Beconi MG. A semi-automated method measuring the potential for protein covalent binding in drug discovery. *J Pharmacol Toxicol Methods* 2005;52:278–285.
90. Dahms M, Spahn-Langguth H. Covalent binding of acidic drugs via reactive intermediates: detection of benoxaprofen and flunoxaprofen protein adducts in biological material. *Pharmazie* 1996;51:874–881.
91. Dong JQ, Liu J, Smith PC. Role of benoxaprofen acyl glucuronides in covalent binding to rat plasma and liver proteins in vivo. *Biochem Pharmacol* 2005;70:937–948.
92. Grillo MP, Benet LZ. Studies on the reactivity of clofibryl-*S*-acyl CoA thioester with glutathione *in vitro*. *Drug Metab Dispos* 2002;30:55–62.
93. Fan PW, Bolton JL. Bioactivation of tamoxifen to metabolite E quinone methide: reaction with glutathione and DNA. *Drug Metab Dispos* 2001;29:891–896.
94. Muldrew KL, James LP, Coop L, McCullough SS, Hendrickson HP, Hinson JA, Mayeux PR. Determination of acetaminophen–protein in mouse liver and serum and human

serum after hepatotoxic doses of acetaminophen using high-performance liquid chromatography with electrochemical detection. *Drug Metab Dispos* 2002;30:446–451.

95. Bu HZ, Kang P, Deese AJ, Zhao P, Pool WF. Human *in vitro* glutathione and protein adducts of carbamazepine-10,11-epoxide, a stable and pharmacologically active metabolite of carbamazepine. *Drug Metab Dispos* 2005;33:1920–1924.
96. Castillo M, Lam YW, Dooley MA, Stahl E, Smith PC. Disposition and covalent binding of ibuprofen and its acyl glucuronide in the elderly. *Clin Pharmacol Ther* 1995; 57:636–644.
97. Williams DP, Pirmohamed M, Naisbitt DJ, Maggs JL, Park BK. Neutrophil cytotoxicity of the chemically reactive metabolite(s) of clozapine: possible role in agranulocytosis. *J Pharmacol Exp Ther* 1997;283:1375–1382.
98. Sadeque AJM, Fisher MB, Korzekwa KR, Gonzales FJ, Rettie AE. Human CYP2C9 and CYP2A6 mediate formation of the hepatotoxin 4-ene-valproic acid. *J Pharmacol Exp Ther* 1997;283:698–703.
99. Li AP. Preclinical *in vitro* screening assays for drug-like properties. *Drug Discov Today* 2003;2:179–185.
100. Flores JR, Nevado JJB, Salcedo AMC, Diaz MPC. Non-aqueous capillary zone electrophoresis method for the analysis of paroxetine, tamoxifen and their main metabolites in urine. *Anal Chim Acta* 2004;512:287–295.
101. Meng QH, Gauthier D. Simultaneous analysis of citalopram and desmethylcitalopram by liquid chromatography with fluorescence detection after solid-phase extraction. *Clin Biochem* 2005;38:282–285.
102. Francois-Bouchard M, Simonin G, Bossant M-J, Boursier-Neyret C. Simultaneous determination of ivabradine and its metabolites in human plasma by liquid chromatography–tandem mass spectrometry. *J Chromatogr B* 2000;745:261–269.
103. Djabarouti S, Boselli E, Allaouchiche B, Ba B, Nguyen AT, Gordien JB, Bernadou JM, Saux MC, Breilh D. Determination of levofloxacin in plasma, bronchoalveolar lavage and bone tissues by high-performance liquid chromatography with ultraviolet detection using a fully automated extraction method. *J Chromatogr B* 2004;799:165–172.
104. Rizzo M, Ventrice D, Sarro VD, Gitto R, Caruso R, Chimirri A. SPE-HPLC determination of new tetrahydroisoquinoline derivatives in rat plasma. *J Chromatogr B* 2005;821: 15–21.
105. Christensen EB, Andersen JB, Pedersen H, Jensen KG, Dalgaard L. Metabolites of [^{14}C]-5(2-ethyl-2*H*-tetrazol-5-yl)-1-methyl-1,2,3,6-tetrahydropyridine in mice, rats, dogs, and humans. *Drug Metab Dispos* 1999;27:1341–1349.
106. Titier K, Deridet E, Moore N. *In vivo* and *in vitro* myocardial binding of risperidone and 9-hydroxyrisperidone. *Toxicol Appl Pharmacol* 2002;180:145–149.
107. Oruc EE, Kabasakal L, Rollas S. The *in vivo* metabolism of 5-(4-nitrophenyl)-4-(2-phenylethyl)-2,4-dihydro-3*H*-1,2,4-triazole-3-thione in rats. *Eur J Drug Metab Pharmacokinet* 2003;28:113–118.
108. Gulerman NN, Oruc EE, Kartal F, Rollas S. *In vivo* metabolism of 4-fluorobenzoic acid [(5-nitro-2-furanyl)methylene]hydrazide in rats. *Eur J Drug Metab Pharmacokinet* 2000;25:103–108.
109. Kocyigit-Kaymakcioglu B, Rollas S, Kartal-Aricioglu F. *In vivo* metabolism of *N*-phenyl-*N*′-(3,5-dimethylpyrazole-4-yl)thiourea in rats. *Eur J Drug Metab Pharmacokinet* 2003;28(4):273–278.
110. Bekce B, Sener G, Oktav M, Ulgen M, Rollas S. *In vitro* and *in vivo* metabolism of ethyl 4-[(2-hydroxy-1-naphthyl)azo]benzoate. *Eur J Drug Metab Pharmacokinet* 2005; 30:91–97.

111. Kaymakcioglu BK, Oruc EE, Unsalan S, Kabasakal LEE, Rollas S. High-pressure liquid chromatographic analysis for identification of *in vitro* and *in vivo* metabolites of 4-phenethyl-5-[4-(1-(2-hydroxyethyl)3,5-dimethyl-4-pyrazolylazo)phenyl]-2,4-dihydro-3*H*-1,2,4-triazole-3-thione in rats. *J Chromatogr B* 2006;831:184–189.
112. Kaymakcioglu BK, Aktan Y, Suzen S, Gokhan N, Koyuncuoglu S, Erol K, Yesilada A, Rollas S. *In vivo* metabolism of 2-[1′-phenyl-3′-(3-chlorophenyl)-2′-propenylyden] hydrazino-3-methyl-4(3*H*)-quinazolinone in rats. *Eur J Drug Metab Pharmacokinet* 2005;3:255–260.
113. Oruc EE, Unsal O, Balkan A, Ozkanli F, Goren MZ, Terzioglu MZ, Rollas S. The *in vivo* metabolism of 3-oxo-5-benzylidene-6-methyl-(4*H*)-2-(benzoylmethyl)pyridazine in rats. *Eur J Drug Metabol Pharmacokinet* 2006;31:21–25.
114. Rollas S, Gulerman N, Erdeniz H. Synthesis and antimicrobial activity of some new hydrazones of 4-fluorobenzoic acid hydrazide and 3-acethyl-2,5-disubstitute-1,3,4-oxadiazolines. *Il Farmaco* 2002;57:171–174.
115. Sincula AA, Yalkowsky SH. Rationale for design of biologically reversible drug derivatives. Prodrugs. *J Pharm Sci* 1975;64:181–210.
116. Chen Y-L, Jong Y-J, Wu S-M. Capillary electrophoresis field-amplified sample stacking and electroosmotic flow suppressant for analysis of sulindac and its two metabolites in plasma. *J Chromatogr A* 2006;1119:176–182.
117. Testa B. Prodrug research: futile or fertile? *Biochem Pharmacol* 2004;68:2097–2106.
118. Chandrasekaran S, Al-Ghananeem AM, Riggs RM, Crooks PA. Synthesis and stability of two indomethacin prodrugs. *Bioorg Med Chem Lett* 2006;16:1874–1879.
119. Sriram D, Yogeeswari P, Srichakravarthy N, Bal TR. Synthesis of stavudine amino acid ester prodrugs with broad-spectrum chemotherapeutic properties for the effective treatment of HIV/AIDS. *Bioorg Med Chem Lett* 2004;14:1085–1087.
120. Wu Q, Wang M, Chen ZC, Lu DS, Lin XF. Enzymatic synthesis of metronidazole esters and their monosaccharide ester derivatives. *Enzyme Microbial Technol* 2006;39: 1258–1263.
121. Chari RVJ. Targeted delivery of chemotherapeutics: tumor-activated prodrug therapy. *Adv Drug Delivery Rev* 1998;31:89–104.
122. Denny WA. Prodrug strategies in cancer therapy. *Eur J Med Chem* 2001;36:577–595.
123. Senter PD, Springer CJ. Selective activation of anticancer prodrugs by monoclonal antibody-enzyme conjugates. *Adv Drug Delivery Rev* 2001;53:247–264.
124. Baselga J. Epidermal growth factor receptor pathway inhibitors. *Update Cancer Ther* 2006;I:299–310.
125. Smyth TP, O'Donnell ME, O'Connor MJ, Ledger JO. β-Lactamase-dependent prodrugs—recent developments. *Tetrahedron* 2000;56:5699–5707.
126. Tang S, June SM, Howell BA, Chai M. Synthesis of salicylate dendritic prodrugs. *Tetrahedron Lett* 2006;47:7671–7675.
127. Li X, Wu Q, Lv D-S, Lin X-F. Controllable synthesis of polymerizable ester and amide prodrugs of acyclovir by enzyme in organic solvent. *Bioorg Med Chem* 2006; 14:3377–3382.
128. Chandrasekar D, Sistla R, Ahmad FJ, Khar RK, Dwan PV. The development of folate–PAMAM dendrimer conjugates for targeted delivery of anti-arthritics and their pharmacokinetics and biodistribution in arthritic rats. *Biomaterials* 2006;28:504–512.
129. Najlah M, Freeman S, Attwood D, Emanuele DA. Synthesis, characterization and stability of dendrimer prodrugs. *Int J Pharm* 2006;308:175–182.
130. Emanuele AD, Jevprasesphant R, Penny J, Attwood D. The use of a dendrimer–propranolol prodrug to bypass efflux transporters and enhance oral bioavailability. *J Controlled Release* 2004;95:447–453.

131. Salamonczyk GM. Acyclovir terminated thiophosphate dendrimers. *Tetrahedron Lett* 2003;44:7449–7453.

132. Ansede JH, Thakker DR. High-throughput screening for stability and inhibitory activity of compounds toward cytochrome P450-mediated metabolism. *J Pharm Sci* 2004; 93:239–255.

133. Di L, Kerns EH, Gao N, Li SQ, Huang Y, Bourassa JL, Huryn DM. Experimental design on single-time point high-throughput microsomal stability assay. *J Pharm Sci* 2004;93:1537–1544.

134. Mandagere AK, Thompson TN, Hwang KK. Graphical model for estimating oral bioavailability of drugs in humans and other species from their Caco-2 permeability and *in vitro* liver enzyme metabolic stability rates. *J Med Chem* 2002;45:304–311.

135. Soars MG, Riley RJ, Findlay KAB, Coffey MJ, Riley RJ, Burchell B. Evidence for significant differences in microsomal drug glucuronidation by canine and human liver and kidney. *Drug Metab Dispos* 2001;29:121–126.

136. Di L, Kerns EH, Li SQ, Petusky SL. High throughput microsomal stability assay for insoluble compounds. *Int J Pharm* 2006;317:54–60.

137. Lorenzi PL, Landowski CP, Song X, Borysko KZ, Breitenbach JM, Kim JS, Hilfinger JM, Townsend LB, Drach JC, Amidon GL. Amino acid ester prodrugs of 2-bromo-5,6-dichloro-1-(beta-dribofuranosyl)benzimidazole enhance metabolic stability *in vitro* and *in vivo*. *J Pharmacol Exp Ther* 2005;314:883–890.

138. Lai F, Khojasteh-Bakht SC. Automated online liquid chromatographic/mass spectrometric metabolic study for prodrug stability. *J Chromatogr B* 2005;814:225–232.

139. Miners JO, Knights KM, Houston JB, Mackenzie PI. *In vitro–in vivo* correlation for drugs and others eliminated by glucuronidation in humans: pitfalls and promises. *Biochem Pharmacol* 2006;71:1531–1539.

140. Pryde JP, Williams RT. The biochemistry and physiology of glucuronic acid I. The structure of glucuronic acid of animal origin. *Biochem J* 1933;27:1197–1204.

141. Williams RT. Studies in detoxication II. (a) The conjugation of isomeric 3-menthanols with glucuronic acid and the asymmetric conjugation of *dl*-menthol and *dl*-isomenthol in the rabbit. (b) *d*-Isomenthylglucuronide, a new conjugated glucuronic acid. *Biochem J* 1938;32:1849–1855.

142. Ebner T, Heinzel G, Prox A, Beschke K, Wachsmuth H. Disposition and chemical stability of telmisartan 1-*O*-acylglucuronide. *Drug Metab Dispos* 1999;27:1143–1149.

143. Chen Z, Holt TG, Pivnichny JV, Leung K. A simple *in vitro* model to study the stability of acylglucuronides. *J Pharmacol Toxicol Methods* 2006;55:91–95.

144. Cannell GR, Vesey DA, Dickinson RG. Inhibition of proliferation of HT-29 colon adenocarcinoma cell by carboxylate NSAIDs and their acyl glucuronides. *Life Sci* 2001;70:37–48.

145. Shipkova M, Wieland E. Glucuronidation in therapeutic drug monitoring. *Clin Chim Acta* 2005;358:2–23.

146. Gad SC. Active drug metabolites in drug development. *Curr Opin Pharmacol* 2003; 3:98–100.

147. Fura A. Role of pharmacologically active metabolites in drug discovery and development. *Drug Discov Today* 2006;11:133–142.

148. Fura A, Shu YZ, Zhu M, Hanson RL, Roongta V. Discovering drugs through biological transformation: role of pharmacologically active metabolites in drug discovery. *J Med Chem* 2004;47:4339–4351.

149. Guengerich FP. Cytochrome P450s and other enzymes in drug metabolism and toxicity. *AAPS J* 2006;8:101–111.

150. Klein CE, Gupta E, Reid JM, Atherton PJ, Sloan JA, Pitot HC, Ratain MJ, Kastrissios H. Population pharmacokinetic model for irinotecan and two of its metabolites, SN-38 and SN-38 glucuronide. *Clin Pharmacol Ther* 2002;72:638–647.
151. Mak IT, Weglicki WB. Potent antioxidant properties of 4-hydroxyl-propranolol. *J Pharmacol Exp Ther* 2004;303:85–90.
152. Davis HR. Ezetimibe: first in a new class of cholesterol absorption inhibitors. *Int Cong Ser* 2004;1262:243–246.
153. Wong JW, Nisar U-R, Yuen KH. Liquid chromatographic method for the determination of plasma itraconazole and its hydroxy metabolite in pharmacokinetic/bioavailability studies. *J Chromatogr B* 2003;798:355–360.
154. Gasparro DM, Almeida DRP, Fülöp F. *Ab initio* multi-dimensional conformational analysis of *R*-(−)-desmethyldeprenyl: a potent neuroprotective metabolite of *R*-(−)-deprenyl. *J Mol Structure THEOCHEM* 2005;725:75–83.
155. Nave R, Meyer W, Fuhst R, Zech K. Formation of fatty acid conjugates of ciclesonide active metabolite in the rat lung after 4-week inhalation of ciclesonide. *Pulm Pharmacol Ther* 2005;18:390–396.
156. Eddershaw PJ, Beresford AP, Bayliss MK. ADME/PK as part of a rational approach to drug discovery. *Drug Discov Today* 2000;5:409–414.
157. Kerns EH, Kleintop T, Little D, Tobien T, Mallis L, Di L, Hu M, Hong Y, McConnell OJ. Integrated high capacity solid phase extraction–MS/MS system for pharmaceutical profiling in drug discovery. *J Pharm Biomed Anal* 2004;34:1–9.
158. Crivori P, Poggesi I. Computational approaches for predicting CYP-related metabolism properties in the screening of new drugs. *Eur J Med Chem* 2006;41:795–808.
159. Lipinski CA. Drug-like properties and the causes of poor solubility and poor permeability. *J Pharmacol Toxicol Methods* 2000;44:235–249.
160. Dickins M, Waterbeemd H. Simulation models for drug disposition and drug interactions. *Drug Discov Today Biosilico* 2004;2:38–45.
161. Davis AM, Riley RJ. Predictive ADMET studies, the challenges and The opportunities. *Curr Opin Chem Biol* 2004;8:378–386.
162. Huisinga W, Telgmann R, Wulkow M. The virtual laboratory to pharmacokinetics: design principles and concepts. *Drug Discov Today* 2006;11:800–805.
163. Ekins S, Waller CL, Swaan PW, Cruciani G, Wrighton SA, Wikel JH. Progress in predicting human ADME parameters *in silico*. *J Pharmacol Toxicol Methods* 2000;44:251–272.
164. Ekins S, Nikolsky Y, Nikolskaya T. Techniques: application of systems biology to absorption, distribution, metabolism, excretion and toxicity. *Trends Pharmacol Sci* 2005; 26(4):202–209.
165. Klopman G, Stefan L, Saiakhov RD. A computer model for the prediction of intestinal absorption in humans. *Eur J Pharm Sci* 2002;17:253–263.
166. Uetrecht J. Curreent trends in drug-induced autoimmunity. *Autoimmun Rev* 2005;4: 309–314.
167. Sams-Dodd F. Drug discovery. Selecting the optimal approach. *Drug Discov Today* 2006;11:465–472.

24

IN VITRO EVALUATION OF METABOLIC DRUG–DRUG INTERACTIONS: SCIENTIFIC CONCEPTS AND PRACTICAL CONSIDERATIONS

ALBERT P. LI
In Vitro ADMET Laboratories Inc., Columbia, Maryland

Contents

Preclinical Development Handbook: ADME and Biopharmaceutical Properties,
edited by Shayne Cox Gad

24.1 INTRODUCTION

Simultaneous coadministration of multiple drugs to a patient is highly probable. A patient may be coadministered multiple drugs to allow effective treatment of a single disease (e.g., cancer, HIV infection) or multiple disease or disease symptoms. It is now known that drug–drug interactions may have serious, sometimes fatal, consequences. Serious drug–drug interactions have led to the necessity of a drug manufacturer to withdraw or limit the use of marketed drugs. Examples of fatal drug–drug interactions are shown in Table 24.1. As illustrated by the examples in Table 24.1, a major mechanism of adverse drug–drug interactions is the inhibition of the metabolism of a drug by a coadministered drug, thereby elevating the systemic burden of the affected drug to a toxic level.

Besides toxicity, loss of efficacy can also result from drug–drug interactions. In this case, the metabolic clearance of a drug is accelerated due to the inducing effects of a coadministered drug on drug metabolism. A well known example is the occurrence of breakthrough bleeding and contraceptive failures in women taking oral contraceptives who were coadministered the enzyme inducer rifampin [7]. Examples of drug–drug interactions leading to the loss of efficacy are shown in Table 24.2.

Estimation of drug–drug interaction potential is therefore an essential element of drug development. Screening for drug–drug interaction in early phases of drug development allows the avoidance of the development of drug candidates with high potential for adverse drug interactions. Estimation of drug–drug interaction potential is a regulatory requirement—it is required for New Drug Applications (NDAs) to the U.S. FDA [11]. In this chapter, the scientific principles, technologies, and experimental approaches for the preclinical evaluation of drug–drug interactions are reviewed.

24.2 MECHANISMS OF ADVERSE DRUG–DRUG INTERACTIONS

Adverse effects in a patient due to coadministration of multiple drugs can be due to pharmacological or pharmacokinetic drug–drug interactions defined as follows:

Pharmacological Interactions. Adverse effects that occur due to combined pharmacological activities, leading to exaggerated pharmacological effects. An example of pharmacological interaction is the serious, sometimes fatal, drop in blood pressure due to coadministration of nitroglycerin and Sildenafil [12].

TABLE 24.1 Drugs that Have Been Withdrawn from the Market Due to Fatal Interactions with Coadministered Drugs

Drug–Drug Interaction	Mechanism of Interactions	References
Terfenadine–ketoconazole interaction, leading to fatal arrhythmia (torsades de pointes). Terfenadine was withdrawn from the market in January 1997 and replaced by a safer alternative drug (fexofenadine), which is the active metabolite of terfenadine.	Terfenadine is metabolized mainly by CYP3A4 and has been found to interact with CYP3A4 inhibitors (e.g., ketoconazole), leading to elevation of plasma terfenadine level that reached cardiotoxic levels.	1–3; www.fda.gov/bbs/topics/answers/ans00853.html
Mibefradil interaction with multiple drugs, leading to serious adverse effects. Mibefradil interactions with statins has led to rhabdomyolysis. Mibefradil was withdrawn from the market in June 1998, less than a year after it was introduced to the market in August 1997.	Mibefradil is a potent CYP3A4 inhibitor known to elevate the plasma levels of over 25 coadministered drugs to toxic levels. Statins, especially simvastatin and cerivastatin, are known to cause rhabdomyolysis.	4; www.fda.gov/bbs/topics/answers/ans00876.html
Sorivudine–5-fluorouracil (5-FU) interaction, leading to severe or fatal gastrointestinal and bone marrow toxicities. Soruvidine was withdrawn from the market in 1993.	Sorivudine inhibits dihydropyrimidine dehydrogenase, an enzyme pathway responsible for fluoropyrimidine metabolism.	5
Gemfibrozil–cerivastatin interaction, leading to rhabdomyolysis. Cerivastatin was withdrawn from the market in August 2001.	Inhibition of cerivastatin metabolism by gemfibrozil, apparently due to CYP2C8 inhibitory effects of gemfibrozil.	6; www.fda.gov/medwatch/safety/2001/Baycol2.html

Pharmacokinetic Interactions. Adverse effects that occur due to altered body burden of a drug as a result of a coadministered drug that can occur because of the ability of one drug to alter the absorption, distribution, metabolism, and excretion (ADME properties) of the coadministered drug. Of the ADME properties, drug metabolism represents the most important and prevalent mechanism for pharmacokinetic interactions.

24.3 DRUG METABOLISM

All drugs administered to a patient are subject to biotransformation. Orally administered drugs are first subjected to metabolism by the intestinal epithelium and, upon

TABLE 24.2 Drug–Drug Interactions Leading to Loss of Efficacy

Drug–Drug Interaction	Mechanism	References
Oral contraceptive–rifampin interactions, leading to breakthrough bleeding and contraceptive failure	Rifampin accelerates the metabolism of the estrogenic component (e.g., 17 α-ethinylestradiol) of oral contraceptives via induction of the metabolizing enzymes (CYP3A4 and estrogen sulfotransferases)	7, 8
Cyclosporin–rifampin interaction, leading to rejection of transplanted organs	Rifampin induces CYP3A, leading to accelerated metabolic clearance of cyclosporine to nonimmunosuppressive level	9
St. John's wort (SJW) interactions with prescribed drugs, leading to loss of efficacy	SJW (*Hypericum perforatum*) is an herbal medicine found to contain ingredients that can induce CYP3A4, CYP2C9, CYP1A2, and various transporters, leading to clinically observed accelerated metabolic clearance and/or loss of efficacy of a large number of drugs including warfarin, phenprocoumon, cyclosporine, HIV protease inhibitors, theophylline, digoxin, and oral contraceptives. The incidents with SJW illustrate the importance of the evaluation of potential drug–drug interaction of herbal medicines.	10

absorption into the portal circulation, are metabolized by the liver before entering the systemic circulation. While multiple tissues have certain degrees of biotransformation capacity, it is generally accepted that hepatic metabolism represent the most important aspect of drug metabolism.

Drug metabolism can be classified into the following major categories:

Phase I Oxidation. This generally is described as the addition of an oxygen atom (e.g., as a hydroxyl moiety) to the parent molecule. Phase I oxidation is carried out by multiple enzyme pathways, including the various isoforms of the cytochrome P450 (CYP) family and the non-P450 biotransformation enzymes such as flavin-containing monooxygenase (FMO) and monamine oxidase (MAO).

Phase II Conjugation. Phase II conjugation represents enzyme reactions that lead to the addition of a highly water-soluble molecule to the chemical that is being metabolized, leading to highly water-soluble "conjugates" that allow efficient excretion. Examples of phase II enzymes are UDP-glucuronosyl transferase (UGT), sulfotransferase (ST), and glutathione-*S*-transferase (GST). Conjugation reactions often occur with the hydroxyl moiety of the parent structure or with the oxidative metabolites.

The major drug-metabolizing enzymes and subcellular locations are summarized in Table 24.3.

TABLE 24.3 Major Pathways for Drug Metabolism, Enzymes, Subcellular Locations, and *In Vitro* Experimental System Containing the Enzymes[a]

Major Classification	Enzyme	Subcellular Location	Representative *In Vitro* Experimental System
Phase I oxidation	Cytochrome P450 mixed function monooxygenases	Endoplasmic reticulum	Microsomes, S9, hepatocytes
	Monoamine oxidase	Mitochondria	Hepatocytes
	Flavin-containing monooxygenase	Endoplasmic reticulum	Microsomes, S9, hepatocytes
	Alchohol/aldehyde dehydrogenase	Cytosol	S9, hepatocytes
	Esterases	Cytosol and endoplasmic reticulum	Microsomes, S9, hepatocytes
Phase II conjugation	UDP-dependent glucuronyl transferase	Endoplasmic reticulum	Microsomes, S9, hepatocytes
	Phenol sulfotransferases; estrogen sulfotransferase	Cytosol	S9, hepatocytes
	N-acetyl transferase	Endoplasmic reticulum	Microsomes, S9, hepatocytes
	Soluble glutathione-S-transferases (GST)	Cytosol	S9, hepatocytes
	Membrane-bound GST	Endoplasmic retuculum	Microsomes, S9, hepatocytes

[a]These enzymes are grouped into phase I oxidation and phase II conjugation enzymes, although it is now believed that such classification may not be possible for all drug-metabolizing enzymes. Representative *in vitro* experimental systems containing these enzymes are shown to guide the selection of the most relevant approach for specific enzyme pathways. It is apparent that intact hepatocytes represent the most complete *in vitro* system for drug metabolism studies as they contain all the key hepatic drug-metabolizing enzyme pathways.

24.4 CYP ISOFORMS

Cytochrome P450-dependent monooxygenases (CYP) are the drug-metabolizing enzymes often involved in metabolic drug–drug interactions. The CYP family is represented by a large number of isoforms, each having selectivity for certain chemical structures. The major hepatic human CYP isoforms are CYP1A2, CYP2A6, CYP2B6, CYP2C8, CYP2C9, CYP2C19, CYP2D6, CYP2E1, and CYP3A4. Of these isoforms, the CYP3A isoforms are the most important in drug metabolism. CYP3A isoforms (CYP3A4 and CYP3A5) collectively represent the most abundant hepatic CYP isoforms (approximately 26%), followed by CYP2C isoforms (approximately 17%). In terms of the isoforms involved in drug metabolism, CYP3 isoforms are known to be involved in the metabolism of the most number of drugs (approximately 33%), followed by CYP2C isoforms (approximately 25%) [13].

P450 isoforms are known to have specific substrates, inhibitors, and inducers (Table 24.4).

TABLE 24.4 Major Human P450 Isoforms[a] Involved in Drug Metabolism

CYP Isoform	Substrate	Inhibitor	Inducer
CYP1A2	Phenytoin	Furafylline	Omeprazole
CYP2A6	Coumarin	Tranylcypromine	Rifampin
CYP2B6	Bupropion	Ticlopidine	Rifampin
CYP2C8	Taxol	Quercetin	Rifampin
CYP2C9	Tolbutamide	Sulfaphenazole	Rifampin
CYP2C19	S-mephenytoin	Omeprazole	Rifampin
CYP2D6	Dextromethorphan	Quinidine	None
CYP2E1	Chlorzoxazone	Diethyldithiocarbamate	Ethanol
CYP3A4	Testosterone	Ketoconazole	Rifampin

[a]The individual isoforms and examples of isoform-specific substrates, inhibitors, and inducers are shown.

24.5 HUMAN *IN VITRO* EXPERIMENTAL SYSTEMS FOR DRUG METABOLISM

Substantial species–species differences occur in drug metabolism pathways, especially for CYP isoforms. Because of the species–species differences, human *in vitro* hepatic experimental systems rather than nonhuman animals are viewed as the most relevant to the evaluation of xenobiotic properties, including human drug metabolism and metabolism-based drug–drug interactions [14–17]. The following are the commonly used *in vitro* experimental systems for the evaluation of metabolism-based drug–drug interactions.

24.5.1 Hepatocytes

Hepatocytes are the parenchymal cells of the liver, which are responsible for hepatic biotransformation of xenobiotics. Isolated hepatocytes represent the most physiologically relevant experimental system for drug metabolism studies as they contain all the major hepatic drug-metabolizing enzyme pathways that are not physically disrupted such as cell free fractions. Furthermore, the drug-metabolizing enzymes and cofactors in the hepatocytes are present at physiological concentrations. Freshly isolated hepatocytes and cryopreserved hepatocytes are generally believed to represent the most complete *in vitro* system for the evaluation of hepatic drug metabolism [18].

In the past, the use of human hepatocytes has been severely limited by their availability, as studies would be performed only if human livers were available for hepatocyte isolation. Furthermore, hepatocyte isolation from human livers is not a technology available to most drug metabolism laboratories. This limitation has been overcome in the past decade due to the advancements in the procurement of human livers for research, and the commercial availability of isolated human hepatocytes. The application of human hepatocytes in drug metabolism studies is also greatly aided by the successful cryopreservation of human hepatocytes to retain drug metabolism activities [8, 19, 20]. Recently, the usefulness of cryopreserved human hepatocytes was further extended through the development of technologies to cryopreserve human hepatocytes to retain their ability to be cultured as attached cultures (plateable cryopreserved hepatocytes), which can be used for longer term

TABLE 24.5 Viability and Plateability (Ability of Hepatocytes to Be Cultured as Monolayer Cultures) of the Various Lots of Cryopreserved Human Hepatocytes[a]

Lot	Yield (cells/vial)	Viability (trypan blue)	Plating	Confluency
HU4003	4.5 × 106	86%	Yes	100%
HU4001	6.0 × 106	80%	No	20%
HU4004	6.0 × 106	80%	No	30%
HU4000	7.2 × 106	93%	Yes	100%
HU4013	7.3 × 106	92%	Yes	75%
HU4016	6.2 × 106	81%	Yes	100%
HU4021	5.4 × 106	89%	Yes	70%
HU4022	5.5 × 106	91%	Yes	80%
HU4026	5.85 × 106	91%	No	10%
HU4027	5.9 × 106	92%	No	30%
HU4028	3.2 × 106	83%	Yes	50%
HU4023	2.1 × 106	89%	No	20%
HU4029	6.0 × 106	90%	Yes	80%

[a]Hepatocytes manufactured by APSciences Inc. in partnership with CellzDirect Inc.

studies such as enzyme induction studies [21]. Examples of the viability and plateability of cryopreserved human hepatocytes prepared in our laboratory are shown in Table 24.5.

24.5.2 Liver Postmitochondrial Supernatant (PMS)

Liver PMS is prepared by first homogenizing the liver, and then centrifuging the homogenate at a speed of either 9000*g* or 10,000*g* to generate the supernatants S9 or S10, respectively. Liver PMS contains both cytosolic and microsomal drug-metabolizing enzymes but lacks mitochondrial enzymes.

24.5.3 Human Liver Microsomes

Liver microsomes are the 100,000*g* pellet for the PMS. Microsome preparation procedures in general involve the homogenization of the liver, dilution of the homogenate with approximately 4 volumes of sample weight with a buffer (e.g., 0.1 M Tris-HCl, pH 7.4, 0.1 M KCl, 1.0 mM EDTA, 1.0 mM PMSF [22]) followed by centrifugation at 9000–14,000*g* to remove nonmicrosomal membranes, and then at 100,000–138,000*g* to pellet the microsomes [23]. Microsomes contain the smooth endoplasmic reticulum, which is the site of the major phase I oxidation pathway, the P450 isoforms, and esterases, as well as a major conjugating pathway, UGT.

24.5.4 Recombinant P450 Isoforms (rCYP)

These are microsomes derived from organisms transfected with genes for individual human P450 isoforms (e.g., bacteria, yeast, mammalian cells) [24–26] and therefore contain only one specific human isoform. The major human P450 isoforms involved in drug metabolism are available commercially as rCYP. This experimental system is widely used to evaluate the drug-metabolizing activities of individual P450 isoforms [15, 16].

TABLE 24.6 Comparison of the Key *In Vitro* Drug-Metabolizing Experimental Systems: Liver Microsomes (Microsomes), Liver Postmitochondrial Supernatant (S9), Liver Cytosol (Cytosol), and Hepatocytes and Their Major Drug-Metabolizing Enzymes[a]

In Vitro System	P450	MAO	UGT	ST	GST
Microsomes	+	–	+[b]	–	+[c]
S9	+	–	+[b]	+[b]	+
Cytosol	–	–	–[b]	+[b]	+[d]
Hepatocytes	+	+	+	+	+

[a]P450, cytochrome P450; MAO, monoamine oxidase; UGT, UDP-glucuronosyl transferase; ST, sulfotransferase; GST, glutathione-*S*-transferase.
[b]Activity of this drug-metabolizing enzyme requires the addition of specific cofactors, for instance, UDP-glucuronic acid (UDPGA) for UGT activity, and 3′-phosphoadenosine 5′-phosphosulfate (PAPS) for ST activity.
[c]Membrane-bound GST but not the soluble GST is found in the microsomes.
[d]Soluble GST but not membrane-bound GST are found in the cytosol.

24.5.5 Cytosol

The supernatant after the 100,000 *g* centrifugation for microsome preparation is the cytosol, which is practically devoid of all membrane associated enzymes. *N*-acetyl transferases, sulfotransferases, and dehydrogenases are examples of cytosolic enzymes. While drug–drug interaction studies are mainly studied using liver microsomes, there are cases of drug–drug interactions involving phase II pathways that can be studied using liver cytosol [27].

A comparison of the different *in vitro* experimental systems and their drug-metabolizing enzymes are shown in Table 24.6.

24.6 MECHANISMS OF METABOLIC DRUG–DRUG INTERACTIONS

Metabolic drug–drug interaction results from the alteration of the metabolic clearance of one drug by a coadministered drug. There are two major pathways of metabolic drug–drug interactions:

Inhibitory Drug–Drug Interaction. When one drug inhibits the drug metabolism enzyme responsible for the metabolism of a coadministered drug, the result is a decreased metabolic clearance of the affected drug, resulting in a higher than desired systemic burden. For drugs with a narrow therapeutic index, this may lead to serious toxicological concerns. Most fatal drug–drug interactions are due to inhibitory drug–drug interactions.

Inductive Drug–Drug Interactions. Drug–drug interactions can also be a result of the acceleration of the metabolism of a drug by a coadministered drug. Acceleration of metabolism is usually due to the induction of the gene expression, leading to higher rates of protein synthesis and therefore higher cellular content of the induced drug–metabolizing enzyme and a higher rate of metabolism of the substrates of the induced enzyme. Inductive drug–drug interactions can lead to a higher metabolic clearance of the affected drug, leading to a decrease in plasma concentration and loss of efficacy. Inductive drug–drug interactions can also lead to a higher systemic burden of metabolites, which, if toxic, may lead to safety concerns.

24.7 MECHANISM-BASED APPROACH FOR THE EVALUATION OF DRUG–DRUG INTERACTION POTENTIAL

Due to the realization that it is physically impossible to evaluate empirically the possible interaction between one drug and all marketed drugs, and that most drug-metabolizing enzyme pathways are well defined, a mechanism-based approach is used for the evaluation of drug–drug interaction potential of a new drug or drug candidate [15, 16, 28]. This mechanism-based approach is now also recommended by the U.S. FDA (www.fda.gov/cber/gdlns/interactstud.htm). The approach consists of the following major studies.

Metabolic Phenotyping. Metabolic phenotyping is defined as the identification of the major pathways involved in the metabolism of the drug in question. The reasoning is that if the pathways are known, one can estimate potential interaction of the drug in question with known inhibitors or inducers of the pathway.

Evaluation of Inhibitory Potential for Drug-Metabolizing Enzymes. The ability of the drug in question to inhibit the activities of known pathways for drug metabolism is evaluated. If a drug is an inhibitor of a drug-metabolizing enzyme pathway, it will have the potential to cause inhibitory drug interactions with coadministered drugs that are substrates of the inhibited pathway.

Induction Potential for Drug-Metabolizing Enzymes. The ability of the drug in question to induce drug-metabolizing enzyme activities is evaluated. If the drug in question is an inducer of a specific pathway, it will have the potential to cause inductive drug interactions with coadministered drugs that are substrates of the induced pathway.

24.8 EXPERIMENTAL APPROACHES FOR THE *IN VITRO* EVALUATION OF DRUG–DRUG INTERACTION POTENTIAL

Because of the known species–species differences in drug metabolism, it is now believed that *in vitro*, human-based, experimental systems are more appropriate than nonhuman animal models for the evaluation of drug–drug interactions. *In vitro* positive findings are usually confirmed with *in vivo* clinical studies. The typical preclinical studies for drug–drug interactions [15, 16, 28] (www.fda.gov/cber/gdlns/interactstud.htm) are described next.

24.8.1 Study 1: Metabolic Phenotyping 1—Metabolite Identification

The objective of this study is to identify the major metabolites of the drug in question. For this study, the drug in question is incubated with an appropriate *in vitro* metabolic system to allow the formation of metabolites [15, 16]. Metabolites are then identified using analytical chemical approaches. The *in vitro* experimental system of choice is human hepatocytes, with high performance liquid chromatography/mass spectrometry (HPLC/MS) or tandem mass spectrometry (HPLC/MS/MS) as the most convenient analytical tool to identify the metabolites.

The metabolites are generally identified as metabolites of phase I oxidation or phase II conjugation. If phase I oxidation is concluded as the major pathway for the

oxidative metabolism of the drug, Experiment 2 will be performed to evaluate which of the several oxidative pathways are involved. Phase II conjugation pathways can generally be identified by the identity of the metabolite and subsequent experiments to further identify the pathways may not be necessary. For instance, if the metabolite is a glucuronide, UGT can be identified as the enzyme involved.

A typical experimental design is as follows:

- *In vitro System.* Cryopreserved human hepatocytes pooled from two donors (male, female).
  - Three drug concentrations: 1, 10, and 100 μM.
  - Hepatocyte concentration: 0.5–1.0 million hepatocytes per mL.
  - Three incubation times: 1, 2, and 4 hours (suspension culture); up to 24 hours (attached culture).
  - Incubation in 24 well plates at 37 °C.
  - Organic solvent (e.g., acetonitrile) to terminate reaction and to extract medium and intracellular metabolites.
  - Stored frozen until analysis.
- *Analytical Chemistry.* HPLC-MS/MS.
  - Quantification of disappearance of parent chemical in all samples.
  - Identification of metabolites from 100 μM samples.
  - Detection of metabolites in 1 and 10 μM samples.

24.8.2 Study 2: Metabolic Phenotyping 2—Identification of Major Metabolic Pathways

If oxidative metabolites are found to be the major metabolites, it is necessary to evaluate which major oxidative pathways are involved in the metabolism. This is performed via the use of liver microsomes and experimental conditions that would inhibit a specific pathway. The major pathways and experimental conditions are shown in Table 24.7.

As P450 pathways are considered the most important for metabolic drug–drug interactions, the study with the general P450 inhibitor, 1-aminobenzotriazole (ABT)

TABLE 24.7 Experimental Conditions to Reduce the Activity of the Major Drug-Metabolizing Enzyme Pathways (P450 Isoforms (CYP), Flavin-Containing Monooxygenases (FMOs), and Monoamine Oxidase (MAO)) Using the *In Vitro* Experimental Systems for Drug Metabolism (Liver Microsomes (Microsomes), Postmitochondrial Supernatant (S9), and Hepatocytes)

In Vitro System	Condition	Inactivated Pathway(s)
Microsomes	NADH omission	CYP, FMO
Microsomes or hepatocytes	1-Aminobenzotriazole treatment	CYP
Microsomes	Heat (45 °C) inactivation	FMO
S9	Pargyline treatment	MAO

Source: Adapted from http://www.fda.gov/cder/guidance/6695dft.pdf.

is the one that should be performed. ABT is known to inhibit all eight human P450 isoforms involved in drug metabolism [29]. Inhibition of metabolism of a test article by ABT would indicate that the test article is metabolized by the P450 pathway. A typical study with ABT is as follows:

- Human liver microsomes (0.5 mg protein/mL).
- Experiment 1: Evaluation of experimental conditions for the accurate quantification of metabolic clearance.
  - Incubation with three concentrations of test article (e.g., 0.1, 1, 10 μM) and three incubation times (e.g., 15, 30, and 60 minutes).
  - Quantification of test article disappearance.
- Experiment 2: Reaction phenotyping.
  - Incubation with one concentration of the test article at one incubation time (chosen from Experiment 1) in the presence and absence of three concentrations of ABT (100, 200, and 500 μM).
  - Quantification of test article disappearance and evaluation of the effects of ABT treatment.

24.8.3 Study 3: Metabolic Phenotyping 3—Identification of P450 Isoform Pathways (P450 Phenotyping)

If ABT is found to inhibit the metabolism of the drug or drug candidate in Study 2, P450 metabolism is ascertained. The next step is to identify which P450 isoforms are involved in the metabolism, a process termed P450 phenotyping [30, 31]. There are several major approaches for this study.

Liver Microsome and Isoform-Selective Inhibitors In this experiment, the test article is incubated with human liver microsomes in the presence and absence of individual selective inhibitors for the eight major CYP isoforms. The ability of an inhibitor to inhibit metabolism of the test article would indicate that the pathway inhibited by the inhibitor is involved in metabolism. For instance, if ketoconazole, a potent CYP3A4 inhibitor, is found to inhibit the metabolism of the test article, then CYP3A4 is concluded to be involved in the metabolism of the test article. It is also a common practice to assign the degree of involvement by the maximum percent inhibition. For instance, if the maximum inhibition, expressed as percentages of the total metabolism in the absence of inhibitor, by sulfaphenazole (CYP2C9 inhibitor) and ketoconazole (CYP3A4 inhibitor) are 20% and 80%, respectively, it can be concluded that the CYP2C9 is involved in 20% and CYP3A4 in 80% of the metabolism of the test article. It is important to realize that the inhibitors are isoform selective rather than isoform specific, so data interpretation must be performed carefully to avoid an inaccurate assignment of enzyme pathways [31]. It is always prudent to confirm the results of this study with results using a different approach (e.g., using rCYP).

Incubation with Individual rCYPs In this experiment, individual rCYP isoforms are used to evaluate which P450 isoforms are involved in the metabolism [30]. The

test article is incubated with each rCYP and its disappearance quantified. A rCYP that leads to the disappearance of the test article would indicate that the isoform is involved in the metabolism of the test article. For instance, if rCYP2C19 incubation leads to the disappearance of the test article, then CYP2C19 is concluded to be involved in the metabolic clearance of the test article. It is important to realize that these studies are performed with a single P450 isoform and therefore lack competing enzyme pathways. Metabolism by a rCYP isoform may not be relevant *in vivo* because of higher affinity pathways.

Correlation Study with Human Liver Microsomes In this experiment, the test article is incubated with multiple lots of human liver microsomes that have been previously characterized for the activities of the individual CYP isoforms [32]. The rate of metabolic clearance of the test article is then plotted against the CYP activities of the different lots of microsomes. A linear correlation between activity and rate of disappearance for a specific CYP would indicate that this pathway is involved in the metabolism of the test article. This study requires the evaluation of at least 10 liver microsome lots with well-distributed gradations of activities.

Liver Microsome/Inhibitor Study Design In general, studies with liver microsomes are believed to be more relevant than studies with rCYP, as studies with individual rCYP does not allow competition in metabolism for isoforms with different affinities for the substrate and therefore may overemphasize the participation of low affinity pathways. It is important to use substrate concentrations similar to expected plasma concentrations. An artifactually high concentration would cause the substrate to be metabolized similarly by high and low affinity enzyme pathways [33]. Using liver microsomes with physiologically relevant substrate concentrations should provide the best results. A typical liver microsome experiment with inhibitors is as follows.

- Human liver microsomes (0.5 mg/mL).
- Experiment 1: Metabolic stability study.
  - Incubation with three concentrations of test article (e.g., 0.1, 1, 10 μM) and three incubation times (e.g., 15, 30, and 60 minutes).
  - Quantification of test article disappearance.
- Experiment 2: Reaction phenotyping.
  - Incubation with one concentration of the test article at one incubation time (chosen from Experiment 1) in the presence and absence of isoform-specific inhibitors.
  - Quantification of test article disappearance.

The isoform-specific inhibitors suggested by the U.S. FDA are shown in Table 24.8.

Evaluation of CYP Isoform Contributions Using Both Liver Microsomes and rCYP Isoforms It is also possible to calculate the relative contribution of individual isoforms using data from both liver microsomes and rCYP isoforms using the following approach [34, 35]:

TABLE 24.8 Preferred and Acceptable P450 Isoform-Specific Inhibitors Suggested by U.S. FDA in the September 2006 Draft Guidance Document for Drug–Drug Interaction Evaluation and Preferred Inhibitors Used in the *In Vitro* ADMET Laboratories (IVAL)

CYP	FDA Preferred Inhibitor	FDA Acceptable Inhibitor	IVAL Preferred Inhibitor
1A2	Furafylline	α-Napthoflavone	Furafylline
2A6	Tranylcypromine, methoxsalen	Pilocarpine, tryptamine	Tranylcypromine
2B6		Ticlopidine, sertraline	Ticlopidine
2C8	Quercetin	Trimethoprim, gemfibrozil, rosiglitazone	Quercetin
2C9	Sulfaphenazole	Fluconazole	Sulfaphenazole
2C19		Ticlopidine	Omeprazole
2D6	Quinidine		Quinidine
2E1		Diethyldithiocarbamate	Diethyldithiocarbamate
3A4/5	Ketoconazole, itraconazole	Troleandomycin, verapamil	Ketoconazole

- The relative activity factor for individual isoforms (using isoform-specific substrates) is calculated first. This is necessary as each lot of liver microsomes would have different relative amounts of each P450 isoform. V_{max} and K_m values are determined for each isoform using isoform-specific substrates for both liver microsomes and rCYP isoforms. The relative activity factor (RAF) is calculated using the following equation:

$$RAF = \frac{(V_{max}/K_m \text{ of CYP in microsomes})}{V_{max}/K_m \text{ of rCYP}}$$

- Contribution of a specific CYP isoform to the metabolism of a test article is then calculated using the following equation:

$$\text{Contribution of CYP (\%)} = RAF \times \frac{V(\text{rCYP})}{V(\text{microsomes})}$$

24.8.4 Study 4: CYP Inhibitory Potential

The objective of this study is to evaluate if the drug or drug candidate in question is an inhibitor of a specific P450 isoform. This study can be performed with rCYP, human liver microsomes, and human hepatocytes.

rCYP Studies rCYP studies represent the most convenient and rapid study for the evaluation of CYP inhibitory potential. As the study involves substrates that form metabolites that can be quantified by fluorescence, the laborious and time-consuming HPLC or LC/MS sample analysis is not required. For this reason, most drug development laboratories perform rCYP inhibition assays as a screen for P450

inhibitory potential of their drug candidates. The study involves the incubation of individual rCYP isoforms with the test article at various concentrations (e.g., seven concentrations plus solvent control) in triplicate, and a substrate that can be metabolized by the specific isoform. As the reaction contains only one isoform, isoform-specific substrates are not required to be used. The requirement is that the substrate generates metabolites that can be measured by a plate reader with the capability to quantify florescence.

Liver Microsome Studies Liver microsomes represent the most appropriate experimental system for the evaluation of the interaction of a drug with P450 isoforms. For the evaluation of CYP inhibitory potential, the test article is incubated with liver microsomes in the presence of individual isoform-specific substrates. The isoform-specific substrates and the metabolites quantified are shown in Table 24.9.

Human Hepatocyte Studies rCYP and human liver microsomes are cell-free systems, allowing direct interaction of the test article with the P450 isoforms. *In vivo*, the inhibitor is initially absorbed into the systemic circulation and then interacts with the enzymes after penetration through the hepatocyte plasma membrane. Once inside the cytoplasm, the inhibitor may be metabolized by phase I and/or phase II metabolism and/or actively transported out of the hepatocytes, for instance, via bile excretion. Furthermore, there may be transporters present to actively uptake the inhibitor. The result is that the intracellular concentration of the inhibitor may be substantially different from the plasma concentration. Results with rCYP and human liver microsomes may not be useful to estimate *in vivo* inhibitory effects based on plasma concentrations if the intracellular concentration of the inhibitor is not known.

The use of intact human hepatocytes may allow a more accurate extrapolation of *in vitro* results to *in vivo*. The study is performed using intact human hepatocytes incubated with isoform-specific substrate and the test article. The intact plasma membrane and the presence of all hepatic metabolic pathways and cofactors allow distribution and metabolism of the test article. The resulting inhibitory effect there-

TABLE 24.9 P450 Isoform-Specific Substrates and Their Respective Metabolites[a]

CYP	Substrate	Metabolite
1A2	Phenacetin	Acetaminophen
	Ethoxyresorufin	Resorufin
2A6	Coumarin	7-OH-coumarin
2B6	Bupropion	Hydroxypropion
2C8	Taxol	6-α-Hydroxypaclitaxel
2C9	Tolbutamide	4′-Hydroxytolbutamide
2C19	*S*-Mephenytoin	4-OH-mephenytoin
2D6	Dextromethorphan	Dextrophan
2E1	Chlorzoxazone	6-Hydroxychlorzoxazone
3A4/5	Testosterone	6-β-Hydroxytestosterone

[a]These substrates are used in *in vitro* experimental systems such as liver microsomes, liver S9, or hepatocytes in which multiple isoforms are expressed.

fore should be physiologically more relevant to the *in vivo* situation than results with cell-free systems.

It is recommended that inhibition studies with intact hepatocytes be performed if inhibitory effects of a drug or drug candidate have been observed with rCYP or liver microsomes to allow a more accurate prediction of the extent of *in vivo* inhibitory effects. Time-dependent inhibition of P450 can also be studied using intact human hepatocytes [36]. One precaution with the use of intact hepatocytes is to concurrently measure cytotoxicity. As dead hepatocytes are not active in drug metabolism, without cytotoxicity information, cytotoxic drug concentrations could be interpreted as inhibitory concentrations.

A recent advancement is to use intact hepatocytes suspended in whole human plasma for inhibition studies to allow correction for plasma protein binding [37]. As drugs *in vivo* are always in contact with 100% human blood, this is conceptually sound and therefore deserves further investigation on its general applicability. One disturbing finding in our laboratory is that testosterone, a compound that is readily metabolized *in vivo*, is not metabolized by intact human hepatocytes in whole plasma (A. P. Li, unpublished).

IC_{50}, K_i, K_{inact} and [I]/K_i Determinations Enzyme inhibition data are often presented as IC_{50}, the concentration of the inhibitor to cause 50% inhibition at one chosen substrate concentration; K_i, the inhibition constant (dissociation constant from the inhibitor–enzyme complex) determined by enzyme kinetic analysis (e.g., Dixon plot); and K_{inact}, the time-dependent inhibition constant for mechanism-based inhibitors. IC_{50} values can be estimated from the study described earlier. A positive inhibition, defined as dose-dependent inhibition, with the inhibited activity lower than 50% of that of the negative control, will require further experimentation to define K_i for a better evaluation of *in vivo* inhibitory potential. Furthermore, study to determine K_{inact} may be performed to evaluate if the inhibitor acts via covalent binding to the active site of the enzyme, leading to time-dependent irreversible inhibition.

IC_{50} is generally determined by plotting the log of the relative activity (activity in the presence of the inhibitor as a percentage of the activity of the negative solvent control), and then estimating the concentration yielding 50% relative activity using linear regression analysis. IC_{50} can also be calculated from the relationship between inhibitor concentrations and percent control activity with the aid of a nonlinear regression program such as SCIENTIST (Micromath, Salt Lake City, UT) [38].

K_i can be determined using a Dixon plot with the reciprocal of the activity as the *y*-axis and inhibitor concentration as the *x*-axis. Results with at least two substrate concentrations below V_{max} are plotted,with K_i calculated as the negative of the *x*-intercept [39]. K_i can also be estimated with the aid of nonlinear regression analysis software such as SYSTAT (SPPS, Inc., Chicago, IL) [40].

Most P450 inhibitors act via reversible (competitive or noncompetitive) mechanisms and their inhibitory potential can be estimated from their IC_{50} or K_i values. Some inhibitors are "mechanism-based" or "time-dependent" inhibitors, which can cause irreversible inhibition due to the formation of reactive metabolites by the CYP isoform, leading to covalent binding to the active site and thereby causing

irreversible inhibition of the affected enzyme molecule [41]. Irreversible inhibitors therefore will have prolonged inhibition of the enzyme even after clearance of the drug in question. K_{inact} is a measure of the potency of such "mechanism-based" inhibitors.

K_{inact} can be determined using the following approach [42]:

1. Plot the relative activity (activity in the presence of the inhibitor as a percentage of the activity of the solvent or negative control) versus time and determine the slope at each inhibitor concentration.
2. Plot (1/slope) versus (1/inhibitor concentration) (Kitz–Wilson plot). K_{inact} is calculated as the reciprocal of the *y*-intercept, and K_i as the negative of the reciprocal of the *x*-intercept.

$[I]/K_i$, the ratio of the anticipated or known steady-state plasma drug concentration to K_i, is generally used to determine the likelihood of clinical drug–drug interactions [43, 44]. A general rule of thumb suggested by the U.S. FDA (http://www.fda.gov/cder/guidance/6695dft.pdf) is as follows:

- $[I]/K_i < 0.1$: Unlikely to cause *in vivo* drug–drug interactions.
- $[I]K_i = 1$: Possible to cause *in vivo* drug–drug interactions.
- $[I]/K_i > 1$: Likely to cause *in vivo* drug–drug interactions.

K_i is estimated by an experiment with varying inhibitor and substrate concentrations. A typical K_i study is as follows:

- *In vitro* experimental system: rCYP, human liver microsomes or hepatocytes.
- Inhibitor concentrations: Five (ideally yielding 10–90% inhibition of activity).
- Substrate concentrations: Minimum of two for the Dixon plot; three is recommended.
- Timepoint: one (within the linear time course) if time course is known; multiple (e.g., 5, 10, and 15 minutes) if time course under the experimental conditions has not been established.
- K_i is determined by a Dixon plot, plotting the reciprocal of activity versus inhibitor concentration. The negative of the *x*-coordinate value corresponding to the intercept of the plots for the low and high substrate concentrations is the K_i.

For mechanism-based inhibitors, K_{inact} is estimated by an experiment with varying inhibitor concentration and preincubation time. A typical K_{inact} study is as follows:

- *In vitro* experimental system: rCYP, human liver microsomes or hepatocytes.
- Preincubation time (preincubation of enzyme with inhibitor): Five values (e.g., 5, 10, 15, 20, 30 minutes).
- Inhibitor concentration: Five (ideally yielding 10–90% inhibition of activity).
- Substrate concentration: one.

- Substrate incubation time: one (within the linear time course) if time course is known; multiple (e.g., 5, 10, and 15 minutes) if time course under the experimental conditions has not been established.
- K_{inact} is determined by the following approach:
  Plot activity as a percentage of the solvent control versus time.
  Estimate the first-order inactivation constants at each inhibitor concentration by multiplying the slope of the linear regression analysis by 2.303.
  Determine $t_{1/2}$ of the inactivation reaction as $0.693/k$.
  Plot the Kitz–Wilson plot of $t_{1/2}$ versus the reciprocal of the inhibitor concentration and estimate K_{inact} as the y-intercept, and K_i as the reciprocal of the x-intercept.

24.8.5 Study 5: Enzyme Induction Potential

Enzyme induction is a major mechanism for drug–drug interactions. Induction of a drug-metabolizing enzyme by one drug would lead to the enhanced metabolism of coadministered drugs that are substrates of the induced enzyme.

Experimental evaluation of enzyme induction involves the treatment of human hepatocytes for several days with the test article followed by evaluation of enzyme activities using P450 isoform-specific substrates [45, 46]. As freshly isolated hepatocytes possess endogenous activities, which may be the result of inducers present in the donor's systemic circulation, the isolated hepatocytes are cultured for 2–3 days to allow the P450 enzyme activities to return to a basal level. Testing for induction potential is initiated by treatment of the cultured hepatocytes for 2–3 days to allow full expression of the induced enzyme. Induction is generally evaluated by measuring enzyme activity, as activity represents the most relevant endpoint for drug–drug interaction. Both freshly isolated and plateable cryopreserved human hepatocytes can be used for the induction study [21, 47, 48].

As of this writing, all known inducers of P450 isoforms *in vivo* are inducers *in vitro* [21]. The known human P450 inducers are shown in Table 24.10.

TABLE 24.10 Clinically Demonstrated Human Enzyme Inducers and Their Respective *In Vitro* Induction Results as Well as Their Association with Severe Hepatotoxicity

In Vivo Enzyme Inducer	*In Vitro* Human Hepatocyte Induction Finding	Severe Clinical Hepatotoxicity
Carbamazepine	+	+
Dexamethasone	+	–
Isoniazid	+	+
Omeprazole	+	+
Phenobarbital	+	+
Phenytoin	+	+
Rifampin	+	+
Rifapentine	+	–
Rifabutin	+	–
Troglitazone	+	+
St. John's wort	+	+

The typical experimental procedures for an enzyme induction study are as follows:

- Day 0: Plate human hepatocytes (freshly isolated or plateable cryopreserved human hepatocytes).
- Day 1: Refresh medium.
- Day 2: Refresh medium.
- Day 3: Change medium to that containing test article, solvent control, or positive controls.
  - Minimum of three test article concentrations, with the high concentration at least one order of magnitude greater than expected plasma concentration.
  - If plasma concentration not known, evaluate concentrations ranging over at least two orders of magnitude (e.g., 1, 10, 100 μM).
- Day 4: Refresh treatment medium.
- Day 5: Refresh treatment medium.
- Day 6: Measure activity (*in situ* incubation with isoform-specific substrates).

The isoform-specific substrates described earlier for CYP inhibition studies are generally used for enzyme induction studies.

The known CYP inducers are now known to induce either CYP1A and/or CYP3A, with inducers of other inducible isoforms such as CYP2A6, CYP2C9, and CYP2C19 found also to be CYP3A inducers. For general enzyme induction evaluation for drug–drug interaction, it may be adequate to simply screen for CYP1A and CYP3A induction. If CYP3A induction is observed, then investigations into CYP2A6, CYP2C9, and CYP2C19 induction are warranted.

The two most common confounding factors for P450 induction studies are as follows:

1. *Inducers that Are Also Inhibitors.* The co-occurrence of P450 inhibition and induction (i. e., the compound is both an inhibitor and inducer) can confound induction results. Ritonavir is an example of a CYP3A4 inducer [49] that is also a potent CYP3A4 inhibitor [50]. The inhibitory effects can overcome any induction effects using activity as an endpoint. For the evaluation of enzyme induction potential of inhibitors, Western blotting for the amount of enzyme proteins would be most appropriate. Studies with mRNA expression would provide data to distinguish between induction of gene expression or protein stabilization as mechanisms. As in the case of ritonavir, induction effects persist after the clearance of the drug from the systemic circulation, leading to enhanced clearance of drugs that are substrates of the induced pathways. It is important to define the induction potential of a drug even if it is found to be an enzyme inhibitor.
2. *Cytotoxic Compounds.* Induction effects can be masked by the decrease of cell viability, as most induction assays quantify substrate metabolism *in situ* (in the same cell culture plate in which the cells are cultured) and assume that there is no change in cell number. Cytotoxicity evaluation therefore should always be performed concurrently with induction studies. In the presence of cytotoxicity, activity should be corrected by the viability for comparison with negative control activity to assess induction potential.

A compound is concluded to be an inducer if reproducible, statistically significant, and dose-dependent induction effects are observed. U.S. FDA recommends the use of the criterion of "40% or higher of the activity of positive controls" as a positive response (www.fda.gov/cber/gdlns/interactstud.htm).

24.8.6 Study 6: *In Vitro* Empirical Drug–Drug Interactions

The physiological significance of the findings based on the mechanistic approach may be substantiated by *in vitro* drug–drug interactions between frequently coadministered drugs that are likely to have interaction with the drug in question [28]. This is particularly important if the drug in question is either a CYP3A4 substrate or a CYP3A4 inhibitor. As CYP3A4 is now known to have different affinities for different substrates and inhibitors [51], the interaction potential for a drug and a particular coadministered drug may be substantially different from that estimated by using a surrogate substrate of CYP3A4.

This study can be performed with liver microsomes or hepatocytes. The use of hepatocytes probably would allow the development of data more relevant to humans *in vivo*.

24.9 DATA INTERPRETATION

The studies described previously allow one to develop data for the estimation of drug–drug interaction potential of the drug or drug candidate in question. Accurate prediction of *in vivo* effects is possible only through thorough and scientifically sound interpretation of the data. While every novel chemical structure will provide a unique set of data and therefore requires individualized data interpretation and/or further experimentation, the following guidelines can be used to aid the evaluation of the data generated.

24.9.1 Pathway Evaluation

Possible outcomes of a study are as follows:

1. The test article is not metabolized by liver microsomes or hepatocytes. This is indicated by the lack of metabolite formation and lack of parent disappearance in Studies 1 and 2. Hepatic metabolism is not involved in the metabolic clearance of the compound. There should be no concern with coadministered drugs that can alter drug-metabolizing enzyme activities.
2. The test article is metabolized but not metabolized by P450 isoforms. As P450-related drug–drug interactions are the most prevalent, non-P450 drug–drug interactions should be considered on a case-by-case basis. For instance, MAO interaction may be important if the drug in question may be coadministered with known MAO substrates or inhibitors. UGT substrates, for instance, may have drug interactions with UGT inhibitory drugs such as probenecid.
3. The test article is metabolized by a single P450 isoform. This represents the easiest data to interpret, albeit not a good scenario for a drug candidate. A drug that is metabolized predominantly by a single P450 isoform will very likely have drug–drug interactions with inhibitors of the isoform. The known cases of serious drug–drug interactions often involve a single P450 pathway,

with CYP3A4 being the most prominent. Drugs that have been withdrawn due to fatal drug–drug interactions are often CYP3A4 substrates or potent CYP3A4 inhibitors. Because of the role of CYP2C8 in the metabolism of statins, which are widely prescribed to combat hypercholesterolemia, CYP2C8 has become the second-most important isoform for drug–drug interactions. Cerivastatin, a CYP2C8 substrate, was withdrawn from the market in August 2001 after reports of fatal interactions with the CYP2C8 inhibitor gemfibrozil [52].

4. The test article is metabolized by multiple P450 isoforms. This is generally interpreted that the test article may not have serious interactions with a specific inhibitor of one of the P450 isoforms, as the metabolic clearance can be carried out by the unaffected pathways. However, there are examples of drugs that have been found to be metabolized by multiple pathways but later were found in clinical or postmarketing studies to have interactions with potent inhibitors of a specific pathway. An example is the antifungal terbinafine, which has been characterized using human liver microsomes and rCYP isoforms to be metabolized by multiple P450 isoforms: CYP1A2, CYP2C8, CYP2C9. CYP2C19, CYP2D6, and CYP3A4, leading to the conclusion that "the potential for terbinafine interaction with other drugs is predicted to be insignificant" [53]. In the same study, as terbinafine was a competitive inhibitor of CYP2D6, it was concluded that it would have interactions with CYP2D6 substrates. *In vivo* studies confirmed the CYP2D6 inhibitory effects as predicted by *in vitro* studies; however, it was also observed clinically that rifampin, a CYP3A4 inducer, caused a 100% increase in terbinafine clearance (www.fda.gov/medwatch/safety/2004/jan_PI/Lamasil_PI.pdf). One possible explanation of this is that, upon CYP3A4 induction, the total metabolism of terbinafine is greatly enhanced due to the high capacity of CYP3A4 for this substrate. It is therefore important to realize that if a drug is metabolized by multiple isoforms, it may still have significant drug interactions with inducers of isoforms with high capacity for the metabolism of the drug.

24.9.2 P450 Inhibition

The outcomes of P450 inhibition studies may include the following:

1. No inhibition is observed. If no inhibitory effects are observed with rCYP, microsomes, and hepatocytes, the substance in question is considered not to have the potential to cause inhibitory metabolic drug–drug interactions *in vivo*. As of now, there are no examples of *in vivo* enzyme inhibitors that are not inhibitors *in vitro*.
2. Significant inhibition is observed. A practical definition of significant inhibition is that the test article is found to cause dose-dependent and >50% inhibition of one or more P450 isoforms at the concentrations evaluated. The conclusion is that the test article is a potent inhibitor. As described earlier, the physiological significance is determined by the $[I]/K_i$ value, with any $[I]/K_i$ value of 0.1 or higher as possible or likely to cause *in vivo* drug–drug interactions. It is recommended that $[I]/K_i$ values obtained from cell-free systems (microsomes and rCYP) are confirmed with intact hepatocytes to aid an accurate prediction

of *in vivo* effects. If the results with hepatocytes are also determined to be significant, *in vivo* studies will need to be performed to estimate human *in vivo* drug–drug interaction potential.

3. No time-dependent inhibition is observed. The inhibitor is not a mechanism-based inhibitor.
4. Time-dependent inhibition is observed. The inhibitor is a time-dependent inhibitor. *In vivo* studies will need to be performed to further define its drug–drug interaction potential.
5. Additional safety concern. A time-dependent inhibitor may need to be further studied to define its hepatotoxic potential, as a number of time-dependent P450 inhibitors are found to cause idiosyncratic hepatotoxicity.

24.9.3 P450 Induction

The following outcomes may be observed:

1. No induction is observed. The substance evaluated is not an enzyme inducer if P450 inhibitory and cytotoxic potential are eliminated as confounding factors.
2. Induction is observed. The substance evaluated is observed to cause dose-dependent and physiologically significant induction (e.g., induced activity greater than twofold the negative control activity). If the doses found to be positive are within clinical plasma concentrations (e.g., within 10× of plasma C_{max}), *in vivo* studies may be needed to further define the test article's *in vivo* enzyme induction and the subsequent drug–drug interaction potential.
3. Additional safety concern. Enzyme inducers may need to be further evaluated for their hepatotoxic potential, as a large number of enzyme-inducing drugs are found to cause severe hepatotoxicity.

24.10 CONCLUSION

Drug–drug interactions can have serious adverse consequences and therefore should be evaluated accurately before a new drug is introduced to the human population. Due to the scientific advances in the understanding of key human drug-metabolizing pathways, and the availability of human *in vitro* systems for drug metabolism studies, human drug–drug interaction evaluations, especially drug metabolism-related interactions, can be performed rapidly and efficiently. A scientific, mechanism-based approach to evaluate drug–drug interactions remains the most appropriate approach:

1. Understanding of the major drug-metabolizing pathways in the metabolism of the drug or drug candidate in question will allow assessment of its potential interactions with existing drugs that are inhibitors or inducers of the pathways involved.
2. A careful and exhaustive evaluation of the inhibitory potential of the drug or drug candidate in question toward the major human drug metabolism enzymes

will allow assessment of its potential to cause interactions with existing drugs that are substrates of the inhibited enzymes.

3. Evaluation of induction potential of the drug or drug candidate in question for the inducible human drug-metabolizing enzymes will allow assessment of potential interactions with drugs that are substrates of the induced enzymes.

This approach is mainly applied toward P450 isoforms but can also be applied to non-P450 drug-metabolizing enzyme pathways. The next wave of major advances in drug–drug interactions is anticipated to be approaches for the evaluation of the interactions between drugs and drug transporters.

The success achieved with the scientific-based approaches in the evaluation of drug–drug interactions is a result of the extensive scientific research in the identification and characterization of drug-metabolizing enzymes, the definition of the mechanisms of metabolism-based drug–drug interactions, and the development, characterization, and intelligent application of the human-based *in vitro* experimental models for drug metabolism. Similar approaches should be adopted for the evaluation of other major adverse drug effects (e.g., idiosyncratic drug toxicity), which so far have eluded the routine drug safety evaluation approaches. It is through an open mind—a willingness to venture toward the development of a hypothesis, the testing of a hypothesis, and the development and adoption of approaches to investigate a problem based on the best science—that the field of drug safety evaluation can move forward.

REFERENCES

1. Vazquez E, Whitfield L. Seldane warnings. *Posit Aware* 1997;8:12.
2. Carlson AM, Morris LS. Coprescription of terfenadine and erythromycin or ketoconazole: an assessment of potential harm. *J Am Pharm Assoc (Wash)* 1996;NS36:263–269.
3. Von Moltke LL, Greenblatt DJ, Duan SX, Harmatz JS, Wright CE, Shader RI. Inhibition of terfenadine metabolism *in vitro* by azole antifungal agents and by selective serotonin reuptake inhibitor antidepressants: relations to pharmacokinetic interactions *in vivo*. *J Clin Psychopharmacol* 1996;16:104–112.
4. Omar MA, Wilson JP. FDA adverse event reports on statin associated rhabdomyolysis. *Ann Pharmacother* 2002;36:288–295.
5. Diasio RB. Sorivudine and 5-fluorouracil; a clinically significant drug–drug interaction due to inhibition of dihydropyrimidine dehydrogenase. *Br J Clin Pharmacol* 1998;46: 1–4.
6. Ozdemir O, Boran M, Gokce V, Uzun Y, Kocak B, Korkmaz S. A case with severe rhabdomyolysis and renal failure associated with cerivastatin–gemfibrozil combination therapy—a case report. *Angiology* 2000;51:695–697.
7. Zhang H, Cui D, Wang B, Han YH, Balimane P, Yang Z, Sinz M, Rodriqus AD. Pharmacokinetic drug interactions involving 17alpha-ethinylestradiol: a new look at an old drug. *Clin Pharmacokinet* 2007;46:133–157.
8. Li AP, Hartman NR, Lu C, Collins JM, Strong JM. Effects of cytochrome P450 inducers on 17 alpha-ethinyloestradiol (EE2) conjugation by primary human hepatocytes. *Br J Clin Pharmacol* 1999;48:733–742.
9. Capone D, Aiello C, Santoro GA, Gentile A, Stanziale P, D'Alessandro R, Imperatore P, Basile V. Drug interaction between cyclosporine and two antimicrobial agents, josamycin

and rifampicin, in organ-transplanted patients. *Int J Clin Pharmacol Res* 1996;16: 73–76.

10. Henderson L, Yue QY, Berqquist C, Gerden B, Arlett P. St. John's wort (*Hypericum perforatum*): drug interactions and clinical outcomes. *Br J Clin Pharmacol* 2002;54: 349–356.
11. Huang SM, Lesko LJ, Williams RL. Assessment of the quality and quantity of drug–drug interaction studies in recent NDA submissions: study design and data analysis issues. *J Clin Pharmacol* 1999;39:1006–1014.
12. Schalcher C, Schad K, Brunner-La Rocca HP, Schindler R, Oechslin E, Scharf C, Suetsch G, Bertel O, Kiowski W. Interaction of sildenafil with cAMP-mediated vasodilation *in vivo*. *Hypertension* 2003;40:763–767.
13. Guengerich FP. Cytochrome P450s and other enzymes in drug metabolism and toxicity. *AAPS J* 2006;8:E101–E111.
14. Li AP, Maurel P, Gomez-Lechon MJ, Cheng LC, Jurima-Romet M. Applications of primary human hepatocytes in the evaluation of P450 induction. *Chem Biol Interact* 1997;107:5–16.
15. Li AP. Screening for human ADME/Tox drug properties in drug discovery. *Drug Discov Today* 2001;6:357–366.
16. Li AP. *In vitro* approaches to evaluate ADMET drug properties. *Curr Top Med Chem* 2004;4:701–706.
17. MacGregor JT, Collins JM, Sugiyama Y, Tyson CA, Dean J, Smith L, Andersen M, Curren RD, Houston JB, Kadlubar FF, Kedderis GL, Krishnan K, Li AP, Parchment PE, Thummel K, Tomaszewski JE, Ulrich R, Vickers AE, Wrighton SA. *In vitro* human tissue models in risk assessment: report of a consensus-building workshop. *Toxicol Sci* 2001;59:17–36.
18. Hewitt NJ, Lechon MJ, Houston JB, Hallifax D, Brown HS, Maurel P, Kenna JG, Gustavsson L, Lohmann C, Skonberg C, Huillouzo A, Tuschi G, Li AP, Elcluyse E, Groothuis GM, Hengstler JG. Primary hepatocytes: current understanding of the regulation of metabolic enzymes and transporter proteins, and pharmaceutical practice for the use of hepatocytes in metabolism, enzyme induction, transporter, clearance, and hepatotoxicity studies. *Drug Metab Rev* 2007;39:159–234.
19. Li AP, Gorycki PD, Hengstler JG, Kedderis GL, Koebe HG, Rahmani R, de Sousas G, Silva JM, Skett P. Present status of the application of cryopreserved hepatocytes in the evaluation of xenobiotics: consensus of an international expert panel. *Chem Biol Interact* 1999;121:117–123.
20. Li AP, Lu C, Brent JA, Pham C, Fackett A, Ruegg CE, Silber PM. Cryopreserved human hepatocytes: characterization of drug-metabolizing enzyme activities and applications in higher throughput screening assays for hepatotoxicity, metabolic stability, and drug–drug interaction potential. *Chem Biol Interact* 1999;121:17–35.
21. Li AP. Human hepatocytes: isolation, cryopreservation and applications in drug development. *Chem Biol Interact* 2007;168:16–29.
22. Raucy J, Lasker JM. Isolation of P450 enzymes from human livers. *Methods Enzymol* 1991;206:577–594.
23. Nelson AC, Huang W, Moody DE. Human liver microsome preparation: impact on the kinetics of L-α-acetylmethadol (LAAM) *N*-demethylation and dextromethorphan *O*-demethylation. *Drug Metab Dispos* 2001;29:319–325.
24. Barnes HJ, Arlotto MP, Waterman MR. Expression and enzymatic activity of recombinant cytochrome P450 17-alpha-hydroxylase in *Escherichia coli*. *Proc Natl Acad Sci USA* 1991;88:5597–5601.
25. Friedberg T, Pritchard MP, Bandera M, Hanlon SP, Yao D, McLaughlin LA, Ding S, Burhell B, Wolf CR. Merits and limitations of recombinant models for the study of human

P450-mediated drug metabolism and toxicity—an intralaboratory comparison. *Drug Metab Rev* 1999;31:523–544.

26. Donato MT, Jimenez N, Castell JV, Gomez-Lechon J. Fluorescence-based assays for screening nine cytochrome P450 (P450) activities in intact cells expressing individual human P450 enzymes. *Drug Metab Dispos* 2004;32:699–706.
27. Vtric F, Haefeli WE, Drewe, J, Krahenbuhl S, Wenk M. Interaction of ibuprofen and probenecid with metabolizing enzyme phenotyping procedures using caffeine as the probe drug. *Br J Clin Pharmacol* 2003;55:191–198.
28. Li AP. Scientific basis of drug-drug interactions: mechanism and preclinical evaluation. *Drug Inf J* 1998;32:657–664.
29. Emoto C, Murase S, Sawada Y, Jones BC, Iwasaki K. *In vitro* inhibitory effects of 1-aminobenzotriazole on drug oxidations catalyzed by human cytochrome P450 enzymes: a comparison with SKF-525A and ketoconazole. *Drug Metab Pharmacokinet* 2003;18: 287–295.
30. Rodriques AD. Integrated cytochrome P450 reaction phenotyping: attempting to bridge the gap between cDNA-expressed cytochromes P450 and native human liver microsomes. *Biochem Pharmacol* 1999;57:465–480.
31. Lu AYH, Wang RW, Lin JH. Commentary: Cytochrome P450 *in vitro* reaction phenotyping: a re-evaluation of approaches for P450 isoform identification. *Drug Metab Dispos* 2003;31:345–350.
32. Ring BJ, Gillespie JS, Eckstein JA, Wrighton SA. Identification of human cytochromes P450 responsible for atomozetine metabolism. *Drug Metab Dispos* 2002;30:319–323.
33. Renwick AB, Surry D, Price RJ, Lake BG, Evans DC. Metabolism of 7-benzyloxy-4-trifluoromethylcoumarin by human hepatic cytochrome P450 isoforms. *Xenobiotica* 2004;30:955–969.
34. Crespi CL. Xenobiotic-metabolizing human cells as tools for pharmacological and toxicological research. *Adv Drug Res* 1995;26:179–235.
35. Uttamsingh V, Lu C, Miwa G, Gan LS. Relative contributions of the five major human cytochromes P450, 1A2, 2C9, 2C19, 2D6, and 3A4, to the hepatic metabolism of the proteasome inhibitor bortezomib. *Drug Metab Dispos* 2005;33:1723–1728.
36. McGinnity DF, Berry AJ, Kenny JR, Grime K, Riley RJ. Evaluation of time-dependent cytochrome P450 inhibition using cultured human hepatocytes. *Drug Metab Dispos* 2006;34:1291–1300.
37. Lu C, Miwa GT, Prakash SR, Gan LS, Balani SK. A novel model for the prediction of drug–drug interactions in humans based on *in vitro* cytochrome p450 phenotypic data. *Drug Metab Dispos* 2007;35:79–85.
38. Chiba M, Jin L, Neway W, Vacca JP, Tata JR, Chapman K, Lin JH. *Drug Metab Dispos* 2001;29:1–3.
39. Kim JY, Baek M, Lee S, Kim SO, Dong MS, Kim BR, Kim DH. Characterization of the selectivity and mechanism of cytochrome P450 inhibition by dimethyl-4,4′-dimethoxy-5,6,5′,6′-dimethylenedioxybiphenyl-2,2′-dicarboxylate. *Drug Metab Dispos* 2001;29: 1555–1560.
40. Wen X, Wang JS, Backman JT, Kivisto KT, Neuvonen PJ. Gemfibrozil as an inhibitor of human cytochrome P450 2C9. *Drug Metab Dispos* 2001;29:1359–1361.
41. Walsh CT. Suicide substrates, mechanism-based enzyme inactivators: recent developments. *Annu Rev Biochem* 1984;53:493–535.
42. Madeira M, Levine M, Chang TKH, Mirfazaelian A, Bellward G. The effect of cimetidine on dextromethorphan *O*-demethylase activity of human liver microsomes and recombinant CYP2D6. *Drug Metab Dispos* 2004;32:460–467.

43. Brown HS, Galetin A, Hallifax D, Houston B. Prediction of *in vivo* drug–drug interactions from *in vivo* data: factors affecting prototypic drug–drug interactions involving CYP2C9, CYP2D6 and CYP3A4. *Clin Pharmacokinet* 2006;45:1035–1050.
44. Kato M, Tachibana T, Ito K, Sugiyama Y. Evaluation of methods for predicting drug–drug interactions by Monte Carlo simulation. *Drug Metab Pharmacokinet* 2003;18:121–127.
45. Li AP, Rasmussen A, Xu L, Kaminski DL. Rifampicin induction of lidocaine metabolism in cultured human hepatocytes. *J Pharmacol Exp Ther* 1995;274:673–677.
46. Li AP. Primary hepatocyte cultures as an *in vitro* experimental model for the evaluation of pharmacokinetic drug–drug interactions. *Adv Pharmacol* 1997;43:103–130.
47. Roymans D, Van Looveren C, Leone A, Parker JB, McMillan M, Johnson MD, Koganti A, Gilissen R, Silber P, Mannens G, Meuldermans W. Determination of cytochrome P450 1A2 and P450 3A4 induction in cryopreserved human hepatocytes. *Biochem Pharmacol* 2004;67:427–437.
48. Roymans D, Annaert P, Van Houdt J, Weygers A, Noukens J, Sensenhauser C, Silva J, van Looveren C, Hendrickx J, Mannens G, Meuldermans W. Expression and induction potential of cytohromes P450 in human cryopreserved hepatocytes. *Drug Metab Dispos* 2005;33:1004–1016.
49. Hariparsad N, Nallani S, Sane RS, Buckley DJ, Buckley AR, Desai PB. Induction of CYP3A4 by efavirenz in primary human hepatocytes: comparison with rifampin and phenobarbital. *J Clin Pharmaol* 2004;44:1273–1281.
50. Lillibridge JH, Liang BH, Kerr BM, Webber S, Quart B, Shetty BV, Lee CA. Characterization of the selectivity and mechanism of human cytochrome P450 inhibition by the human immunodeficiency virus–protease inhibitor nelfinavir mesylate. *Drug Metab Dispos* 1998;26:609–616.
51. Wang RW, Newton DJ, Liu N, Atkins WM, Lu AYH. Human cytochrome P-450 3A4: *in vitro* drug–drug interaction patterns are substrate-dependent. *Drug Metab Dispos* 2000;28:360–366.
52. Backman JT, Kyrklund C, Neuvonen M, Neuvonen PJ. Gemfibrozil greatly increases plasma concentrations of cerivastatin. *Clin Pharmaol Ther* 2002;72:685–691.
53. Vickers AE, Sinclair JR, Zollinger M, Heitz F, Glanzel U, Johanson L, Fischer V. Multiple cytochrome P450s involved in the metabolism of terbinafine suggest a limited potential for drug–drug interactions. *Drug Metab Dispos* 1999;27:1029–1038.